



MICROENCAPSULATION OF FLAXSEED OIL
PRODUCED THROUGH THE COMBINATION OF
DIFFERENT EMULSIFICATION METHODS AND
DRYING TECHNOLOGIES

Doctoral (Ph.D.) dissertation by
Asma Yakdhane

Under the supervision of
Prof. András Koris
and
Dr. Habil Arijit Nath

Hungarian University of Agriculture and Life Sciences
Institute of Food Science and Technology
Department of Food Engineering

Budapest, 2024

The PhD School

Name: Doctoral School of Food Science

Discipline: Food science

Head: **Dr. Livia Simonné Sarkadi**
Professor, DSc,
Hungarian University of Agriculture and Life Sciences
Institute of Food Science and Technology
Department of Nutrition

Supervisor: **Dr. András Koris**
Full Professor, PhD,
Hungarian University of Agriculture and Life Sciences
Institute of Food Science and Technology
Department of Food Process Engineering

Co-supervisor: **Dr. Arijit Nath**
Scientific Associate, PhD-Habil,
Hungarian University of Agriculture and Life Sciences
Institute of Food Science and Technology
Department of Food Process Engineering

Approval signature of Head of the doctoral school and supervisors:

The candidate has fulfilled all the conditions prescribed by the Doctoral School of Hungarian University of Agriculture and Life Sciences, the comments and suggestion at the thesis workshop were taken into consideration when revising the thesis, so the dissertation can be submitted to a public debate.

.....
Signature of Head Food Science
PhD School

.....
Signature of Supervisor

.....
Signature of Supervisor

TABLE OF CONTENT

1. INTRODUCTION	1
2. OBJECTIVES	2
3. LITERATURE REVIEW	3
3.1. Nutritional profile of flaxseed oil	3
3.2. Microencapsulation technology	5
3.2.1. Emulsification for microencapsulation purposes	6
3.2.1.1. Emulsions	6
3.2.1.2. Membrane emulsification	8
3.2.1.3. Rotor-stator homogenization	10
3.2.2. Coating techniques	11
3.2.2.1. Spray drying	13
3.2.2.2. Freeze drying	14
3.2.3. Matrix (Wall material)	16
3.2.3.1. Emulsifier	17
3.2.4. Characterization of microencapsulated flaxseed oil	17
3.3. Applications of microencapsulated flaxseed oil	18
4. MATERIALS AND METHODS	20
4.1. Materials	20
4.1.1. Flaxseed oil	20
4.1.2. Wall materials	20
4.1.3. Emulsifier	20
4.1.4. Solvents and chemicals	20
4.2. Methods	20
4.2.1. Preparation of the emulsion through membrane emulsification	20
4.2.1.1. Membrane emulsification apparatus setup	20
4.2.1.2. Apparatus cleaning procedure	22

4.2.2. Preparation of the emulsion through the rotor-stator homogenization	23
4.2.3. Spray drying	24
4.2.4. Freeze drying	25
4.2.5. Emulsions preparation for the pilot study	25
4.2.6. Experimental design	26
4.2.7. Emulsion characterization	29
4.2.7.1. Emulsion stability	29
4.2.7.2. Droplet Sizing	29
4.2.7.3. Morphological analysis of emulsion droplets	30
4.2.8. Microcapsules characterization	31
4.2.8.1. Encapsulation efficiency	31
4.2.8.2. Moisture Content	31
4.2.8.3. Bulk density	32
4.2.8.4. Tapped density	32
4.2.8.5. Flowability and Cohesiveness	32
4.2.8.6. Powder wettability	32
4.2.8.7. Morphological study by scanning electron microscopy	32
4.2.8.8. Particle size distribution	33
4.2.8.9. Solubility	33
4.2.8.10. Oxidative stability of flaxseed oil	33
4.2.9. Statistical analysis	34
5. RESULTS AND DISCUSSION	35
5.1. Wall materials and oil load impact on encapsulation results: pilot study	Erreur ! Signet non défini.
5.1.1. Size and morphology study	35
5.1.2. Emulsions stability	37
5.1.3. Particle size	39

5.1.4. Encapsulation Efficiency	41
5.2. Discussion of the results	42
5.3. Optimization of flaxseed oil microcapsules using Response Surface Methodology with Box-Behnken Design	43
5.3.1. Encapsulation of flaxseed oil using combination of membrane emulsification and spray drying	43
5.3.1.1. Optimization and verification formula of flaxseed oil microcapsules	51
5.3.2. Encapsulation of flaxseed oil using combination of rotor stator homogenizer and spray drying	52
5.3.2.1. Optimization and verification formula of flaxseed oil microcapsules	59
5.3.3. Encapsulation of flaxseed oil using combination of membrane emulsification and freeze drying	59
5.3.3.1. Optimization and verification formula of flaxseed oil microcapsules	67
5.4. Optimized emulsions and microcapsules characterization	68
5.4.1. Emulsions stability	68
5.4.2. Size and morphology study of emulsion	70
5.4.3. Flaxseed oil microcapsules size and morphology	72
5.4.4. Oxidative stability of encapsulated flaxseed oil	74
5.4.5. Microcapsules characteristics	76
6. SUMMARY	79
7. NEW SCIENTIFIC RESULTS	81
8. APPENDIX	84
9. REFERENCES	95
10. LIST OF PUBLICATIONS AND CONFERENCES	107
ACKNOWLEDGEMENTS	109

LIST OF TABLES

Table 1: Comparison between ω -6 and ω -3 composition in different oils.....	4
Table 2: Summary of different emulsification technologies	8
Table 3: Brief description of some FO encapsulation techniques.....	12
Table 4: Description of formulations for emulsion preparation.....	26
Table 5: Coding of independent variables.....	27
Table 6: Droplet size and span measurements	36
Table 7: Zeta-potential measurements	38
Table 8: Phase separation measurements	39
Table 9: Particle size and span measurements	40
Table 10: Experimental responses of the optimization experimental design.....	44
Table 11: Fit summary.....	45
Table 12: Box-Behnken design and observed responses.	45
Table 13: Constraints	52
Table 14: Experimental responses of the optimization experimental design.....	52
Table 15: Fit summary	53
Table 16: Box-Behnken design and observed responses	53
Table 17: Constraints	59
Table 18: Experimental responses of the optimization experimental design.....	60
Table 19: Fit summary	61
Table 20: Box-Behnken design and observed responses	61
Table 21: Constraints	67
Table 22: Evaluation of separation % of different optimized formulation	70
Table 23: Evaluation of separation % of different optimized formulation	72
Table 24: Evaluation of particle size and distribution of different optimized formulation.	73
Table 25: Evaluation of moisture%, wettability and solubility% of optimized formulations	76
Table 26: Evaluation of Bulk and tapped density for ME-SD-C and RSH-SD-C	77

List of Figures

Figure 1. Different types of ω -3 and ω -6 fatty acids present in FO.....	3
Figure 2. Applications of FO in different food matrixes and biopharmaceuticals for the prevention of different diseases	4
Figure 3. Different types of water and oil emulsions	6
Figure 4. Membrane emulsification process for O/W emulsion preparation	9
Figure 5. Difference between crossflow and premix emulsification processes.....	9
Figure 6 : Rotor stator homogenizer mechanism	11
Figure 7. Schematic diagram of the SD process.....	13
Figure 8. Schematic diagram of the FD process.....	15
Figure 9. Geometry of the helix reducer.....	21
Figure 10. Experimental set-up of ME	22
Figure 11. Rotor-Stator Homogenizer device	24
Figure 12. Spray drying apparatus.....	24
Figure 13. Freeze drying apparatus	25
Figure 14. Microscopic observations of emulsions.....	35
Figure 15. Encapsulation efficiency % of different formulations.....	41
Figure 16. Plots of residuals for response and plot of actual response against predictive values.....	47
Figure 17. Surface plot (A) and contour plot (B) for EE response (X1;X2)	48
Figure 18. Surface plot (A) and contour plot (B) for EE response (X1;X3)	49
Figure 19. Surface plot (A) and contour plot (B) for EE response (X2;X3)	50
Figure 20. Plots of residuals for response and plot of actual response against predictive values.....	55
Figure 21. Surface plot (A) and contour plot (B) for EE response (X1; X2)	56
Figure 22. Surface plot (A) and contour plot (B) for EE response (X1; X3)	57
Figure 23. Surface plot (A) and contour plot (B) for EE response (X2; X3)	58
Figure 24. Plots of residuals for response and plot of actual response against predictive values.....	63
Figure 25. Surface plot (A) and contour plot (B) for EE response (X1;X2)	64
Figure 26. Surface plot (A) and contour plot (B) for EE response (X1;X3)	65
Figure 27. Surface plot (A) and contour plot (B) for EE response (X2;X3)	66

Figure 28. Zeta potential distribution of ME-SD-E.....	69
Figure 29. Zeta potential distribution of RSH-SD-E.....	69
Figure 30. Zeta potential distribution of ME-FD-E.....	70
Figure 31. Microscopic images of ME-SD-E (A), ME-FD-E (B) and RSH-SD-E (C).....	71
Figure 32. SEM images of ME-SD-C (A), RSH-SD-C (B) and ME-FD-C (C).....	74
Figure 33. TBARS measurements in FO, ME-SD-C and RSH-SD-C after 30 days storage...	75

Abbreviations

ALA	α -linolenic acid
ANOVA	Analysis of variance
MANOVA	Multivariate analysis of variance
DE	Dextrose equivalent
FD	Freeze drying
FO	Flaxseed oil
GA	Gum arabic
MD	Maltodextrin
ME	Membrane emulsification
ME-FD-C	Membrane emulsification-Freeze drying capsule
ME-FD-E	Membrane emulsification - Freeze drying emulsion
MS	Modified starch
ME-SD-C	Membrane emulsification -Spray drying capsule
ME-SD-E	Membrane emulsification -Spray drying emulsion
PSD	Particle size distribution
PUFA	polyunsaturated fatty acids
R ²	Coefficient of determination
RSH-SD-C	Rotor stator homogenization-Spray drying capsule
RSH-SD-E	Rotor stator homogenization-Spray drying emulsion
RSH	Rotor stator homogenization
RSM	Response surface methodology
SD	Spray drying
O/W	Oil-in-water
O/W/O	Oil-in-water-in-oil
W/O	Water-in-oil
W/O/W	Water-in-oil-in-water

1. INTRODUCTION

Flaxseed oil (FO) thrive of essential nutrients with an abundance of polyunsaturated fatty acids (PUFAs), particularly α -linolenic acid (ALA), an ω -3 fatty acid. PUFAs, like ω -3 and ω -6 fatty acids, are crucial for human health and can play vital roles in cell membrane development and serve in controlling inflammatory reactions, blood pressure, and preventing cardiovascular diseases. Additionally, ω -3 fatty acids offer benefits such as reduced risk of diabetes and certain cancers. In many food products, the addition of ω -3 fatty acids helps maintain a healthy balance between ω -3 and ω -6 fatty acids in the diet which is, unfortunately, in many modern diets, falling within the concerning range.

Due to this nutritional profile of flaxseed oil, many industries have aimed to incorporate it into various products leading to an increase demand in the food and biopharmaceutical industries. As an example, it was incorporated in formulations to prepare ice cream, soup powder, and bread, and it was also used to prepare formulations for the treatment and prevention of gastrointestinal disorders, cardiovascular disease, eczemas, hypertension, atherosclerosis, diabetes, and cancer.

In the other hand while FO offers all these benefits, unfortunately it is prone to oxidation which not only deteriorate its nutritional value but also negatively impact the organoleptic properties of food products containing it. Therefore, microencapsulation of FO emerges as a critical step to ensure its stability within the food matrix.

Encapsulation is an evolving technology that aims to satisfy the demands of a stable product with high quality. It is used to protect food ingredients, to assure their quality and effectiveness and to control the release of property of active agents by coating small droplets of liquid or solid particles with a thin film of wall materials. Depending on the core material to be protected, wall materials can include a variety of polymers, carbohydrates, proteins, and waxes etc. Different techniques have been used for food-grade compounds encapsulation.

2. OBJECTIVES

The objective of my PhD work is to dive into the details of various microencapsulation techniques for flaxseed oil (FO) and to offer promising formulations for the development of stable microcapsules systems that can protect FO from lipid deterioration.

Optimizing microencapsulation techniques for FO, will pave the way for its wider application in the food and biopharmaceutical industries and will ultimately lead to an increase development of functional food products enriched with the health benefits of FO, while ensuring its stability.

The focus on membrane emulsification technique (ME) as an initial step for emulsion preparation can offer a cost-effective solution providing a foundation to achieve desired results in term of characteristics and properties of FO capsules.

In this regard, the following steps were set to accomplish:

- Preparing a base study through literature review and screening with preliminary and pilot studies for the selection of adequate wall materials and oil load in the case of ME and spray drying (SD).
- Optimizing the FO capsules obtained through ME and SD with different oil content and different composition of wall material such as, maltodextrin (MD), Gum arabic (GA), and modified starch (MS).
- Optimizing the FO capsules obtained through rotor stator homogenization (RSH) and SD with different oil content and different composition of wall material.
- Optimizing the FO capsules obtained through ME and freeze drying (FD) with different oil content and different composition of wall material.
- Evaluating and comparing of differently formed FO capsules from optimized formulations in the aim of studying their efficacy in offering the needed protection for FO. This evaluation consists of comparing the produced optimized emulsions stability and the droplet size and distribution and also studying the capsules characteristics by conducting an evaluation of particle size and distribution, oxidative stability, moisture content, and analysis that are in correlation with FO encapsulation efficiency and stability.

3. LITERATURE REVIEW

3.1. Nutritional profile of flaxseed oil

Flaxseed (latin name *Linum usitatissimum*) is an abundant source of PUFAs, short chain PUFAs (Kaur et al., 2014), soluble and insoluble fibers (Singh et al., 2011), phytoestrogenic lignans, antioxidants (Touré and Xueming, 2010), and proteins (Hall et al., 2006). In flaxseed, the total amount of fat is quite high (41% weight basis) compared to the carbohydrate (29% weight basis) and protein (20% weight basis). In FO, the contents of palmitic acid (C16:0), stearic acid (C18:0), oleic acid (C18:1), α -linolenic acid (C18:3) (ω -3), and linoleic acid (C18:2) (ω -6) are 4.90–8.00%, 2.24–4.59%, 13.44–19.39%, 39.90–60.42%, and 12.25–17.44%, respectively (Goyal et al., 2014). Different types of ω -3 and ω -6 fatty acids present in FO are represented in Figure 1.

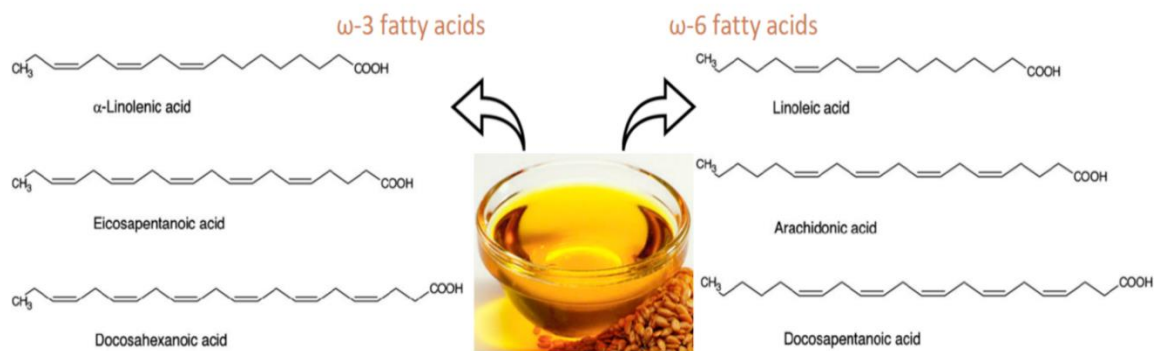


Figure 1. Different types of ω -3 and ω -6 fatty acids present in FO (self-developed, the concept was adopted from (Goyal et al., 2014))

Polyunsaturated essential fatty acids, such as ω -3 and ω -6 fatty acids are characterized by the presence of a double bond in three and six atoms, respectively away from the terminal methyl group in their chemical structure (Kaur et al., 2014). Both ω -3 and ω -6 fatty acids are important for cell membrane development and precursor molecules of many physiological elements, which are involved in controlling inflammatory reactions, blood pressure, and mortal cardiac diseases. Additionally, ω -3 fatty acids reduce the risk of diabetes and certain types of cancer. Eicosapentaenoic and docosahexaenoic acids can be synthesized from the α -linolenic acid (Gibson et al., 2011). In many foods, the addition of ω -3 fatty acid maintains the ratio of ω -3 fatty acid to ω -6 fatty acid (Ludwig, 2020). Clinically, it has been proven that the ratio of 4:1 or less of ω -6 fatty acid to ω -3 fatty acid in a diet is beneficial for health. Unfortunately, in many diets, this ratio ranges between 10:1 and 50:1 (Simopoulos, 2008). Therefore, FO, being an alternative to balance the intake of ω -3 and ω -6 compared to other vegetable oils, has witnessed an increasing use in food and

biopharmaceutical industries. A brief comparison of FO composition with other vegetable oils is given in Table 1. In the food industry, FO was used to prepare dahi (Indian yogurt) (Goyal et al., 2016), healthy milk (Goyal et al., 2017), ice cream (Gowda et al., 2018), soup powder (Rubilar et al., 2012), and bread (Gallardo et al., 2013). Presently, its application to develop the ketogenic diet has gained lots of attention (Dell et al., 2001; Harvey et al., 2019; Parikh et al., 2019).

Table 1: Comparison between ω -6 and ω -3 composition in different oils (Rabail et al., 2021; Goyal et al., 2014; El-Beltagi & Amin Mohamed, 2010)

PUFAs	Flaxseed oil	Olive oil	Sunflower oil	Rapeseed oil
Linoleic acid (C18:2) (ω -6) %	12.25–17.44	4.8-15.26	54.17-65.76	10.52-13.74
α -Linolenic acid(C18:3)(ω -3) %	39.90–60.42	0.3-1.2	0.09-5.16	8.83-10.32

In the biopharmaceutical industry, FO is used to prepare formulations for the treatment and prevention of gastrointestinal disorders, cardiovascular disease, eczemas, hypertension, atherosclerosis, diabetes, and cancer (Goyal et al., 2014). The application of FO in different food matrixes and biopharmaceuticals for the prevention of different diseases are represented in Figure 2.

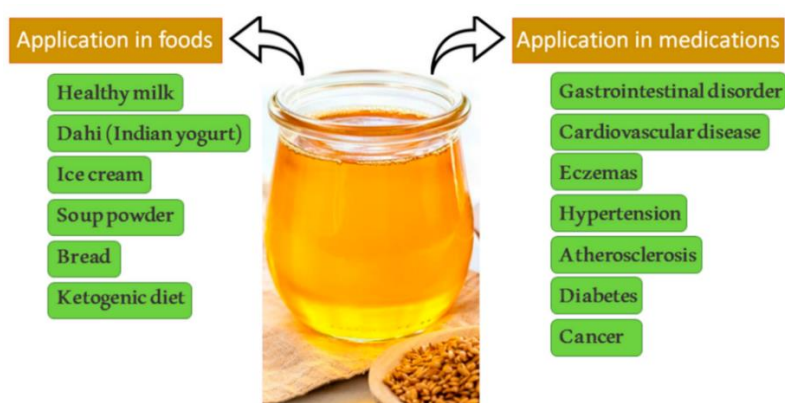


Figure 2. Applications of FO in different food matrixes and biopharmaceuticals for the prevention of different diseases (self-developed, the concept was adopted from (Gallardo et al., 2013; Gowda et al., 2018; Goyal et al., 2014, 2016, 2017; Rubilar et al., 2012))

Biological activities of FO against various autoimmune and chronic inflammatory diseases are associated with several mechanisms, such as (a) modifications in cell membrane lipid

composition, (b) expression of genetic activity, (c) cellular metabolism and (d) signal transduction (Balić et al., 2020). Furthermore, orbitides or cyclolinopeptides with an antitumor activity are abundant in FO (Zou et al., 2017). The micronutrient tocopherol present in FO, acts as an antioxidant, and suppresses the activity of reactive oxygen species. Even though FO is rich in antioxidants, after its extraction from the seed and purification, fatty acids in FO are easily oxidized. Oxidized fatty acids change the organoleptic property of food and deteriorate the nutritional status (Gunstone, 2011; Holstun and Zetocha, 1994; Shahidi, 2005). Therefore, the microencapsulation of FO is a prerequisite that ensures its stability in the food matrix. However, despite several reported biological activities of FO, its industrial production and utilization is still limited in comparison with other vegetable oils (Harvey et al., 2019). It might be due to the lack of technologically needed information that can enhance the flaxseed oil stability and resolve its shelf life issues due to its high unsaturated fatty acid content. Considering the great potentiality of FO as well as the microencapsulation technology, some laboratory-scale investigations were performed by several research groups. In this study, information about different technologies on the microencapsulation of FO and biochemical characteristics of the microcapsule are discussed in a comprehensive way.

3.2. Microencapsulation technology

Microencapsulation has been explored in order to satisfy the increasing expectation of developing food ingredients with complex properties and functional values. It is an emerging technology which has been receiving interest in food and biopharmaceutical industries. It is used to protect encapsulated bioactive compounds and control their release. In the microencapsulation technology, small droplets of liquid or solid particles are coated within a thin film, known as a wall material or matrix (Gouin, 2004; Liu and Yang, 2011). For the microencapsulation of food-grade bioactive compounds, different techniques have been adopted and they can be classified into three distinctive categories. Those include (a) chemical methods: Entrapping the bioactive compound within the polymerized matrix, (b) physical methods: spray drying, spray coating, freeze drying, and supercritical encapsulation processes, and (c) physico-chemical methods: Complex coacervation, entrapment within the nanostructured lipid matrix, ionotropic gelation, and molecular inclusion (Comunian and Favaro-Trindade, 2016). For the microencapsulation of FO, two major steps are: Preparation of FO emulsion with an aqueous solution of the matrix and subsequently, SD or FD.

3.2.1. Emulsification for microencapsulation purposes

3.2.1.1. Emulsions

Emulsions are potential delivery systems commonly used in food industries and are acknowledged to have a considerable importance in food products fabrication (Roohinejad et al., 2018). An emulsion is a system of two or more immiscible liquids. It consists of two phases, a dispersed phase and a continuous phase where the dispersed phase is present as suspension in the continuous phase. Depending on the size, emulsions can be classified into nanoemulsions for droplet size between 1 nm and 100 nm, and miniemulsions for droplet size between 100 nm and 1000 nm which are both thermodynamically unstable and microemulsions for droplet size between 0.5 μm and 100 μm which is thermodynamically stable (Santana et al., 2013). They are used in the fabrication of a wide range of food products such as salad dressings, margarines, cream liqueurs and are as well evolved in the first step of encapsulation of bioactive compounds (Charcosset, 2009; Van Der Graaf et al., 2005). Depending on the nature of the dispersed and continuous phases, emulsions can be classified into different types (Figure 3) including oil-in-water emulsions (O/W), water-in-oil (W/O) emulsions, double emulsions of water in-oil-in-water (W/O/W) and oil-in-water-in-oil (O/W/O) (Van Der Graaf et al., 2005).

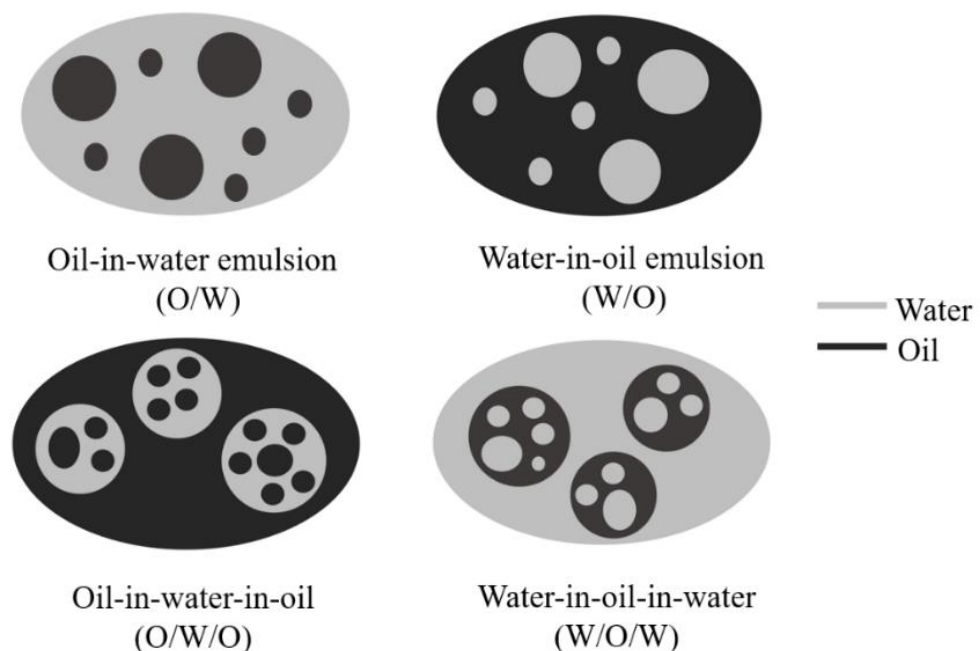


Figure 3. Different types of water and oil emulsions (Bakry et al., 2015)

Emulsions face different types of destabilizations such as flocculation, coalescence, phase inversion, creaming and sedimentation. Resort to emulsifier has always been considered in order to enhance the stability of the emulsion by the reducing the interfacial tension. This is possible thanks to their amphiphilic nature consisted of both hydrophobic and hydrophilic parts (Rosen and Kunjappu, 2012).

The emulsion preparation plays a key role in the encapsulation efficiency. An emulsion is a mixture of two or more immiscible liquids (Malik et al., 2012). The emulsion stability is controlled by many factors. Flocculation, a reversible aggregation of droplets and coalescence, an irreversible fusion of droplets are two main types of emulsion instabilities. The emulsifier can make a bridge between polar and non-polar components, and provides stability in the emulsion (Aronson, 1989). To prepare the emulsion, two different types of technologies can be adopted. Those are (a) high energy consuming technologies using mechanical devices to mix up the water and oil phase, such as (i) ultrasound generator and (ii) high pressure homogenizers, as well as (b) low energy consuming technologies, such as (i) phase inversion temperature, (ii) membrane emulsification, and (iii) spontaneous emulsification of two immiscible liquids without any significant external thermal or mechanical energy (Nazari et al., 2019). In Table 2, a summary of different emulsification technologies is provided. The emulsion stability, droplets size, and their distribution are considerably affected by the adopted technologies (Charcosset, 2009). It has been reported that the fine emulsion increases the organoleptic properties of microcapsules (Shima et al., 2004).

Table 2. Summary of different emulsification technologies

Emulsification techniques		Description	Reference
High energy consuming methods	Ultrasound generator	Due to ultrasound (physical shear force) fine droplets are created. At a certain range of sound source pressure amplitude, cavitation takes place and emulsification of the immiscible liquids occurs.	(Gaikwad and Pandit, 2008)
	High pressure homogenizer	In a homogenizer, with the help of a pump, the liquid is pressed with high pressure to a narrow channel, which offers shear force on immiscible liquids. It creates cavitation and leads to emulsion with small droplet size.	(Stang et al., 2001)
	Rotor stator homogenization	Rotor-stator homogenizer can operate in discontinuous or continuous systems. It generally consists of a rotor and a stator that is axially fixed around it. Due to the rotor high velocity, high shear stress in the gap between rotor and stator is created, leading to breaking the droplets into smaller ones.	(Urban et al., 2006)
Low-Energy Techniques	Phase inversion temperature	Due to change of factors, such as temperature or pH, activity of emulsifier in term of its hydrophilic – lipophilic balance is affected. It helps to create emulsion.	(Friberg et al., 2011)
	Membrane emulsification	ME is performed with the porous membrane. Hydrophobic liquid (oil) in dispersed phase is pressed through membrane pores to continuous phase, generally hydrophilic liquid and emulsion is formed in continuous phase.	(Charcosset et al., 2004)
	Spontaneous emulsification	In spontaneous emulsification, the immiscible liquids, such as oil and water along with emulsifier create the emulsion without external energy source.	(Lapez-Montilla et al., 2002 ; Solans et al., 2016)

As in our study we have produced emulsions using RSH; a high energy consuming method that is commonly used for emulsion preparation for the purpose of encapsulation; and ME; an emerging low energy consuming method employed in the preparation of stable emulsions production, a more focus will be giving to these two techniques to have an overview and a description of the functioning and the parameters.

3.2.1.2. Membrane emulsification

ME has grabbed a lot of attention during the last years as a relatively new technique capable of producing emulsions with better control of droplet characteristics and low energy

consumption (Figure 4). Premix ME; during which a coarse pre-mix is pressed the membrane resulting in finer droplets and cross-flow ME where a dispersed phase is pressed into a continuous phase flowing through microporous membrane pores with the help of an applied pressure (Figure 5), can be adopted for the production of oil in water emulsions (Charcosset et al., 2004; Van Der Graaf et al., 2005).

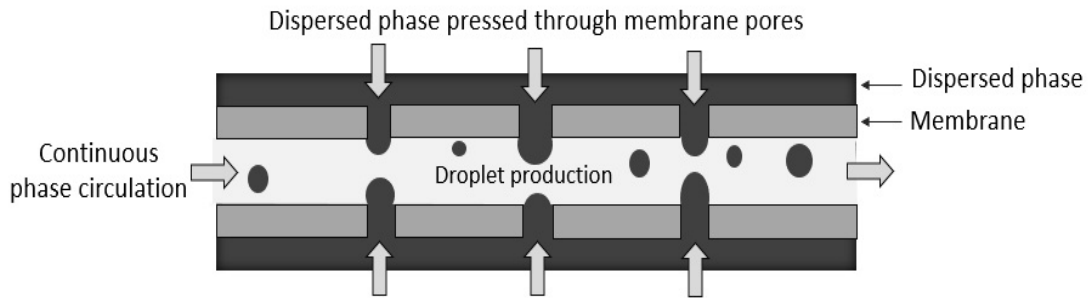


Figure 4. Membrane emulsification process for O/W emulsion preparation (Charcosset et al., 2009)

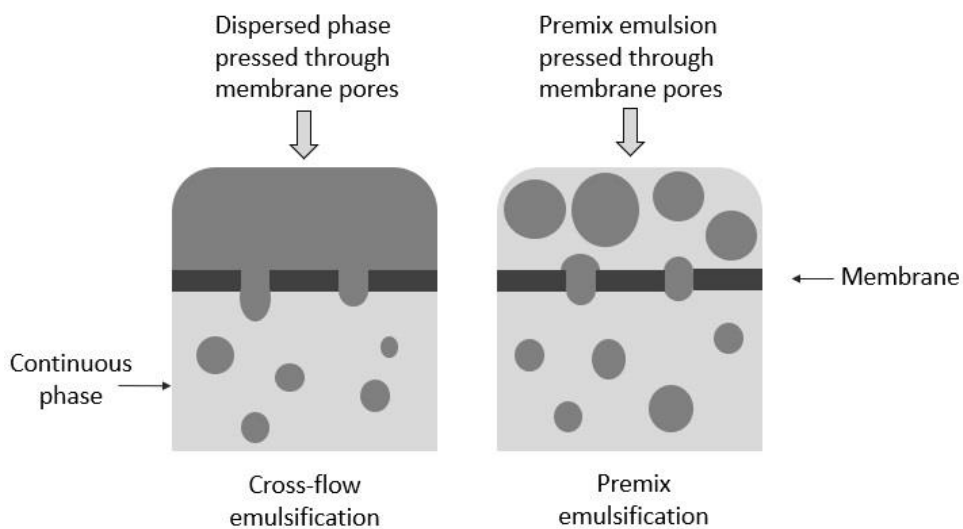


Figure 5. Difference between crossflow and premix emulsification processes (Charcosset et al., 2004; Van Der Graaf et al., 2005)

Several membrane types have been used for the preparation of oil in water emulsions such as, Shirasu-porous-glass (SPG) membranes which are widely used for their narrow pores size distribution and tubular shape and are characterized by a high porosity and mean pore size ranging from 0.1 μm to 20 μm , silicon and silicon nitride micro-engineered membranes characterized by their hierarchical structures exhibiting super-hydrophobic properties, and ceramic membranes which are suitable for oil-in-water emulsion treatment due to their

mechanical and chemical and thermal stability (Charcosset, 2009; Wagdare et al., 2010; Wang et al., 2022; Jun-Wei et al., 2023).

During membrane emulsification numerous parameters must be taken in consideration for effective emulsification regarding the final droplet size and stability of the produced emulsion. These parameters can be divided into three categories which are 1) continuous and dispersed phases formulations and parameters, 2) membrane parameters and 3) process parameters.

Among continuous and dispersed phases formulations and parameters, we can cite the surfactant type and content and the viscosity of both phases. The selection of the adequate surfactant at the right concentration is crucial for the production of a stable emulsion as it can reduce water-oil interfacial tension, help with the detachment of the droplets from the pores, prevent from coalescences and has an effect on the determination of droplet size (Charcosset, 2009; Schröder et al., 1998; Van Der Graaf et al., 2004). Membrane parameters are the characteristics of the chosen membrane for emulsification such as porosity, pores geometry, pore size and distribution, activated pores and membranes wettability, in fact for the production of oil-in-water emulsions, the membrane must be hydrophilic, and must be hydrophobic in case of water-in-oil emulsion production. The membrane parameters highly affect the droplet size and distribution as well as stability of the emulsion (Abrahamse et al., 2002; Kukizaki, 2009; Nakashima et al., 2000). Regarding Process parameters, transmembrane pressure used to press the dispersed phase through the membrane pores, continuous phase flow rate and dispersed phase flux are essential parameters that should be taken in consideration in order to control the average droplet size and size distribution and to avoid droplets coalescence (Charcosset, 2009).

3.2.1.3. Rotor-stator homogenization

The rotor-stator homogenization method is a widely employed mechanical technique for producing emulsions. The core principle of RSH relies on a high-speed rotating shaft (rotor) within a stationary casing (stator) which breaks down larger droplets into smaller and more uniform sizes and leading to a stable emulsion. As the rotor spins, it creates intense shear forces within the sample, promoting the disruption and dispersion of one immiscible liquid phase (dispersed phase) into another (continuous phase) (Urban et al., 2006). The RSH method Includes a rotor with multiple blades concentrically placed inside a stator with vertical or slant slots which creates a vacuum to circulate the liquid for emulsification (Figure 6). It operates on two key forces that have an impact on reducing droplet size which

are, mechanical impingement against the wall due to high fluid acceleration and shear force from the rotor-stator gap. At high rotational speeds, turbulent flow occurs enhancing emulsification efficiency. Additionally, fluid dynamics simulation can help in understanding the fluid flow within the device in a way to optimize the parameters for achieving desired droplet size distribution and reducing energy consumption making this method a valuable tool for industrial emulsification processes (Urban et al., 2006).

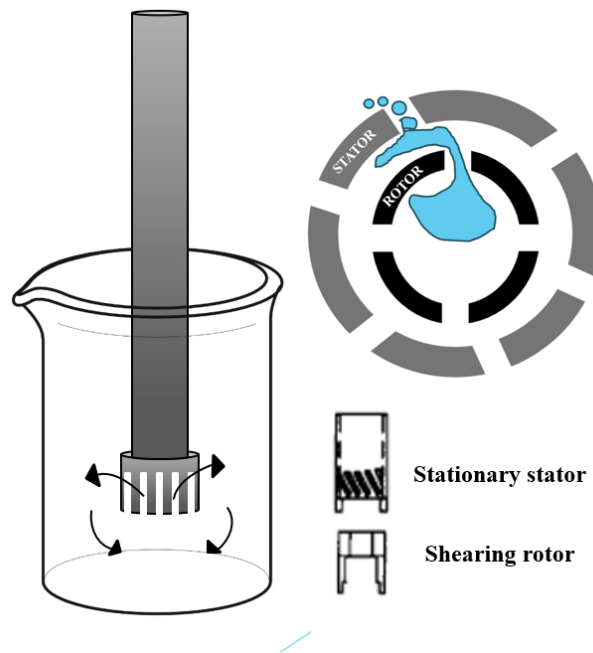


Figure 6. Rotor stator homogenizer mechanism (Maa & Hsu, 1996)

3.2.2. Coating techniques

Choosing the adequate encapsulation techniques plays a key role in the efficiency of oil encapsulation and protection. The principal processes used for encapsulation of flaxseed include SD, FD, spray freeze drying, coacervation, in situ polymerization and encapsulation by extrusion method. A brief description of these encapsulation techniques is giving in Table 3.

Table 3 : Brief description of some FO encapsulation techniques (Bakry et al., 2015; Elik et al., 2021; Guesmi et al., 2022)

Microencapsulation technique	Description
Spray drying	This technique is known for its rapidity and its low cost. Water removal is instantly happening due to high temperature and crust is formed entrapping the oil. SD can operate with a continuous mode.
Freeze drying	FD also referred to as lyophilization consist of freezing the oil with the carrier material, and then conducting a sublimation of the water. It is considered an expensive drying technology.
Spray Freeze Drying	Spray Freeze Drying is a fusion between SD and FD common steps. In fact, the emulsion is atomized into a cold vapor phase of cryogenic liquid. Frozen droplets are produced and are consecutively dried through FD. Spray Freeze Drying can provide a good control over particle size, but it is time and energy consuming.
Coacervation	This process is based on phase separation through simple or complex coacervation. Simple coacervation is a low-cost process but its scale-up is complex.
In situ polymerization	In situ polymerization results in the formation of a wall via the introduction of a reactant externally from the core material. During this process consists of emulsifying oil with a reactive resin solution through sonication, followed by polymerization initiation through sonication or pH adjustment to facilitate microcapsule shell formation.
Encapsulation by extrusion method	It is a physical method for FO encapsulation. During extrusion method a solution containing within it the FO is pressed through a nozzle, the droplets will undergo a solidification by gelation forming a membrane in the surface.

As in our study we have produced microcapsules using SD and FD techniques, a more focus will be giving to these two techniques to have an overview and a description of the functioning and the parameters.

3.2.2.1. Spray drying

SD is a commonly used technology to prepare the encapsulation of vegetable oil (Carneiro et al., 2013). In the SD process, due to high heat, the water content is evaporated. Subsequently, the phase of the matrix is altered, and solidification of the matrix takes place. Oil droplets are encapsulated within the molten matrix in a non-homogeneous way and the size of the microcapsule ranges between 10 to 400 μm depending on the initial parameters (Mishra, 2015). Compared to other microencapsulation technologies, SD is simple, may operate with a continuous mode, and has a low production cost. On the other hand, the disadvantages of SD are (a) the availability of water-soluble matrixes is limited and (b) loss of heat energy (Gharsallaoui et al., 2007). In Figure 7, the process flow diagram of the SD technology is represented.

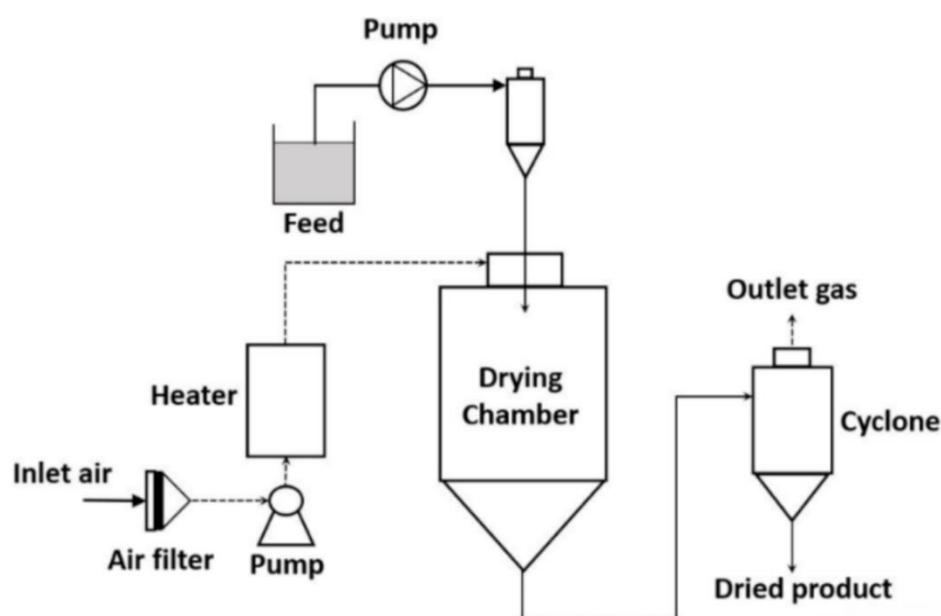


Figure 7. Schematic diagram of the SD process (self-developed, the concept was adopted from (Bakry et al., 2016; Fang and Bhandari, 2012)).

To obtain an optimum encapsulation efficiency with a minimum amount of oil on the surface of the matrix and maximum retention of the active compound, the composition of the emulsion, technology to prepare the emulsion, and parameters of the SD process are taken into consideration (Gharsallaoui et al., 2007; Keogh, 2005; Mori et al., 2019). The composition of the emulsion, size of droplets, and the viscosity of emulsion influence the quality of the spray-dried product. In the emulsion, the ratio of oil and matrix affects the stability of emulsion and encapsulation efficiency. It also affects the physical and biochemical properties of the spray-dried product (Anandharamakrishnan and Padma

Ishwarya, 2015; Rezvankhah et al., 2020). The lower oil content and higher matrix to oil ratio led to a smaller droplet of oil bodies in the emulsion. In this case, the amount of oil on the surface of the matrix is reduced and encapsulation efficiency is increased. In the emulsion, viscosity is directly proportional to the droplet size and inversely proportional to the emulsion stability. These two conditions affect the encapsulation efficiency. The type of atomizer and its operating parameters are important to prepare the microcapsule since they influence the particle size. Among the existing atomizers used for breaking the bulk feed into a smaller droplet, the centrifugal wheel atomizer and spray pressure nozzle are the most used for the encapsulation of oil (Anandharamakrishnan and Padma Ishwarya, 2015; Fang and Bhandari, 2012). In the SD process, the particle size of the product is increased with the increase in the emulsion flow. In the case of the spray pressure nozzle, the particle size of the spray-dried product is increased with the increase in the nozzle orifice diameter and decrease in the atomization pressure. In the case of the centrifugal wheel atomizer, an increase in the wheel diameter and speed provides a smaller size of the particle (Anandharamakrishnan and Padma Ishwarya, 2015). Furthermore, drying parameters provide the desired quality of the final product. The major drying parameters are the drying air flow, and inlet and outlet temperatures (Anandharamakrishnan and Padma Ishwarya, 2015; Rezvankhah et al., 2020). A high inlet temperature in the SD process may lead to deterioration of the encapsulated active compound and an imbalanced evaporation of water from the matrix, which affects the encapsulation efficiency. On the other hand, a higher water content in the encapsulated product and agglomeration of the microcapsule may take place at a very low inlet temperature in the SD process. Furthermore, the outlet temperature in the SD process influences the stability of the microcapsule and retention of the encapsulated product. However, the outlet temperature in the SD process cannot be regulated in a direct way, it can be monitored in an indirect way by controlling the solid content in the feed, inlet temperature, and feed flow rate. The spray air flow rate affects the quality of the final product. It controls the stickiness of the dried particles, deposited onto the wall of the drying chamber (Anandharamakrishnan and Padma Ishwarya, 2015).

3.2.2.2. Freeze drying

FD is also known as the lyophilization process. It is used for the dehydration of high temperature sensitive bioactive compounds, including FO and aromas. During the FD process, a reduction of the surrounding pressure, heating of the emulsion, and sublimation of the frozen water in the material take place (Bakry et al., 2016). After crystallization of

water in the emulsion, sublimation of water takes place at a minimal temperature. It promotes the transformation of water from a solid phase to vapor, directly (Haseley and Oetjen, 2017). In Figure 8, the process flow diagram of the FD technology is represented.

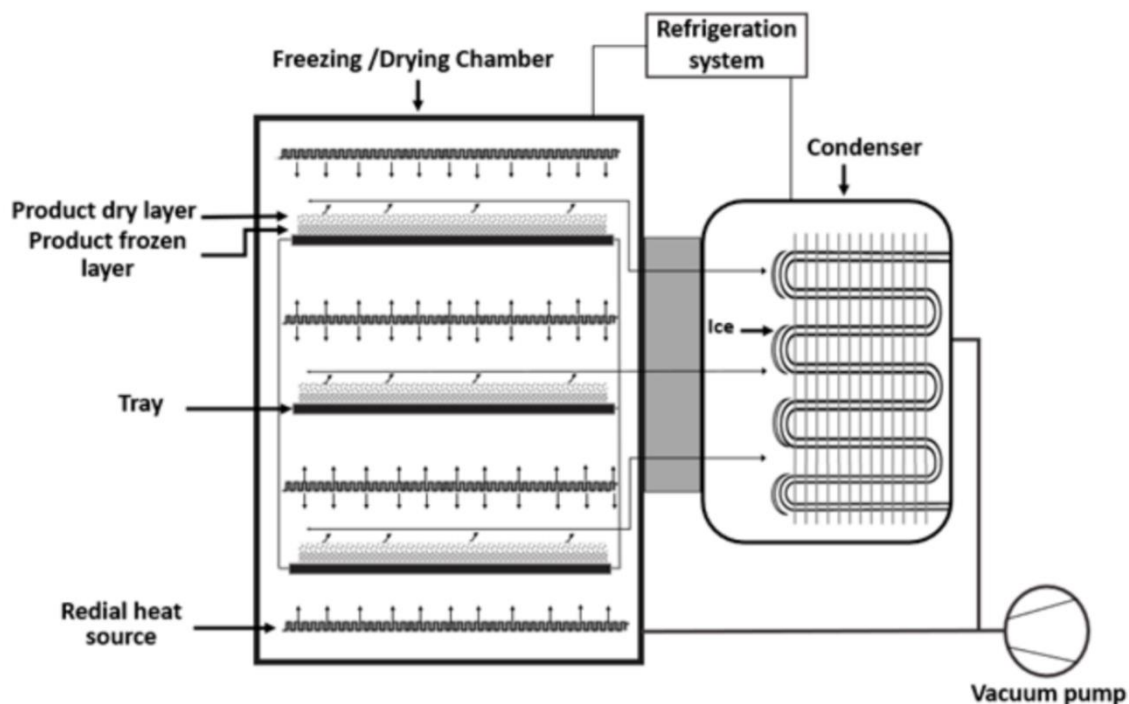


Figure 8. Schematic diagram of the FD process (self-developed, the concept was adopted from (Bakry et al., 2016; Mawilai et al., 2019). Reproduced with permission from Mawilai et al., 2019). Copyright Elsevier, 2016.

It is considered an expensive drying technology compared to the SD process (Desobry et al., 1997). Furthermore, FD is a time occupying process, which consumes high energy. Due to the use of low temperature in the FD process, there is no thermal deterioration in the bioactive compound and less degradation in the heat-sensitive product. The moisture content in the final product is controlled by FD. Therefore, this technology provides a better quality of the product with a remarkable preservation of sensory properties of food ingredients (Bakry et al., 2016; Haseley and Oetjen, 2017; Massounga Bora et al., 2019). Similar to SD, the properties of the emulsion, characteristics of the matrix, and ratio of the matrix and oil are major factors to ensure the quality of the freeze-dried product. MD, GA, and protein are commonly used as a wall material or matrix for microencapsulation through FD (Fang and Bhandari, 2012). The freezing rate can affect the morphology of the microcapsule. A faster rate of freezing of the emulsion can lead to aggregation of the FD products. In the FD process, the system pressure and temperature influence the properties of the microcapsule. Furthermore, the operational time of drying is important to achieve a stable moisture content

in the microcapsule and the stability of the final product (Haseley and Oetjen, 2017; Rezvankhah et al., 2020). Depending on the process parameters, a particle size of the freeze-dried product remains between 20 to 5000 μm (Haseley and Oetjen, 2017).

3.2.3. Matrix (Wall Material)

For the microencapsulation of FO, a selection of the suitable matrix, accepted in the food industry has a great importance. The matrix provides the desired stability of the encapsulated product, increases the encapsulation efficiency, and controls the release of the encapsulated item into the environment. Furthermore, the matrix provides unique physico-chemical and bio-chemical characteristics of the microcapsule (Anandharamakrishnan and Padma Ishwarya, 2015; Desai and Park, 2005). The inexpensive wall material may reduce the cost of the process (Desai and Park, 2005). The water-soluble wall material is preferable for the encapsulation of FO. In the case of SD, the wall material should be soluble in an aqueous medium to shield the encapsulated material from the external environment (Fang and Bhandari, 2012). The drying characteristics of the matrix influence the moisture content of microcapsules. If the matrix has a chance to dry with high temperature at a minimal time, the moisture content in the microcapsule is reduced. Therefore, the encapsulated item has less chance to be contaminated with water (Anandharamakrishnan and Padma Ishwarya, 2015; Desai and Park, 2005). An aqueous solution of the selected wall material is needed to have low viscosity with a high concentration of the solid. It helps obtain a fine microcapsule (lower particle size) and control the release of the encapsulated product. The Newtonian behavior of the emulsion is desirable for SD, a continuous industrial drying process. In the case of SD, previous knowledges about the glass transition temperature of the oil and matrix are a prerequisite to ensure the stability of the microcapsule and avoid the stickiness of the obtained powder in the SD chamber (Anandharamakrishnan and Padma Ishwarya, 2015). In Appendix 1, the biochemical characteristics of different matrixes along with their advantages and disadvantages for preparing the microcapsule are represented.

Many studies are trying to identify the optimal wall materials for encapsulating FO through different emulsification and drying processes. An ideal matrix should form a dense network upon drying, offer exceptional stability and has the ability to dissolve easily in water. In order to offer stability, the wall materials used need to have strong emulsifying properties to prevent oil separation during the process (Calvo et al., 2012; Gharsallaoui et al., 2007). These crucial characteristics provide the ability to shield the encapsulated FO from degradation, particularly oxidation, throughout storage. Of course, cost-effectiveness and materials

availability are also important considerations. Since no single material possesses all these desirable qualities, researchers often strategically combine them to achieve optimal results. (Hogan et al., 2001; Jafari et al., 2008).

3.2.3.1. Emulsifier

The emulsifier, also known as “emulgent” and “surface active agents”, has a great influence on the preparation of FO emulsion in the aqueous solution of the matrix, prior to the drying process. Emulsifiers are amphiphilic with hydrophilic/polar and hydrophobic/non-polar moieties (Kinyanjui et al., 2003). The emulsifier reduces the interfacial tension between hydrophilic and hydrophobic compounds and makes them miscible (Rosen and Kunjappu, 2012). Furthermore, emulsifiers have an antimicrobial property (Nabilah et al., 2020). During the emulsification process, the hydrophilic group of emulsifier binds with water or the wall material and the hydrophobic group binds with the FO. The concentration of the emulsifier and hydrophile–lipophile balance influence the stability of the emulsion, as well as the encapsulation efficiency (Liu and Yang, 2011; Rosen and Kunjappu, 2012; Yang et al., 2020). For the preparation of FO encapsulation, emulsifier Polysorbate 80 known also as Tween 80 (Thirundas et al., 2014) and soya lecithin (Gallardo et al., 2013) were used by several researchers.

3.2.4. Characterization of microencapsulated flaxseed oil

Several physical and biochemical aspects were considered to characterize FO microcapsules. The physical and biochemical properties include particle size, particle morphology, color, moisture content, water activity, oxidative stability, encapsulation efficiency, and the release of bioactive compounds from the matrix (Barroso et al., 2014; Can Karaca et al., 2013). These properties of FO microcapsule depend on the type of matrix, ratio of oil and matrix or wall component, and type and amount of the emulsifier. Furthermore, the technology of microencapsulation preparation and operational parameters influence the characteristics of the FO microcapsule. The most important characteristic of the encapsulation of FO is the encapsulation efficiency, which is generally estimated by measuring the surface oil and total entrapped oil. Sometimes, high-performance liquid chromatography (HPLC) is used for this purpose (Onsaard and Onsaard, 2019). The mean particle size and their distribution is generally evaluated by the dynamic light scattering analytical instrument (Mourtzinou and Biliaderis, 2017). The particle morphology and size are measured by electron microscopy. The moisture content influences the shelf life of the microcapsule and is measured by the

evaporation of water. The moisture analyzer is used for this purpose (Mourtzinis and Biliaderis, 2017; Onsaard and Onsaard, 2019). The zeta potential of a microcapsule is a good indicator to understand the stability of the microcapsule in colloid and is measured by the zeta potential analyzer (Mourtzinis and Biliaderis, 2017). Fourier transform infrared (FTIR) spectroscopy allows the understanding of the functional groups' modification of the oil, matrix, and emulsifier in the microcapsule (Mohseni and Goli, 2019; Mourtzinis and Biliaderis, 2017). The oxidation of oil and fat with the time progress is a considerable important factor since the oxidation of oil and fat changes the organoleptic property of food items. The oxidation of the encapsulated oil can be evaluated by determining the peroxide value, oxidation induction period, and thiobarbituric acid reactive substances (TBARS) (Onsaard and Onsaard, 2019). Bulk density, tap density and flowability properties play an important role in powder handling. Bulk density is the ratio of mass to volume of powders, while tap density is the ratio of mass to volume after tapping of the powder. High bulk density is desired during handling, as it signifies that large mass of powder can be stored in a small volume container. This also ensures higher stability, as it removes air in the spaces between particles. The Hauser ratio is used to determine flowability and Hausner ratio was used to determine the Cohesiveness (Santomaso et al., 2003). An overview of the FO microencapsulation process and characterization of the microcapsule in terms of the oil content, particle size, encapsulation efficiency, moisture content, and oxidative stability are represented in Appendix 2.

3.3. Applications of microencapsulated flaxseed oil

The application of microencapsulated ingredients, such as FO in food formulations has improved product development by overcoming limitations associated with sensory properties and stability under unfavorable environmental conditions.

The study of Beikzadeh et al. (2020) has compared the properties of breads enriched with FO encapsulated in β -glucan and *saccharomyces cerevisiae* yeast cells. The reported results were that encapsulation has significantly improved dough rheological properties, firmness and density, and decreased lightness. Bread containing FO encapsulated in yeast cells showed a lower peroxide index and a higher α -linolenic acid value than two other samples containing oil.

A similar study of Kairam, Kandi, and Sharma (2021) investigated bread properties after fortification with encapsulated FO, garlic oil, and FO + garlic oil hybrid microcapsules. It was documented that microencapsulation of FO, garlic oil, and FO + garlic oil has

significantly improved the oxidative stability of these oils in fortified bread. The sensory evaluation showed a positive intention of consumers to accept and buy the fortified bread. Encapsulated FO has been also incorporated in some dairy product such as market milk giving an acceptable oxidative and storage stability. The study of Gowda et al. 2018 has investigated the supplementation of microencapsulated FO for the fortification of α -linolenic acid in ice cream. The fortified ice cream has showed stable oxidative proprieties and acceptable organoleptically attributes during the storage period.

Another application was also studied by Bolger et al, 2018 who investigated the use of microencapsulated FO in sausages. Since meat products are often high in saturated fat and can lack essential ω -3 fatty acid. microencapsulation of FO can offer a good strategy to enrich meat products with ω -3 fatty acid while minimizing the impact on sensory characteristics and product quality. During this study it was observed that method of FO incorporation and encapsulation technique had more significant impact on the sausages' physical characteristics compared to direct or pre-emulsified oil addition.

Also, a similar study by Jafari et al, 2019 has investigated the use of microencapsulated FO in mayonnaise. It was documented that mayonnaise formulated with microcapsules had good stability and texture throughout storage. An improvement of the oil's dispersibility in the water phase was also observed, leading to a more homogenous product. This ability to incorporate FO without compromising texture can pave the way for the development of measurable fat spreads and dressings with a similar texture.

4. MATERIALS AND METHODS

4.1. Materials

4.1.1. Flaxseed oil

FO was selected for the process of microencapsulation employing both SD and FD techniques mainly because of its abundant presence of ω -3 fatty acids, notably α -linolenic acid (ALA). The cold-pressed FO was purchased from a local shop in Hungary. Its composition per 100 ml comprised 100 grams of fat, consisting of 10 grams of saturated fatty acids, 20 grams of monounsaturated fatty acids, and 70 grams of PUFAs.

4.1.2. Wall materials

Maltodextrin (MD) with dextrose equivalent (DE)=19 was purchased from Buda Family Kft and Gum arabic (GA) was purchased from Bi-Bor Kft. High amylose maize modified starch (MS) was also used as wall material in emulsion formulation.

4.1.3. Emulsifier

Soya lecithin was purchased for a local shop in Hungary.

4.1.4. Solvents and chemicals

Hexane was used to extract oil from the surface of microcapsules. It was purchased from (Sigma Aldrich, France). Milli-Q ultrapure deionized (DI) water (18.2 M Ω ·cm) used in all experiments, was obtained from Milli-Q Synergy/Elix water purification system (Merck-Millipore, France). For the ME machine cleaning, Ultrasil P3- 11 and Citric acid were used. Ultrasil P3-11 was purchased from Ecolab-Hygiene Kft (Ecolab-Hygiene Kft, Budapest, Hungary) while Citric acid (99%) was purchased from Reanal Kft (Reanal Kft, Budapest, Hungary). Thiobarbituric acid (TBA), and trichloroacetic acid (TCA) were obtained from (SIGMA, Germany). Solvents, such as methanol and ethanol, were purchased from (Sigma Aldrich, USA).

4.2. Methods

4.2.1. Preparation of the emulsion through membrane emulsification

4.2.1.1. Membrane emulsification apparatus setup

All emulsions had total solid material equal to 30% (w/w) and wall materials were dissolved in water under magnetic stirring one day before emulsification.

Emulsions were produced utilizing a continuous, crossflow specialized laboratory apparatus for ME, developed at the Department of Food Engineering within the Hungarian University of Agriculture and Life Sciences, Faculty of Food Science. The device includes a vessel for measuring the dispersion phase (25 ml) and a reservoir for the continuous phase (1000 ml). This emulsification apparatus was used with a tubular ceramic membrane (PALL Austria Filter GmbH) composed of α - alumina with 1,4 μm pore size and an active membrane surface area of 50 cm^2 . To enhance emulsion quality in terms of droplet size distribution and stability, a turbulence static promoter from stainless steel (SS316) takes the form of a double-helix-shaped ribbon reducer (helix reducer) (**Figure 9**), was integrated into the membrane module. Its dimensions are 5.8 mm in width, 1.6 mm in thickness, with a spiral turn length of 24 mm (Koris et al., 2011).

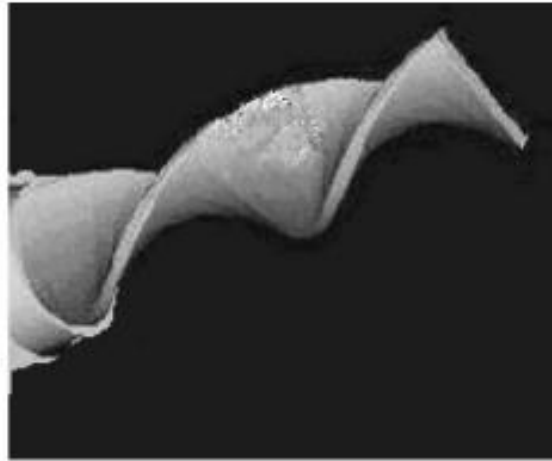


Figure 9. Geometry of the helix reducer (Koris et al., 2011).

The wall material was dissolved in the continuous phase (water) and FO was pressed through the membrane pores with a pressure of 2 bars and dispersed into the continuous phase to create the emulsion. During the emulsification process the recirculation flow rate of the continuous phase was 150 $\text{dm}^3 \text{h}^{-1}$ with a velocity of 1.08 m s^{-1} .

In ME knowing the flux is important as it can affect the droplet size and distribution. So, to understand the behavior of the dispersed phase, the flux was measured during the emulsion preparation process. This involved recording the time it took for the oily phase (dispersed phase) once added to the vessel to disperse throughout the mixture using a stopwatch.

The dispersed phase flux ($\text{dm}^3 \text{m}^{-2} \text{h}^{-1}$) through the membrane is determined as follow:

$$\text{Flux } (J_d) = \frac{G_d}{\rho \cdot A} \quad (1)$$

where A is the membrane surface area (50 cm^2), ρ the dispersed phase density, and G_d the mass flow rate of the dispersed phase through the membrane determined from the stopwatch. According to Darcy's law J_d is related to the transmembrane pressure ΔP_{tm} as follow:

$$J_d = \frac{K \Delta P_{tm}}{\eta L} \quad (2)$$

where K is the membrane permeability, L the membrane thickness, and η the dispersed phase viscosity.

The experimental setup, depicted in Figure 10 below is described as follow:

- The temperature of the continuous phase within tank (1) can be adjusted using a thermostat, facilitating the maintenance of membrane moisture and temperature regulation.
- A pump (4) facilitates the circulation of the continuous phase, drawn from a 1 dm^3 feed tank (1), within the membrane module.
- Monitoring of the recirculated volume of the continuous phase is done through a rotameter (7).
- Compressed air, sourced from a compressor (5), pressurizes the dispersed phase extracted from a separate tank (2).
- Pressure gauges (6) positioned on either side of the membrane (3) gauge the transmembrane pressure difference.
- A pressure control valve (8) regulates the pressure of the dispersed phase on the outer side of the membrane.
- The final emulsion exits through drain valves (9).

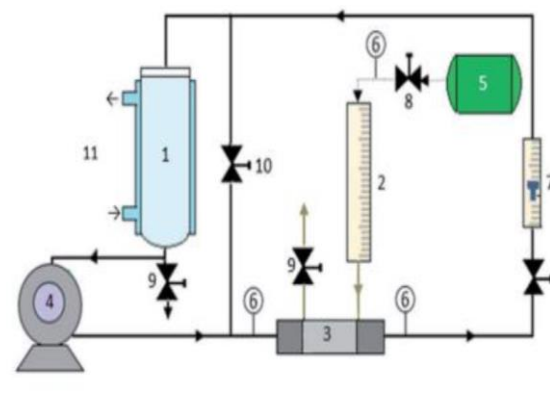


Figure 10. Experimental set-up of ME (Koris et al., 2011).

4.2.1.2. Apparatus cleaning procedure

The apparatus and the membrane have been cleaned before and after each use. It involves placing the membrane in a module and running five cleaning cycles as follow:

- Cycle 1 (water): Cleaning with deionized water for 45 minutes at a pressure of 2 to 4 bar and a flow rate of 200 L/h as measured by the rotameter.
- Cycle 2 (ultrasil 1%): Cleaning with a heated (70°C) solution of 15g ultrasil in 1.5L water for 45 minutes.
- Cycle 3 (water): Removing ultrasil residue with deionized water for 45 minutes.
- Cycle 4 (citric acid 1%): Cleans with a heated (70°C) solution of 15g citric acid in 1.5L water for 45 minutes.
- Cycle 5 (water): Removing citric acid residue with deionized water.

In order to verify the membrane cleanliness, the final step in the cleaning process is assessing the membrane integrity through the measurement of water flux as a function of transmembrane pressure. To achieve this, at the beginning of each experiment, the flux of deionized (DI) water is determined. This value serves as a direct indicator of membrane permeability and, consequently, the effectiveness of the preceding cleaning procedure. In order to do this, we have to collect a specific volume of permeate and record the corresponding time using a stopwatch. Subsequently, the water flux was calculated using equation (1). As dictated by equation (1), increasing the driving force leads to an enhancement in water flux. Therefore, during the flux measurement, the transmembrane pressure was systematically increased in increments of 0.5 bar, ranging from 1 bar to 3 bar. Additionally, a constant flow rate of 200 L/h was maintained using a rotameter. Following the measurements, the obtained flux values were plotted against the corresponding transmembrane pressure values. A linear trendline with a zero-point intercept was then fitted to the data points. A correlation coefficient exceeding 0.96 signifies a successfully cleaned membrane. Conversely, if this criterion is not met, the cleaning process must be repeated until it is.

4.2.2. Preparation of the emulsion through the rotor-stator homogenization

Oil-in-water emulsions were prepared by the addition of FO (dispersed phase) dropwise to the wall material solutions (continuous phase) under high shear. The homogenization process was carried out using a rotor-stator homogenizer (T25 digital ULTRA-TURRAX, Hungary) equipped with a dispersing shaft made of SS 316L stainless steel. The homogenization speed was set to 15,000 rpm for a duration of 5 minutes (Figure 11).



Figure 11. Rotor-Stator Homogenizer device

4.2.3. Spray drying

Microencapsulation was achieved using a laboratory-scale spray dryer (LabPlant SD-05, Hungary) equipped with a 0.5 mm diameter nozzle (Figure 12). During the SD process, the emulsions were continuously stirred using a magnetic stirrer to ensure homogeneity. Compressed air pressure was set to 3.6 bars to facilitate atomization. An inlet air temperature of $185 \pm 5^\circ\text{C}$ and an outlet air temperature of $105 \pm 5^\circ\text{C}$ were employed. An airflow rate of $74 \text{ m}^3/\text{h}$ was maintained throughout. The resulting microcapsules were collected from the dryer's collection chamber and stored in a dark environment until further analysis.



Figure 12. Spray drying apparatus.

4.2.4. Freeze drying

This process was carried out using a freeze-dryer (ScanVac, coolsafe, 110-4 apparatus, Labogene, Lillerod, Denmark) located in the Department of Food Chemistry and Analytics of MATE (Figure 13). As a first step the emulsions were put to freeze for 24 hours at -40°C to promote solidification. Subsequently, a lyophilization process was employed in which the emulsions were maintained at a constant temperature of -109°C and a vacuum pressure of 12 Pa for a duration of 24 hours. Finally, after FD, the samples were manually ground into a fine powder.



Figure 13. Freeze drying apparatus

4.2.5. Emulsions preparation for the pilot study

In this study I have investigated the potential of multiple combinations of wall materials for FO encapsulation. ME was employed as emulsification technique and SD as the drying method. During this investigation, I have incorporated GA for its superior emulsification properties, MD for its coating benefits and cost efficiency and MS for added stability and emulsifying property. Soya lecithin (SL) was used as emulsifier in all formulation. The solid content of O/W emulsions was kept at 30% w/v for all formulations (Table 4). Subsequently, a detailed characterization of the resulting particles was conducted which focused on key aspects including morphology, PSD, and overall stability, which are crucial factors influencing the encapsulation efficiency. By understanding these characteristics, it becomes clearer and easier to optimize the wall material combinations for specific applications depending on available conditions and desired results. For instance, if a longer shelf life is

desired, prioritizing materials with better oxidation resistance might be necessary. In the other hand, if cost is a major concern, formulations with a higher concentration of MD might be preferred.

This investigation can help in optimizing the FO encapsulation which can lead to a more stable and shelf-life extended product and thus, can have significant implications for the food industry, allowing the development of novel functional foods with enhanced health benefits.

Table 4 : Description of formulations for emulsion preparation

Emulsion Combinations				
	GA-MS	MD-GA	MD-GA-MS-1	MD-GA-MS-2
MD (g)	0	48.7	58.4	75
GA (g)	116.8	97.35	58.4	75
MS (g)	29.2	0	29.2	37.6
SL (g)	5	5	5	5
FO (g)	65	65	65	21.4
DI water (g)	500	500	500	500
Solid % w/v^a	30	30	30	30
O/W Ratio (g/g)^b	0.43	0.43	0.43	0.43
Wall material /Oil ratio (g/g)	2.2	2.2	2.2	8.8
Oil load %	30	30	30	10

^aSolid content in emulsion including FO.

^bRatio between dispersed phase and continuous phase.

MD: maltodextrin, GA: Gum Arabic, MS: Modified starch, and FO: Flaxseed oil, SL: Soya lecithin.

4.2.6. Experimental design

To design the experiments the software Design-Expert 13.0.1.0. was used. Response surface methodology RSM was applied to investigate the effect of different formulation on the encapsulation efficiency. 3 factor – 3 level Box-Behnken experimental design was used.

The response surface method (RSM) is a combination of experimental design, statistics, empirical modelling, and mathematical optimization techniques used to improve the performance of processes and products. The use ensures the adoption of a more direct and economical strategy. The number of tests to be performed is determined in a rational way,

which avoids redundant information and facilitates time management and cost control. Also, the implementation of an optimization procedure makes it possible to study the interactions between the different factors (Bas and Boyaci, 2007).

This design based on the response surface method is the most commonly used in this type of experiment. It consists in modelling the results in the form of second-degree polynomial functions which is a quadratic model. Thus, the observed response Y can be expressed as a function of the other explanatory variables in addition to the measurement error ϵ (Bas and Boyaci, 2007):

$$Y = f(X_1, X_2, \dots, X_i) + \epsilon$$

To estimate the function f, we consider that it can be written in the form of a polynomial of second degree:

$$Y = a_0 + \sum a_i X_i + \sum a_{ii} X_i^2 + \sum a_{ij} X_i X_j$$

$$Y_{TL} = a_0 + a_1 X_1 + a_2 X_2 + a_3 X_3 + a_{11} X_1^2 + a_{22} X_2^2 + a_{33} X_3^2 + a_{12} X_1 X_2 + a_{13} X_1 X_3 + a_{23} X_2 X_3$$

Where:

a_i : linear effects regression coefficients.

a_{ii} : regression coefficients of quadratic effects.

X_i and X_j : coded experimental variables.

For the optimization of the encapsulation efficiency, three independent variables were used and were coded according to Table 5 to facilitate the analysis. These variables are the ratio MD/GA (X_1) between MD and GA ranging from 0 to 1, the concentration of MS in wall material (X_2) from 0 to 40% (w/w), and FO content (X_3) from 10% to 40% (w/w).

Table 5 : Coding of independent variables

Variable	Coded X_i	Coded level		
		-1	0	1
Ratio between maltodextrin and gum arabic (MD/GA)	X_1	0	0.5	1
Concentration of modified starch in wall material (MS%)	X_2	0	20	40
FO content %	X_3	10	25	40

This level selection is based on the literature review regarding the used amounts of wall materials and the content of oil in the encapsulation efficiency process while considering factors like stability, oxidative resistance, and physical properties of wall material and the expected produced microcapsules. The lower and upper limits were selected in a way to

provide a view covering a wide range of different scenarios investigating the limit condition in order to obtain the optimal combination in this defined range for achieving high encapsulation efficiency. 0,02% of soya lecithin was used in all formulation and was kept invariant to not affect the assessment of the effect of varying the wall material and flaxseed oil content in encapsulation efficiency and to not alter the optimization of the process.

Ratio between MD/GA (X1): 0 represents excluding maltodextrin and 1 means that same content of GA and MD was used. GA was considered in all formulations as it is the main area of my study and an essential component in producing microcapsules in both spray drying and freeze-drying technologies due to its film forming and emulsifying properties. In addition, producing microcapsules with only maltodextrin is tricky and can provide unsatisfactory results.

Concentration of modified starch (X2): 0% represents no MS, allowing the study of the baseline efficiency without it. 40% is a reasonable upper limit for the concentration of MS in the wall material because any higher value might lead to issues like weak capsules due to excessive rigidity.

Flaxseed oil content (X3): 10% is a low enough concentration to ensure successful encapsulation and avoid issues like capsule formation problems due to insufficient oil droplets to encapsulate. 40% represents a relatively high oil content, pushing the limits of efficiently encapsulated.

Since our primary interest is understanding the interaction between factors and their quadratic effects on the response as encapsulation efficiency, a full factorial analysis was not necessary. And the identification of the main effects of individual factors was based on the literature studies in order to provide details and information needed to pick the different factors and their ranges. In this regard, direct estimation of quadratic effects was offered by adopting Box-Behnken design as efficient approach offering this possibility without requiring a full factorial analysis before. Our study made strategic use of a Box-Behnken design. This method shortened the experiment by allowing for direct calculation of quadratic effects, eliminating the requirement for a complete factorial analysis beforehand. The Box-Behnken design was chosen over its central composite equivalent, largely to avoid unworkable combinations. For example, employing exceptionally high MD levels may cause issues during the drying process. Furthermore, the Box-Behnken design uses fewer experimental runs than a central composite design with the same number of variables. This

efficiency is especially useful when working with expensive substances or time-consuming studies.

4.2.7. Emulsion characterization

4.2.7.1. Emulsion stability

Phase separation

Emulsion stability was evaluated through phase separation. 25ml of emulsion was poured into a graduated cylinder and was kept for 24 hours at room temperature. The upper phase formed was then measured and used for the calculation of separation's percentage according to the following formula:

$$S\% = \left(\frac{H_{up}}{H_i} \right) \times 100 \quad (3)$$

where H_{up}: height upper phase; H_i: emulsion initial phase, S%: Separation, %

Zeta potential

A Malvern Zetasizer located in the department of food engineering at MATE was used to measure the zeta potential of oil-in-water emulsion. Zeta potential is crucial for understanding emulsion stability and reflects the tendency of dispersed particles to aggregate, with values above ± 30 mV indicating good stability.

Adequate cuvettes (DTS1060) were used. The process involved careful loading of the emulsion into the cuvette, avoiding electrode contact and air bubbles. The cuvette was then sealed and illuminated by a laser within the Zetasizer to measure electrophoretic mobility. Measurements occurred at a constant 25°C with 120 seconds of equilibration. Triplicate measurements were performed with fresh samples for data reliability.

4.2.7.2. Droplet sizing

Droplet size and dispersion were promptly assessed following emulsion preparation through two laser diffraction techniques in triplicate measurements.

Approach 1 / Laser Diffraction Technique 1:

Fritsch Analysette 22: A wet dispersing apparatus located in the Department of Food Process Engineering at MATE was used. Operating on laser diffraction principles, this instrument is adept at scanning emulsions, suspensions, and aerosols. The following measurement protocol was adapted:

1. Sample Preparation: Emulsions were diluted with distilled water in the 100 ml transparent glass container of the apparatus, enabling visual monitoring during the process.

2. Calibration: The device underwent calibration using a small quantity of circulated distilled water.

3. Sample Measurement: An adequate volume of the prepared emulsion was introduced via the dosing opening using a pipette until achieving desired absorbance.

4. Cleansing: following each measurement, the apparatus was flushed with a mild degreasing solution. Additionally, a methanol rinse was conducted every 4-5 measurements.

Data Evaluation: For emulsion specimens, the geometric mean diameter (GMD) in μm and the span value were determined. The span value provides details regarding the size distribution through the following equation:

$$\text{Span} = \frac{D_{90} - D_{10}}{D_{50}} \quad (4)$$

Where, D_{10} correspond to the value of particle diameter below of 10% of the particle diameter of the whole sample.

D_{50} correspond to the value of particle diameter below of 50% of the particle diameter of the whole sample.

D_{90} is the value of particle diameter below of 90% of the particle diameter of the whole sample.

Approach 2 / Laser Diffraction:

Bettersize ST: This technique employed a Bettersize ST laser particle size analyzer (LAB-EX, Laborkereskedelmi Kft., Hungary).

Measurement Protocol:

1. Sample Preparation: A small quantity of emulsion was suspended in water under agitation.

2. Measurement: The droplet size distribution was monitored until consecutive readings stabilized.

3. Cleansing: Following each measurement, a washing cycle with methanol was executed.

Data Evaluation: Both methods are based on laser diffraction to determine droplet size and distribution and the choice of method may depend on specific needs and available instrumentation. The Fritsch Analysette 22 offers a wider size measurement range and a dedicated wet dispersing unit, while the Bettersize ST provides Sauter and volume mean diameter measurements. The droplet mean diameter was expressed utilizing both the Sauter mean diameter $D_{[3,2]}$ and the volume mean diameter $D_{[4,3]}$. The span value was also determined.

4.2.7.3. Morphological analysis of emulsion droplets

Characterization of emulsion droplets was carried out through optical microscopy technique

that was employed to evaluate the size, shape, and overall morphology of the emulsion droplets. The analysis was carried out through a microscope (DELTA OPTICAL, USA) located in the Department of Food Engineering at MATE equipped with oil immersion objectives for enhanced resolution at high magnification ($\times 100$). The microscope was linked to a dedicated image analysis software.

Following preparation, emulsion samples were poured out onto microscope slides which were then covered with glass coverslips to minimize evaporation and facilitate clear observation. Digital images of the droplets were captured using a camera integrated with the microscope.

Evaluation of droplet size distribution was achieved by measuring a statistically significant number of randomly selected individual droplets using the microscope's image analysis software. This software offers the advantage of automated image analysis, ensuring accurate and consistent size data across all samples.

4.2.8. Microcapsules characterization

4.2.8.1. Encapsulation efficiency

For the evaluation of encapsulation efficiency, 15mL of Hexane were added to 2g of powder at room temperature and shaken for 2 min in order to extract the surface oil. Then, using a Whatman No.1 filter paper, the solvent mixture was filtered and the powder that remained on the filter was rinsed three times with 20mL of Hexane. The filtrate solution was put in the oven and left at 60 C temperature for the solvent to evaporate. When constant weight was reached the difference between the empty flask weight and the final flask weight containing the extracted oil residue was determined and considered as the surface oil content. Total oil content was assumed to be the same as the initial oil content in powder.

Microencapsulation efficiency was then calculating using the following formula:

$$EE\% = \left(\frac{m_{\text{Total oil}} - m_{\text{Surface oil}}}{m_{\text{Total oil}}} \right) \times 100 \quad (5)$$

4.2.8.2. Moisture content

Moisture content can affect the storage stability of microcapsules. In fact, high moisture can promote microbial growth and possibly lead to product spoilage. For this reason, during microencapsulation process, it is very important to maintain an accurate moisture content as it is primordial for ensuring optimal product quality, and extended shelf life. (Premi, M., and Sharma, R., 2017). For the determination of moisture content, 1g of powder was placed in a

vacuum oven at 70°C until constant weight was reached, then calculating is done using the following formula:

$$\text{Moisture content \%} = \left(\frac{m_{\text{initial}} - m_{\text{final}}}{m_{\text{initial}}} \right) \times 100 \quad (6)$$

4.2.8.3. Bulk density

Bulk density (BD) was measured according to the protocol of Getachew and Chun., 2016 in which 1g of powder was put in a 20ml graduated cylinder and was gently tapped to collect the powder sticking at the wall of the cylinder. The height of powder after being tapped by hand on a bench 50 times from a height of 10 cm was measured and expressed as g/mL.

$$\text{BD} \left(\frac{\text{g}}{\text{mL}} \right) = \frac{\text{Mass}}{\text{Volume}} \quad (7)$$

4.2.8.4. Tapped density

Tapped density (TD) was measured according to the protocol of (Goula and Adamopoulos, 2008) with some modification. 1 g of powder was put in a 20ml graduated cylinder and then was repeatedly manually tapped by lifting and dropping it under its own weight from 5 cm height until a negligible difference in volume between successive measurements was observed.

$$\text{TD} \left(\frac{\text{g}}{\text{mL}} \right) = \frac{\text{Mass}}{\text{Tapped volume}} \quad (8)$$

4.2.8.5. Flowability and Cohesiveness

Flowability of the powders was evaluated in terms of Carr Index (CI) and was assessed from the value of the bulk density and tapped density.

$$\text{CI}(\%) = \frac{\text{TD} - \text{BD}}{\text{BD}} \times 100 \quad (9)$$

Cohesiveness of the powders was evaluated in terms of Hausner ratio (HR) and was assessed from the value of the bulk density and tapped density.

$$\text{HR} = \frac{\text{TD}}{\text{BD}} \quad (10)$$

4.2.8.6. Powder wettability

According to Fuchs et al, (2006) method, powder wettability was calculating as follow: 1g of powder was added to 100 mL of distilled water at room temperature without agitation. The duration of time that took the powder to sediment below the surface of water was measured.

4.2.8.7. Morphological study by scanning electron microscopy (SEM)

Scanning electron micrographs were made with a JEOL 5500 (JEOL, Japan) electron microscope located in the Department of Inorganic and Analytical Chemistry of Budapest

University of Technology and Economics in high vacuum mode with a secondary electron detector. Powder samples were fixed onto double-sided sticky tape mounted on SEM stubs. The samples were coated with gold and platinum (60:40) for 10 min with a 10-mA plasma current.

4.2.8.8. Particle size distribution

The Bettersize ST laser particle size analyzer (LAB-EX, Laborkereskedelmi Kft., Hungary) was used to determine the PSD of the samples following the same protocol as initially done for emulsion droplet size analysis, under continuous agitation, small quantity of FO powder was carefully suspended in anhydrous ethanol. The instrument continuously monitored the PSD during measurement until consecutive readings achieved consistent values and providing stable measurement. The analysis gave result of two key parameters: the Sauter mean diameter $D_{[3,2]}$ and the volume mean diameter $D_{[4,3]}$. As previously described in the section on emulsion droplet size analysis, the span value was utilized to quantify the width of this distribution.

4.2.8.9. Solubility

Solubility was determined by solving 1 gram of powder in 25 ml distilled water with gentle stirring. The solutions were then filtered through Whatman paper No. 42 and the filter papers and residues were put to dry in an oven at 105°C for three hours and then were cooled and weighed. The solubility percentage then was calculated using equations:

$$\text{Solubility \%} = 100\% - \text{Residue\%} \quad (11)$$

Residue% is determined as follow:

$$\text{Residue\%} = \frac{m_{\text{filter paper and residue}} - m_{\text{weight of filter paper}}}{m_{\text{sample}}} 100\% \quad (12)$$

4.2.8.10. Oxidative stability of flaxseed oil

The study of oxidative stability of encapsulated FO was examined through the determinations of thiobarbituric acid-reactive substances (TBARS). Samples were stored for one month in a dark storage at room temperature before analyzing. To assess lipid oxidation, a modified version of the TBARS method described by Tarladgis et al. (1960) was utilized; 4g of FO powder for the capsules measurements and 1 ml of FO for bulk oil measurement, was placed in mixing tubes and homogenized with 15 ml of distilled water using a Digital Ultra-Turrax Disperser (Germany). Then 5 ml of 25 % trichloroacetic acid (TCA) was added to the homogenized mixture to precipitate proteins. The mixture was then centrifuged in 50-

ml polypropylene conical centrifuge tubes at 5000 rpm for 10 min. After the filtration 3.5 ml, was added to 1.5 ml of 0.6 % w/v thiobarbituric acid (TBA) (0.02 M) This mixture facilitates the formation of colored TBARS complexes, which indicate the presence of lipid oxidation products. The tubes were then kept in a water bath at 100 °C for 30 minutes to promote TBARS formation. The solution was cooled, and the absorbance was measured at 532 nm using a Spectrophotometer (U-2900 Hitachi Ltd., Japan) against a blank. TBARS were expressed as malonaldehyde (MDA) mmol/kg of FO.

4.2.9. Statistical analysis

To perform the statistical analysis IBM SPSS (v 29.0.1.0, Armonk, NY: IBM Corp) was used. All measurements were done in triplicate and the mean value with standard deviation was calculated. One-way analysis of variance (ANOVA) and one-way multivariate analysis of variance (MANOVA) followed by the Tukey's post hoc test were performed, and the differences between different groups were considered significant when $P < 0.05$.

5. RESULTS AND DISCUSSION

5.1. Wall materials and oil load impact on encapsulation results: pilot study

5.1.1. Size and morphology study

Microscopic observations revealed well-defined spherical encapsulated droplets in all formulations which are visible in Figure 14, illustrates the size and morphology of the four emulsion formulations. The average droplet size for each emulsion type was determined by measuring multiple randomly selected individual droplets. Formulation containing only GA and MS as wall material, exhibited the smallest average droplet diameter value (approximately 14 μm) in Figure 14.A. Conversely, the emulsions containing MD displayed the largest average droplet diameter (around 21 μm).

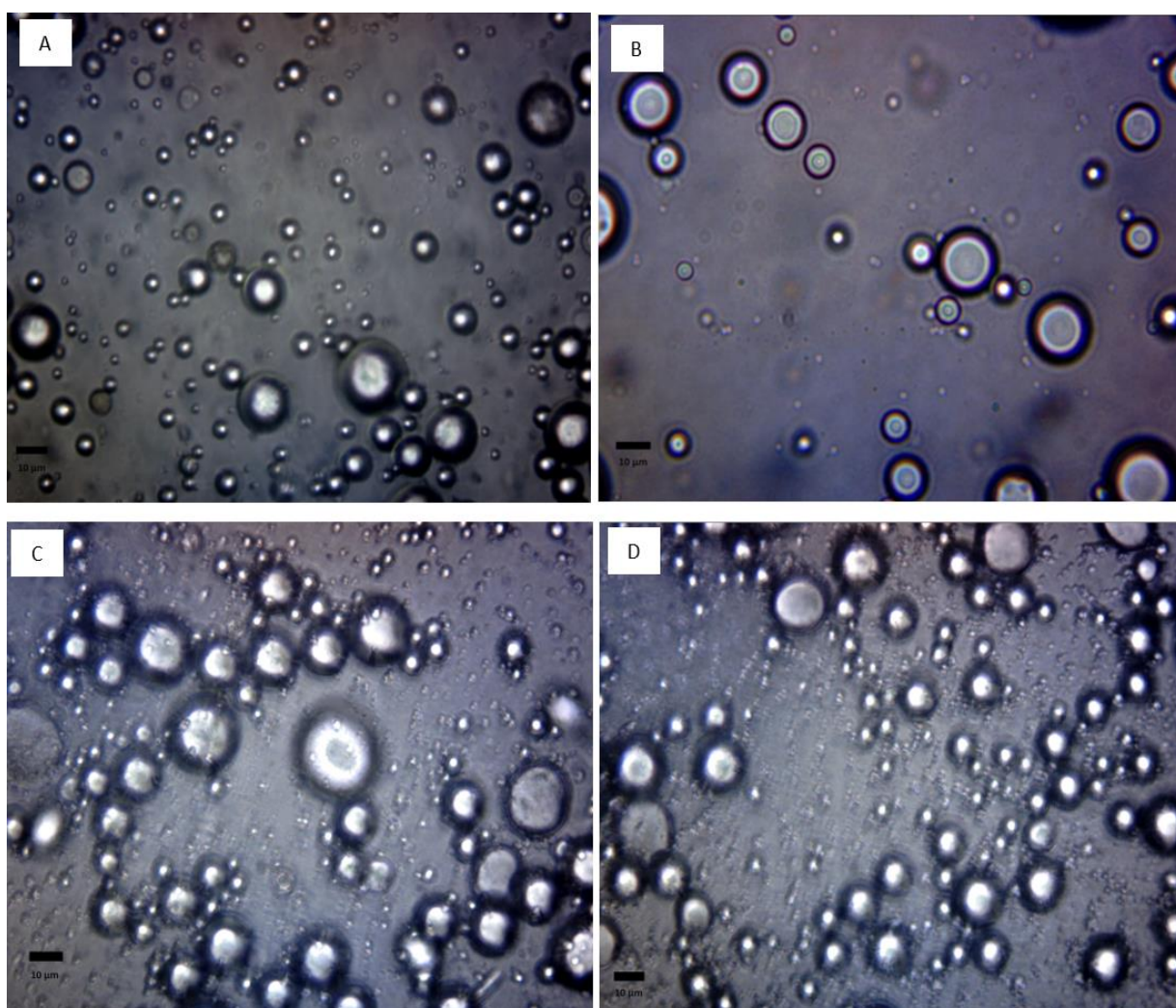


Figure 14. Microscopic observations of emulsions.

Where A: GA-MS / B: MD-GA-MS-2 / C: MD-GA/ D: MD-GA-MS-1

These observations align with established knowledge regarding the influence of formulation parameters on emulsion properties and particularly the well-known relationship between

membrane pore size and droplet size. Generally, a linear scaling law has been observed between these two parameters, with a slope typically ranging from 2 to 10. However, literature reports values as high as 50 in some cases (Vladislavljević, G. T. (2019)).

To gain a comprehensive understanding of the relationship between wall material composition and droplet size distribution, the average droplet diameter ($D_{[4,3]}$) and span values for each emulsion formulation (GA-MS / MD-GA/ MD-GA-MS-1/ MD-GA-MS-2) were determined and summarized in Table 6. The aim is to investigate the impact of varying the ratios of MD, GA, and MS as wall materials as well as the impact of reducing the FO load on the droplet size and distribution characteristics of our oil-in-water emulsions prepared using ME.

Table 6: Droplet size and span measurements

Emulsion	GA-MS	MD-GA	MD-GA-MS-1	MD-GA-MS-2
$D_{[4,3]} \mu\text{m}$	17.94 ± 0.14^a	19.62 ± 0.13^c	23.34 ± 0.17^d	18.57 ± 0.15^b
Span	0.67 ± 0.02^b	0.74 ± 0.03^c	0.84 ± 0.02^d	0.53 ± 0.04^a

Where, MD: maltodextrin, GA: Gum Arabic, MS: Modified starch, and FO: Flaxseed oil. GA-MS / MD-GA/ MD-GA-MS-1/ MD-GA-MS-2 are the emulsion identification depending on the material and oil load used. Results are represented by mean value with standard deviation (\pm values). In superscript, dissimilar alphabet represents the significant difference between different groups of wall materials composition within diameter ($D_{[4,3]}$ μm) and span, separately (horizontal way), interpretation is performed with MANOVA, with the output of Wilks' Lambda ($p < 0,001$) and evaluated by the Tukey's HSD post hoc method.

The analysis revealed a clear trend in which formulations containing MD (MD-GA, MD-GA-MS-1) exhibited progressively larger average droplet diameters with the increase of MD in the formulation. In this regard, formulation GA-MS, which lacked MD entirely had the lowest average size diameter. Formulation MD-GA-MS-2 in the other hand did not follow this rule even though it had the highest amount of MD, the average droplet size was lower than MD-GA-MS-1 and MD-GA. This can be attributed to the lower concentration in oil (10%) compared to the other 3 formulations. This aligns with the findings of Tonton et al, 2012, in which while studying the effect of oil load in microencapsulation found that the higher oil concentration is, the higher droplet mean diameter are obtained for all of the wall materials used. This can be attributed to the higher amount of wall material for the same total solids content in the emulsion containing less oil. Which leads to an effective emulsification

by fully covering the droplets and exhibiting higher emulsifying properties that can protect the oil droplets from flocculation and coalescence. Another explanation can be the increase of emulsion viscosity with the decrease of the oil content. In fact, while the interplay between different wall materials can be complex and that the increase of viscosity is generally associated to larger droplets in ME (Alam et al., 2015), this higher viscosity in our case could have potentially created resistance during the emulsification process, limited the sedimentation or creaming of the particles, leading to enhanced emulsion stability, and preventing droplet coalescence. Formulation MD-GA-MS-1, with MD content of 58.4g, displayed the largest average droplet size. This observation aligns with findings from Alam et al. (2015) in which it was reported that increasing the concentration of bulking agents in ME may lead to larger droplets in the emulsion. Studies like (Li et al., 2010) suggest that specific combinations of wall materials can influence interfacial properties, potentially mitigating the viscosity effect on droplet size. This explains why usually MD and GA are used in combinations. Furthermore, the span values can give an insight on the dispersity of droplet sizes within each emulsion. Formulation MD-GA-MS-2 (0.53 ± 0.04) exhibited the most uniform (monodisperse) distribution, while formulation MD-GA-MS-1 (0.84 ± 0.02) had a broader size range (polydisperse). This suggests that the specific combination of wall materials in each formulation might influence the ability to stabilize droplets of varying sizes. Research by (McClements, 2017) highlights the importance of wall material interactions and their affinity for the oil-water interface in controlling droplet size distribution during ME. In our case, the specific interplay between MD, GA, and MS might influence their ability to stabilize droplets of varying sizes, contributing to the observed variations in span values.

5.1.2. Emulsions stability

Emulsion stability was studied through two different ways the first was through determining the zeta potential (ZP) of the emulsion and the second was through studying the phase separation after 24 hours.

ZP is a crucial parameter for assessing the stability of emulsions, particularly oil-in-water systems like those used for encapsulation. ZP measures the electrical charge on the surface of the dispersed droplets oil droplets. All value obtained during measurement were negative values. A highly negative ZP indicates a strong negative charge on the droplet surface which creates electrostatic repulsion between droplets. This helps preventing droplets from aggregating that leads to destabilizing the emulsion. Emulsions with a ZP of < -60 mV are

considered very stable, those with between -30 mV and -60 mV indicates moderate stability and finally those with a ZP of >-30 mV are considered unstable and prone to aggregation or flocculation, but other factors like droplet size distribution also play a significant role in studying the emulsion stability. The results of zeta-potential for the different formulations are summarized in Table 7.

Table 7: Zeta-potential measurements

Emulsion	Zeta potential
GA-MS	-37.3 ± 0.91^b
MD-GA	-34.2 ± 0.20^a
MD-GA-MS-1	-33.8 ± 0.25^a
MD-GA-MS-2	-40.6 ± 0.25^c

MD: maltodextrin, GA: Gum Arabic, MS: Modified starch, and FO: Flaxseed oil. GA-MS/ MD-GA/ MD-GA-MS-1/ MD-GA-MS-2 are the emulsion identification depending on the material and oil load used. Results are represented by mean value with standard deviation (\pm values). In superscript, dissimilar alphabet represents the significant difference between results, interpretation is performed with one-way ANOVA, and evaluated by the Tukey's

HSD post hoc method.

All four emulsions showed moderate stability. The absolute value of zeta potential in emulsion GA-MS, MD-GA, and MD-GA-MS-1 decreased with the increase of MD content which aligns with Albert et al. (2016) finding in which it was proved that low concentration of MD can positively improve the emulsion stability. Additionally, sample MD-GA-MS-2 had the highest absolute value of zeta potential, this can be explained by the lower concentration of FO that impacts positively the stability, as it was mentioned before, low oil concentration means higher amount of wall material and thus higher matrix availability to fully cover the droplets and exhibiting higher emulsifying properties that can protect the oil droplets from flocculation and coalescence and offer better stability. The ZP results are aligning with the results of separation mentioned in Table 8.

Table 8: Phase separation measurements

Emulsion	Separation %
GA-MS	11.27 ± 0.17 ^b
MD-GA	12.43 ± 0.30 ^c
MD-GA-MS-1	12 ± 0.22 ^c
MD-GA-MS-2	4.63 ± 0.15 ^a

MD: maltodextrin, GA: Gum Arabic, MS: Modified starch, SL: Soya lecithin and FO: Flaxseed oil. GA-MS / MD-GA/ MD-GA-MS-1/ MD-GA-MS-2 are the emulsion identification depending on the material and oil load used. Results are represented by mean value with standard deviation (\pm values). In superscript, dissimilar alphabet represents the significant difference between results, interpretation is performed with one-way ANOVA, and evaluated by the Tukey's HSD post hoc method.

Spontaneous breakdown of the emulsion was measured after storage on ambient temperature for 24 hours by measuring the amount of free oil with tip filter test and as it can be seen in Table 8 difference was found between the test samples. MD-GA-MS-2 proved the best stability from this aspect containing released or untrapped free oil only of 4.63% while in case of the other mixtures (GA-MS, MD-GA, and MD-GA-MS-1) this number was approximately 2.4-2.7 times higher. These results also suggests that correlation of added oil and separation % of oil after storage exists, but this fact would need further investigation in future.

5.1.3. Particle size

Size distribution analysis provides valuable insights into the physical characteristics of powders and their potential implications for encapsulation efficiency and stability. Result obtained are mentioned in Table 9. Formulation GA-MS analysis resulted an average size diameter of $65.37 \pm 0.01 \mu\text{m}$ with a span value of 2.87 ± 0.04 . Formulation GA-MS stands out by its higher concentration of GA (116.8g) along with a reasonable amount of MS (29.2g) and FO of 65g. This specific formulation showed a lower particle average size that could be due to the low average droplet size found while examining the emulsion before drying, and comparatively greater range of sizes. This wide size distribution after encapsulation process may have been due to a higher concentration of GA and the non-presence of MD known to be effective in SD which made the encapsulation less consistent. These results are corroborated by earlier study by Chen et al. (2019), which showed that emulsions containing

too much GA may produce wider size distributions, which is consistent with the observations in formulation GA-MS.

In the other hand a more balanced mixture of MD, and GA, in formulation MD-GA and of MD, GA and MS in MD-GA-MS-1, have resulted in higher average particle size of $112.06 \pm 0.03 \mu\text{m}$ and $107.90 \pm 0.10 \mu\text{m}$ respectively and lower span value of 2.65 ± 0.02 and 2.51 ± 0.01 respectively. This shows that two formulations had a somewhat narrower size distribution than GA-MS, suggesting that the encapsulation and emulsification procedures may have allowed for more control over particle size thanks to the presence of MD and MS in MD-GA-MS-2. This finding was supported by a study conducted by Patel et al. (2020), in which it was demonstrated that a well-balanced emulsion could have a narrower microcapsule size distribution because GA and MD increase stability and homogeneity.

Table 9. Particle size and span measurements

	GA-MS	MD-GA	MD-GA-MS-1	MD-GA-MS-2
D_[4,3] μm	65.37 ± 0.01^a	112.06 ± 0.03^d	107.90 ± 0.10^c	74.84 ± 0.09^b
Span	2.87 ± 0.04^d	2.65 ± 0.02^c	2.51 ± 0.01^b	2.21 ± 0.01^a

MD: maltodextrin, GA: Gum Arabic, MS: Modified starch, SL: Soya lecithin and FO:

Flaxseed oil. GA-MS / MD-GA/ MD-GA-MS-1/ MD-GA-MS-2 are the emulsion identification depending on the material and oil load used. Results are represented by mean value with standard deviation (\pm values). In superscript, dissimilar alphabet represents the significant difference between different groups of wall materials composition within diameter ($D_{[4,3]} \mu\text{m}$) and span, separately (horizontal way), interpretation is performed with MANOVA, with the output of Wilks' Lambda ($p < 0,001$) and evaluated by the Tukey's HSD post hoc method.

Microcapsules created by formulation MD-GA-MS-2 measured $74.84 \pm 0.09 \mu\text{m}$ average size diameters with a span of 2.21 ± 0.01 , making it the most homogeneous formulation and the narrowest size distribution out of all the four formulations. This formulation just like MD-GA-MS-1 was characterized by balanced mixture MD, and GA and a moderate amount of MS, but with a lower FO load. This indicates that the decreased of oil concentration may have improved the stability and consistency of the particle size.

5.1.4. Encapsulation Efficiency

The provided data in Figure 15 reveals the analysis of encapsulation efficiency (EE%) across the four formulations, exploring the potential influence of wall material composition and oil load on these results used in the ME process.

The data collected points to a possible relationship between the encapsulation efficiency and the type and quantity of wall components (MD, GA, and MS). Compared to GA-MS, which had no MD at all, formulations MD-GA, MD-GA-MS-1, and MD-GA-MS-2 showed higher EE%. MD-GA-MS-2 had the best encapsulation efficiency ($91.42 \pm 0.25\%$) while having one of the highest MD contents but also the lower oil content which also raises the question on the effect of oil load on the encapsulation process. In this regard, research by (Jafari et al., 2019) discusses the importance of optimizing the oil-to-wall material ratio for efficient encapsulation during emulsification processes. While GA-MS, MD-GA, MD-GA-MS-1 had the same oil load of 30 %, MD-GA-MS-1 had the best encapsulation efficiency which implies the better stabilization and coating potential offered by combining GA, MD, and MS which can all function as emulsifiers and stabilizers, forming a coating over the oil droplets to keep them from leaking or coalescing.

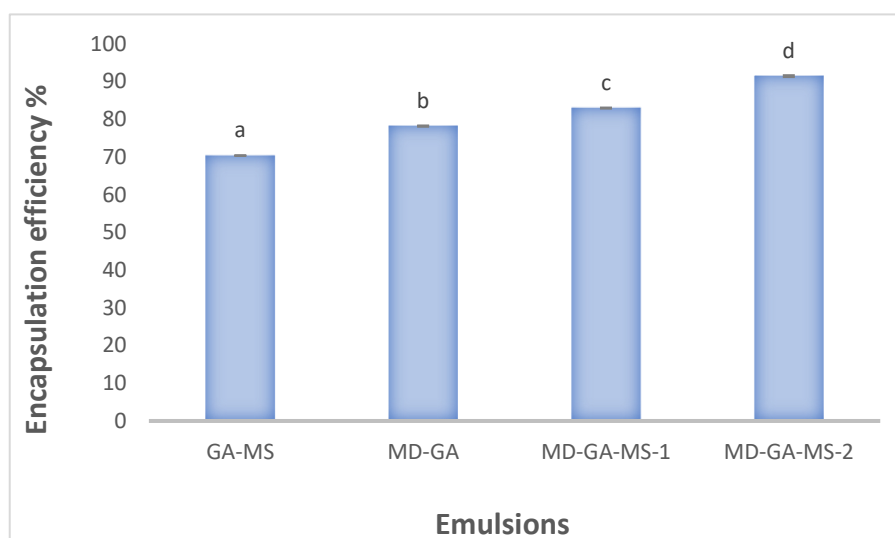


Figure 15. Encapsulation efficiency % of different formulations

MD: maltodextrin, GA: Gum Arabic, MS: Modified starch, SL: Soya lecithin and FO: Flaxseed oil. GA-MS / MD-GA/ MD-GA-MS-1/ MD-GA-MS-2 are the emulsion identification depending on the material and oil load used. Results are represented by mean value with standard deviation (\pm values). In superscript, dissimilar alphabet represents the significant difference between results, interpretation is performed with one-way ANOVA, and evaluated by the Tukey's HSD post hoc method

5.2. Discussion of the results

This work investigated the complex interactions between wall material composition (MD, GA, and MS) and oil load on the size, distribution, stability, and encapsulation effectiveness of microcapsules produced via ME and SD. Four formulations (GA-MS, MD-GA, MD-GA-MS-1, and MD-GA-MS-2) with varied proportions of these components were investigated where MD: maltodextrin, GA: Gum Arabic, MS: Modified starch, and FO: flaxseed-oil.

While studying the MD effect on encapsulation process, it was noticed that the present of MD even though it resulted in bigger droplet sizes, its capacity to improve encapsulation efficiency is notable. In this regard, there may be a trade-off between droplet size and encapsulation efficacy depending on the application,

In the other hand, formulations MD-GA-MS-1, and MD-GA-MS-2, which include a balanced mix of MD and GA, and MS, provided an effective combination. MD have enhanced the drying process by quickly forming a drying coat around the passing oil through the SD nozzle which led to efficient oil droplet coating and reducing leakage. GA has contributed to increased encapsulation efficiency by its emulsifying and film-forming capabilities. Furthermore, MS, present in all formulations, have contributed to overall stability, although its precise effect requires additional exploration.

Another important aspect that arose was the oil load as the observed tendencies indicated that a lower oil load may be beneficial for enhanced emulsion stability resulting in an effective encapsulation. Even though more research and analysis that put into account a wider range of oil concentrations is needed to reach a conclusive conclusion about its effect. This was observed in formulation MD-GA-MS-2 that had the lowest oil load resulting in obtaining the maximum encapsulation efficiency and a narrower size distribution. So, this is consistent with the idea that a larger oil-to-wall material ratio might make total encapsulation more difficult, possibly due to a lack of wall material to adequately cover all oil droplets.

This finding paves the way for additional research into improving microcapsule preparation via ME. Further investigations into Wall material interactions might be emphasized. The upcoming research should undertake the interaction effect of MD, GA, and MS on microencapsulation proprieties. Furthermore, tailoring Wall material ratios has to be taken into consideration since achieving an optimal balance between MD and GA has been proven to result optimal microcapsule quality. The impact of process parameters such as membrane pore size, pressure, and drying conditions has to be considered since they can provide additional information for fine tuning the microencapsulation process.

In conclusion, the significance influence of wall material composition, FO load on the average droplet, and the size distribution and the span values within the oil-in-water emulsions prepared via ME has been proven. The results emphasize the significant influence of wall material composition, and the FO load on the average droplet size, the size distribution and the span values within the oil-in-water emulsions prepared via ME. These findings provide good insights that can help to optimize wall material selection. Future studies could explore the specific interactions between wall materials and their impact on droplet stabilization during ME to further refine the formulation process also it would be beneficial to study the possibly adjusting ME parameters and drying parameters to achieve the desired droplet size and distribution and encapsulation efficiency for specific applications.

5.3. Optimization of FO particle using Response Surface Methodology with Box-Behnken Design

In this subchapter the details of optimization of flaxseed oil microcapsule's fabrication with different technology combinations, namely membrane emulsification-spray drying, rotor stator emulsification-spray drying, and membrane emulsification-freeze drying, are introduced.

5.3.1. Encapsulation of flaxseed oil using combination of membrane emulsification and spray drying

The experimental responses of the optimization experimental design are mentioned in the Table 10. 15 runs were conducted with a central point in order to have a clear view and to be able to optimize the encapsulation process. Our variables are the ratio between MD and GA MD/GA (X1), the concentration of MS in wall material % (X2), and FO content % (X3). These variables were coded according to Table 5 mentioned before. The encapsulation efficiency collected results indicates a possible relationship between the encapsulation efficiency and the matrix components (MD, GA, and MS).

Table 10 : Experimental responses of the optimization experimental design

Run	X1	X2	X3	EE%
1	0	-1	1	73.42
2	-1	0	1	67.35
3	0	0	0	86.33
4	-1	0	-1	72.56
5	0	0	0	86.5
6	1	1	0	77.62
7	0	-1	-1	82.9
8	1	0	-1	92.05
9	-1	1	0	67.06
10	0	1	-1	83.88
11	-1	-1	0	62.95
12	1	-1	0	79.85
13	1	0	1	76.6
14	0	1	1	74.46
15	0	0	0	87.1

Run 8 had the best encapsulation efficiency (92.05%) out of all the runs performed. This formulation had a ratio MD/GA equal to 1 and 20% of MS with only 10% of oil load which is the same formulation as formulation MD-GA-MS-2 in chapter 4.1. Run 11 in the other hand, having only GA as wall material with a FO load of 25% had the lowest encapsulation efficiency (62.95%). These results emphasize the findings that the encapsulation efficiency is inversely proportional to the FO load. In addition, it is shown that MD is essential in microencapsulation through SD to enhance the capsules protection.

To choose the correct model we need to focus on maximizing both adjusted coefficient of determination R^2 and predicted R^2 and the lack of fit should be also insignificant. For the optimization of encapsulated FO sample, a quadratic polynomial model was suggested as a fit model with an adjusted R^2 of 0.9974 and a predicted R^2 of 0.9898 and a nonsignificant lack of fit (p value > 0.05) (Table.11).

Table 11: Fit summary

Source	Sequential p-value	Lack of Fit p-value	Adjusted R ²	Predicted R ²	
Quadratic	< 0.0001	0.4821	0.9974	0.9898	Suggested

Regarding the effect of independent variables on response, there were 15 runs with the predicted value of responses shown in Table 11 and ANOVA of all responses shown in Table 12.

Table 12: Box-Behnken design and observed responses (variables are the ratio between maltodextrin and Gum arabic MD/GA (X1), the concentration of modified starch in wall material % (X2), and flaxseed oil content % (X3).).

Source	Sum of Squares	df	Mean Square	F-value	p-value	
Model	1007.72	9	111.97	607.40	< 0.0001	significant
X1	394.80	1	394.80	2141.68	< 0.0001	
X2	1.90	1	1.90	10.31	0.0237	
X3	195.62	1	195.62	1061.19	< 0.0001	
X1X2	10.05	1	10.05	54.51	0.0007	
X1X3	26.21	1	26.21	142.20	< 0.0001	
X2X3	0.0009	1	0.0009	0.0049	0.9470	
X1²	245.20	1	245.20	1330.14	< 0.0001	
X2²	162.02	1	162.02	878.89	< 0.0001	
X3²	6.77	1	6.77	36.73	0.0018	
Residual	0.9217	5	0.1843			
Lack of Fit	0.5945	3	0.1982	1.21	0.4821	not significant
Pure Error	0.3273	2	0.1636			
Cor Total	1008.65	14				

Std. Dev.	0.4294	R²	0.9991
Mean	78.04	Adjusted R²	0.9974
C.V. %	0.5502	Predicted R²	0.9898
		Adeq Precision	82.4313

According to Table 12 showing the results of analysis of variance it can be observed that the model has an F-value of 607.40 and the p-value which is less than 0.05 implies the model is significant. the ratio between MD and GA, the concentration of MS in wall material, and FO content significantly affects microencapsulation efficiency with a p-values <0.05 for the three independent variables. The interaction between MD/GA ratio and MS and the interaction between MD/GA and oil also had a significant effect with p values of 0.0007 and < 0.0001 respectively. Meanwhile, the interaction between MS and oil did not significantly affect the EE% with a p value of 0.9470 >0.05.

Final coded equation obtained from the model to describe the behavior of EE% is the following:

$$EE\% = 86.64 + 7.02X_1 + 0.49X_2 - 4.95X_3 - 1.58X_1X_2 - 2.56X_1X_3 - 8.15X_1^2 - 6.62X_2^2 - 1.35X_3^2 \quad (13)$$

The actual equation is:

$$EE\% = 63.01 + 58.35 \frac{MD}{GA} + 0.76MS + 0.14FO - 0.16 \frac{MD}{GA} MS - 0.34 \frac{MD}{GA} FO - 32.60 \left(\frac{MD}{GA}\right)^2 - 0.02 MS^2 - 0.01FO^2 \quad (14)$$

The relationship between the independent variables (MD, GA, MS and FO) and the response (EE%) is provided through the coded equation (Equation 13) generated by the model which can be used to predict EE% for different combinations of factors within the studied range. In addition, for a more practical understanding and an easier interpretation of coefficients and their impact on EE%, the actual equation (Equation 14) is also presented allowing the use of the actual units of the variables, to interpret the coefficients and their impact on EE%. To further assess the model's performance, examining plots of residuals for the response variable can reveal any patterns, indicating potential shortcomings of the model. Plots of residuals for response and plot of actual response in comparison with the predictive values of the model can be seen in Figure 16.

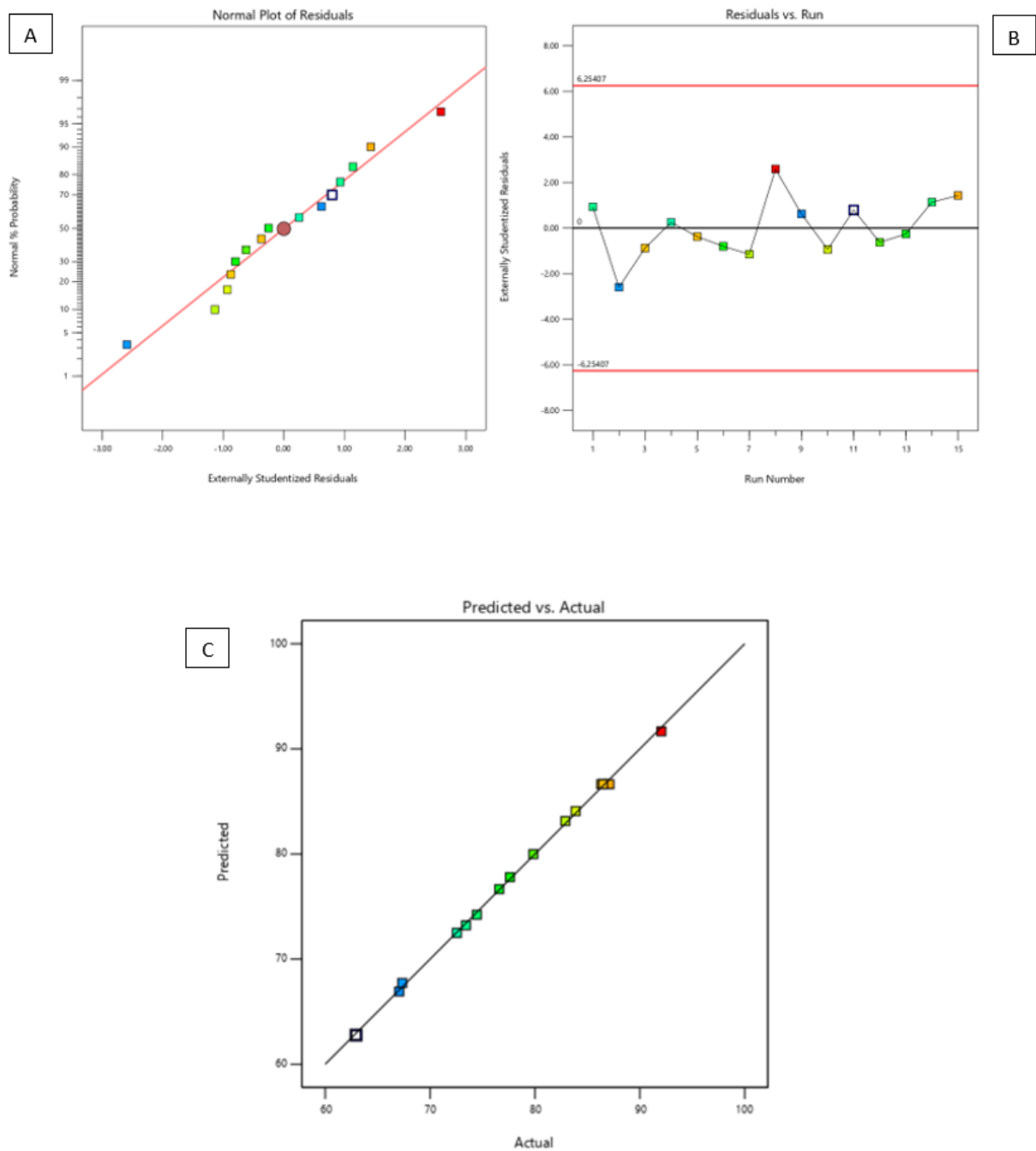


Figure 16. Plots of residuals for response and plot of actual response against predictive values, where (A) normal plot (B) externally studentized residuals vs run and (C) plot of predicted responses vs actual.

Comparing the actual response values with the model's predicted values through a plot can provide valuable insights into the model's accuracy. The experimental values lie reasonably close to the plot which indicates good correlation with the predicted data. The normal % probability of residuals is normally distributed, and all data points are situated within the limits ± 6.25 .

The results of the different response surfaces are shown in the following Figures 17, 18 and 19. According to these results, strong quadratic effect of X1 and X2 on EE% is visible on Figure 17, shaping vault form with clear maximum located around the middle of the investigated spectra and lowest responses at the sides for both independent factors. Figure 17 also verified that the maximal and minimal values have been chosen properly.

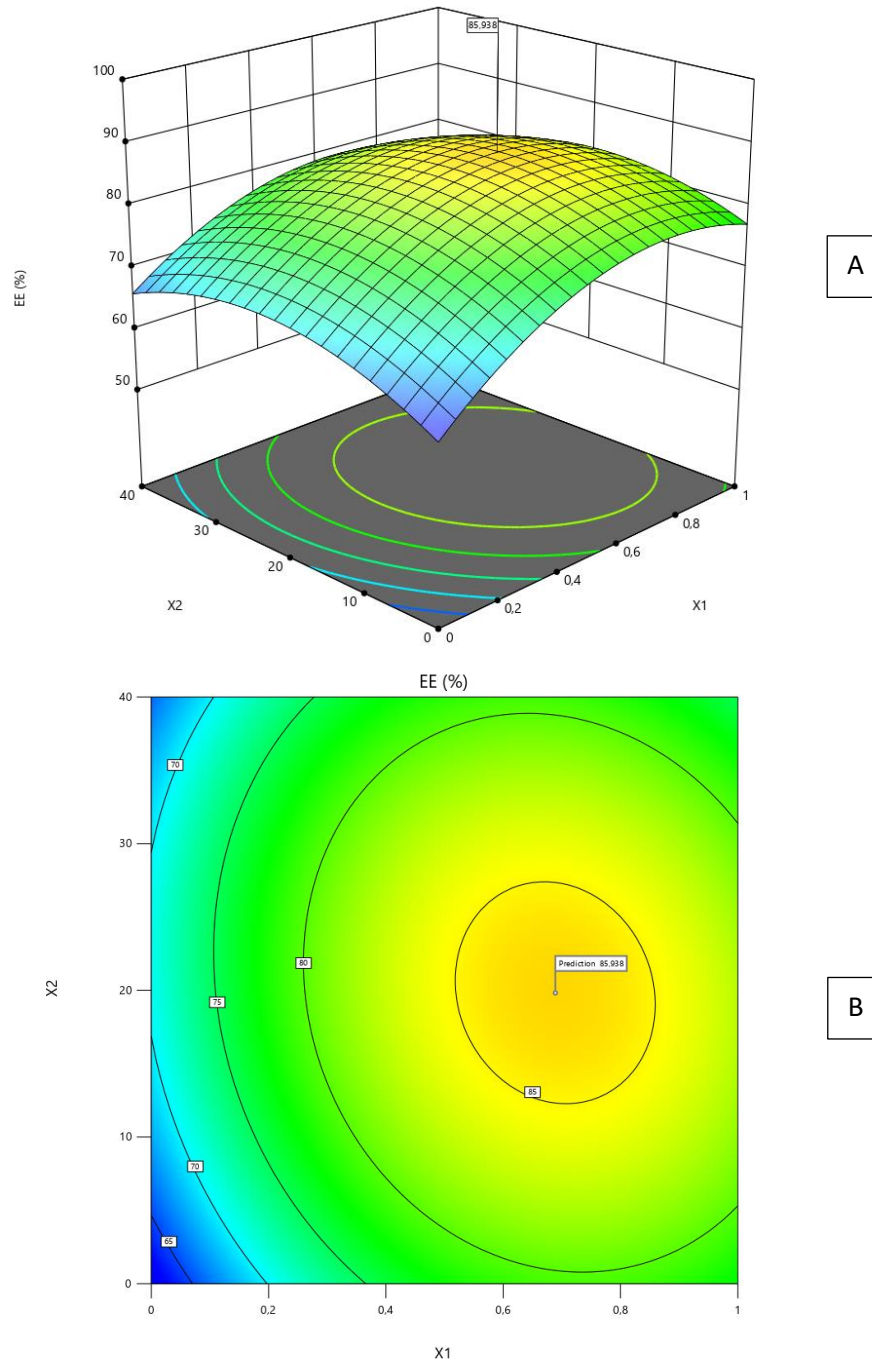


Figure 17. Surface plot (A) and contour plot (B) for EE response (X1;X2) (variables are the ratio between maltodextrin and Gum arabic MD/GA (X1) and the concentration of modified starch in wall material % (X2))

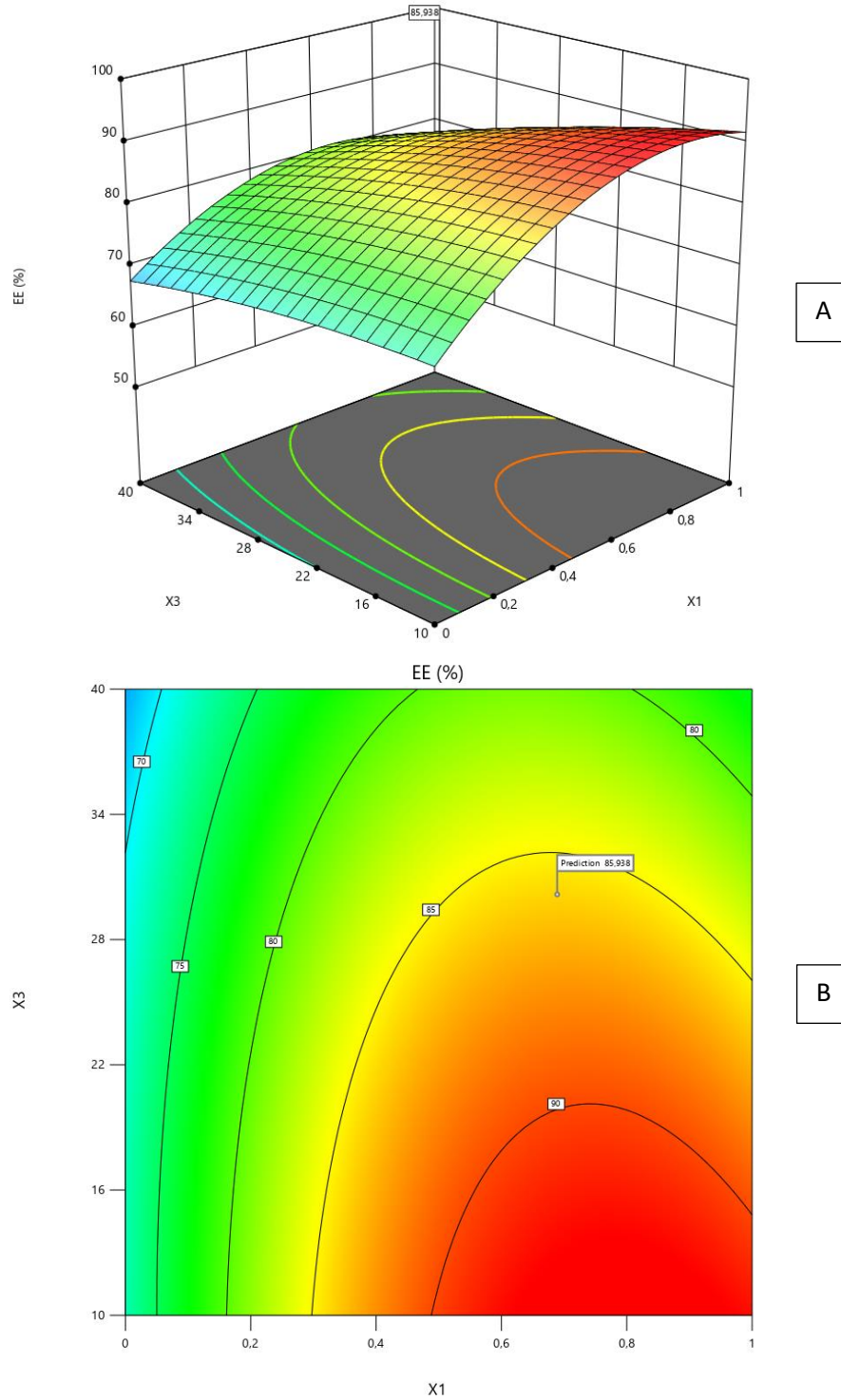


Figure 18. Surface plot (A) and contour plot (B) for EE response (X1;X3) (variables are the ratio between maltodextrin and Gum arabic MD/GA (X1), and flaxseed oil content % (X3))

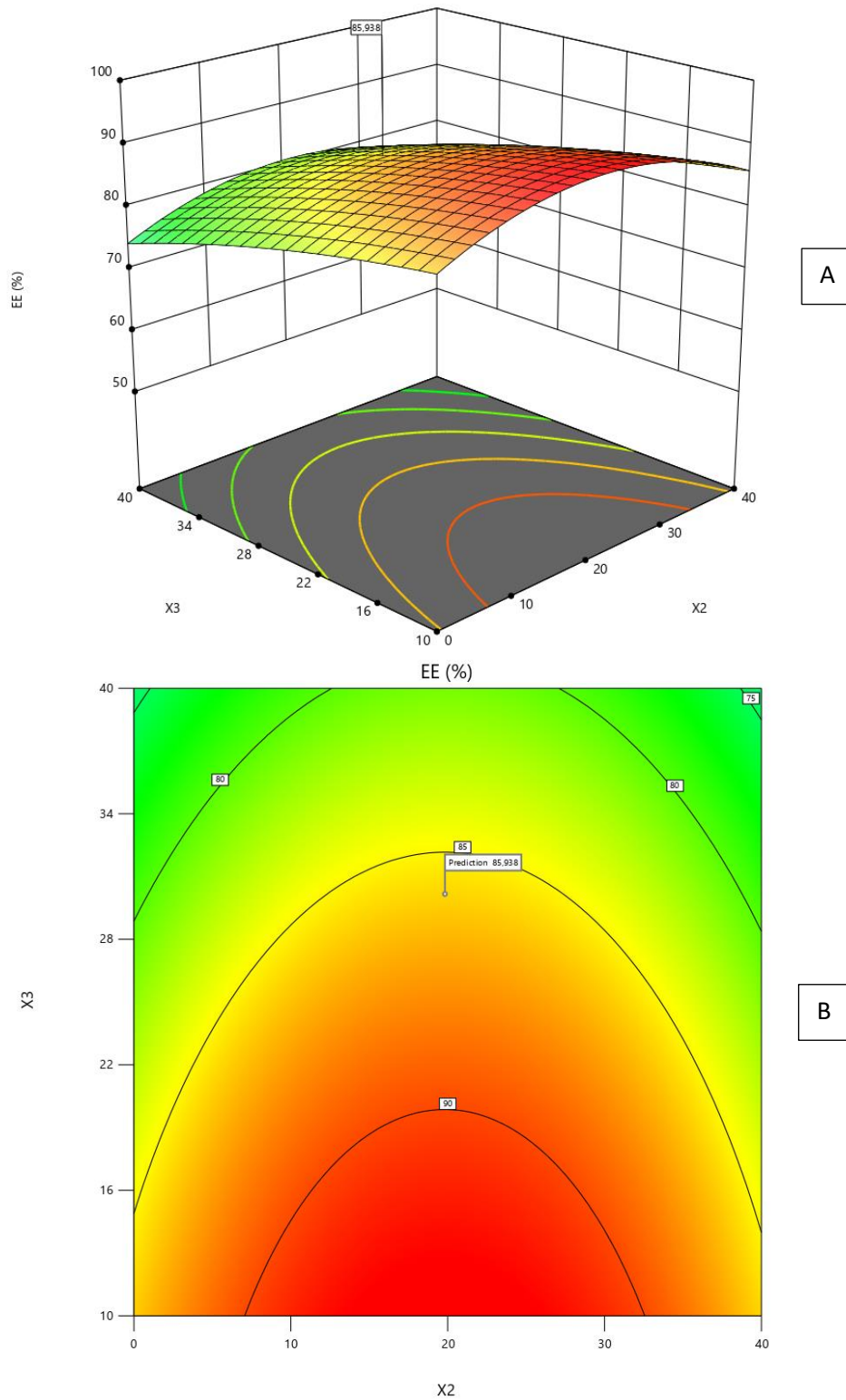


Figure 19. Surface plot (A) and contour plot (B) for EE response (X2;X3) (variables are the concentration of modified starch in wall material % (X2), and flaxseed oil content % (X3).)

Contraversially to the quadratic effect of X1 and X2 the third factor (X3) showed strong linear correlation which is obvious in Figure 18 thus the response surface diagram forms

saddle, suggesting further increase in EE% when the oil load would have less than 10% which is not true for X1 since in its case the maximal setting and the plateau cannot be exceeded. The case is very similar on Figure 19 because it shows the linear increase in EE% with the decreasing oil load (X3), as well the quadratic change of X2 with a clear inflexion point right in the middle of the investigated range.

Surface plots show that the maximum encapsulation efficiency was achieved by minimizing the oil content and maximizing the MD/GA ratio up to a certain limit (~0.7-0.8) starting from which an increase in the ratio leads to a decrease in encapsulation efficiency. This result was in correlation with the findings of Pedro et al. (2011) in which an increase of oil content in the encapsulation of FO with GA as wall material led to a decrease in encapsulation efficiency. Same results were also found in the research of Rubilar et al. (2012) where the highest encapsulation efficiency was obtained with the lowest oil content. Other researchers investigated the best ratios between MD and GA in encapsulation using SD. Turchiuli et al. (2004) have observed that lower free non-encapsulated oil was observed at a (2:3) MD/GA ratio. For MS, from the surface plot it's observed that EE is directly proportional to MS content until a value of ~ 20% starting from which EE is decreasing. Krishnan et al. (2005) have reported similar result in the encapsulation of cardamom oleoresin by SD with MD, GA, and MS as wall materials where a higher oxidation protection, proportional to encapsulation efficiency, was observed with 4:1:1 ratios of GA/MD/MS than with only GA.

5.3.1.1. Optimization and verification formula of flaxseed oil microcapsules

The Design Expert program provides formula composition solutions based on determining the importance of each variable and response and depending on the goal aimed from each one of them (maximize, minimize, target, in range, equal to). In case the goal regarding all the variables is set as in range the optimal combination to optimize the encapsulation efficiency will result in an EE around 92%. As our goal is to have as much oil encapsulated as possible the optimum formula suggested according to the constraints set in Table 13 is 0.69 MD/GA, 19.84% MS and 30.15 % FO with a desirability of 0.75. To validate this prediction, we conducted experiments using the optimal formula. The RSM model predicted an optimal formula for FO microcapsules with an EE of 85.93% shown as well in Figure 17,18 and 19. Experiments for verification result using this formula achieved an actual EE of 86.05%. This value falls within the range predicted by the model's 95% confidence interval, indicating good correlation. To further confirm this, a one-sample t-test using SPSS

was conducted. The test showed no significant difference between the predicted and actual EE values ($p > 0.05$).

Table 13 : Constraints

Name	Goal	Lower Limit	Upper Limit	Lower Weight	Upper Weight	Importance
X1	is in range	0	1	1	1	2
X2	is in range	0	40	1	1	2
X3	maximize	10	40	1	1	2
EE%	maximize	62.95	92.05	1	1	5

It can be concluded that the RSM models is accurate and could be used to study the quadratic effects of MD, GA and MS concentrations, and FO content on EE. Therefore, the application of the RSM with Box-Behnken was suitable for optimizing flaxseed particles with desirable EE.

5.3.2. Encapsulation of flaxseed oil using combination of rotor stator homogenizer and spray drying

The experimental responses of the optimization experimental design are mentioned in the Table 14.

Table 14: Experimental responses of the optimization experimental design

Run	X1	X2	X3	EE%
1	0	-1	1	50.08
2	-1	0	1	49.87
3	0	0	0	75.66
4	-1	0	-1	65.12
5	0	0	0	75.75
6	1	1	0	69.89
7	0	-1	-1	70.64
8	1	0	-1	80.43
9	-1	1	0	59.72
10	0	1	-1	72.39
11	-1	-1	0	56.77
12	1	-1	0	70.14
13	1	0	1	55.02
14	0	1	1	50.3
15	0	0	0	76.22

Run 8 had the best encapsulation efficiency (80.43%) out of all the runs performed. This formulation had a ratio MD/GA equal to 1 and 20% of MS with 10% of oil load which is the same formulation for which we got the highest encapsulation efficiency for FO encapsulation through ME and SD. Run 2 in the other hand, having no MD, 20% of MS and 40% of FO had the lowest encapsulation efficiency (49.87%). These results again emphasize the findings that the encapsulation efficiency is inversely proportional to the FO load and are showing the importance of MD in microencapsulation through SD.

For the optimization of encapsulated FO sample, a quadratic polynomial model was suggested as a fit model with an adjusted R² of 0.9797 and a predicted R² of 0.9583 and a nonsignificant lack of fit (p value > 0.05) (Table 15)

Table 15: Fit summary

Source	Sequential p-value	Lack of Fit p-value	Adjusted R ²	Predicted R ²	
Quadratic	<0.0001	0.1373	0.9966	0.9822	Suggested

For the effect of independent variables on response, ANOVA of all responses is shown in Table 16.

Table 16: Box-Behnken design and observed responses

Source	Sum of Squares	df	Mean Square	F-value	p-value	
Model	1590.24	9	176.69	458.16	< 0.0001	significant
X1	242.00	1	242.00	627.50	< 0.0001	
X2	2.73	1	2.73	7.07	0.0450	
X3	867.57	1	867.57	2249.58	< 0.0001	
X1X2	2.56	1	2.56	6.64	0.0496	
X1X3	25.81	1	25.81	66.92	0.0004	
X2X3	0.5852	1	0.5852	1.52	0.2728	
X1²	92.11	1	92.11	238.83	< 0.0001	
X2²	168.33	1	168.33	436.49	< 0.0001	
X3²	252.65	1	252.65	655.13	< 0.0001	
Residual	1.93	5	0.3857			
Lack of Fit	1.75	3	0.5825	6.44	0.1373	not significant
Pure Error	0.1809	2	0.0904			
Std. Dev.	0.62		R ²	0.998		
Mean	65.2		Adjusted R ²	0.996		
C.V. %	0.95		Predicted R ²	0.982		
			Adeq Precision	62.76		

According to Table 16 showing the results of analysis of variance ANOVA it can be observed that the model F-value of 458.16 and the p-value which is less than 0.05 implies the model is significant. The ratio between MD and GA the concentration of MS in wall material and FO content significantly affects microencapsulation efficiency with a p values <0.05 for the three independent variables. Only the interaction between MS and oil had a non-significant effect with p values of 0.2728>0.05.

The equation in terms of coded factors obtained from the model to describe the behavior of EE is the following:

$$EE\% = 75.88 + 5.50X_1 + 0.58X_2 - 10.41X_3 - 0.8X_1X_2 - 2.54X_1X_3 - 4.99X_1^2 - 6.75X_2^2 - 8.27X_3^2 \quad (15)$$

The actual equation is the following:

$$EE\% = 46.75 + 41.05 \frac{MD}{GA} + 0.78MS + 1.34FO - 0.08 \frac{MD}{GA} MS - 0.34 \frac{MD}{GA} FO - 19.98 \left(\frac{MD}{GA} \right)^2 - 0.02 MS^2 - 0.04 FO^2 \quad (16)$$

Plot of actual response in comparison with the predictive values of the model can be seen in Figure 20.

In plot (A) the data points are fall roughly along the straight line indicating a normal distribution. Plot (B) shows that the residuals are randomly scattered around zero line and are situated within the limits ± 6.25 . The experimental values in predicted vs actual plot are falling close to the plot demonstrating an adequate fit with the predicted data. This indicates that the model's has valid accuracy.

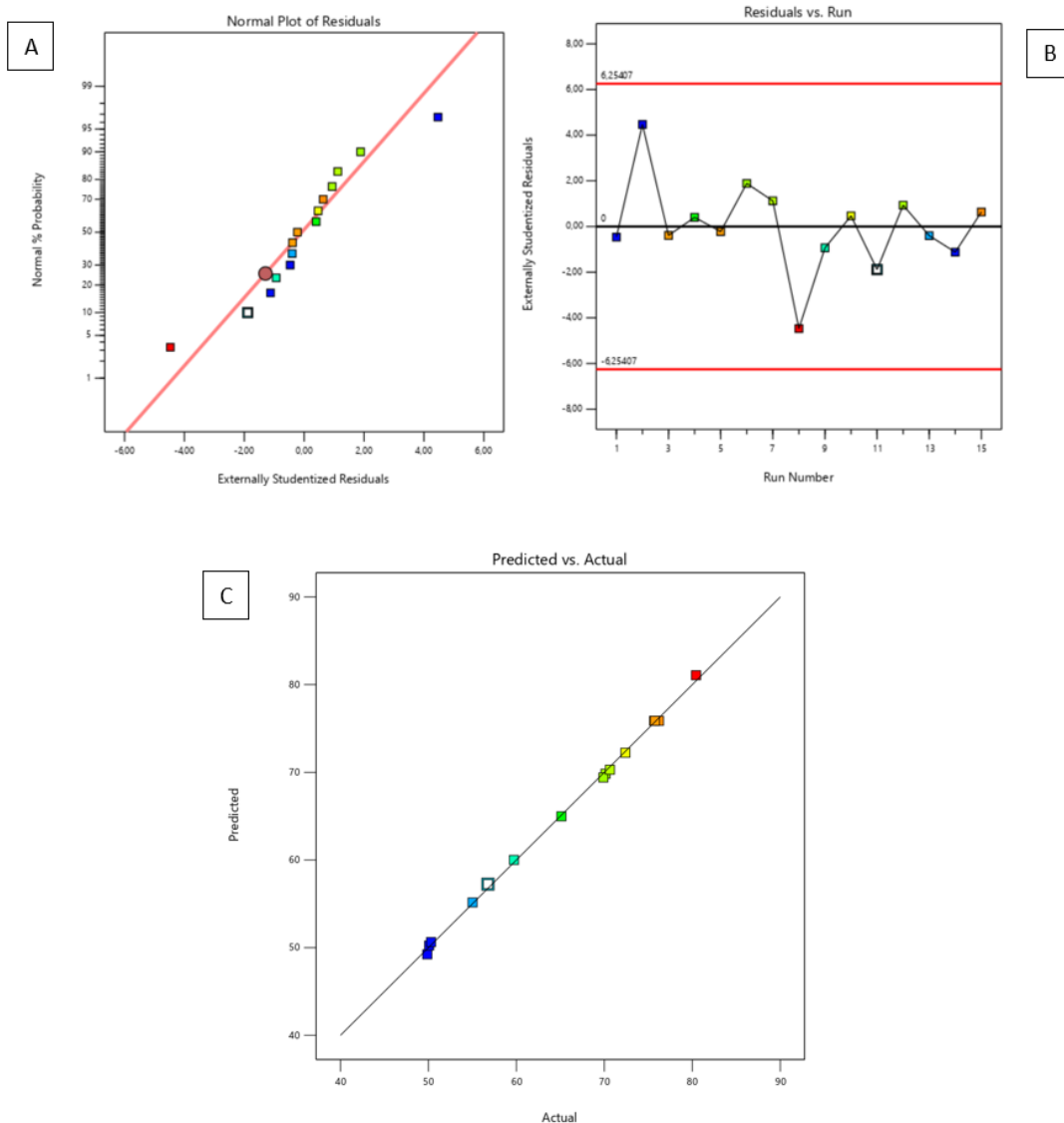


Figure 20. Plots of residuals for response and plot of actual response against predictive values where (A) normal plot of residuals (B) externally studentized residuals vs run and (C) plot of predicted responses vs actual.

The results of the different response surfaces are shown in the Figures 21, 22 and 23. Based on the result of these figures, a distinct quadratic influence of all factor X1, X2, X3 on EE% is visible. Figure 21 shows a vault-like shape with a noticeable peak around the midpoint of the studied spectra. Figure 22 shows that EE% increased significantly with rising X1 until a certain value beyond which the tendency to increase becomes less significant. Figure 23 in in other hand demonstrates a tendency of decrease in EE% with the increase of X3. It also shows an initial increase in EE% followed by decline with increasing X2.

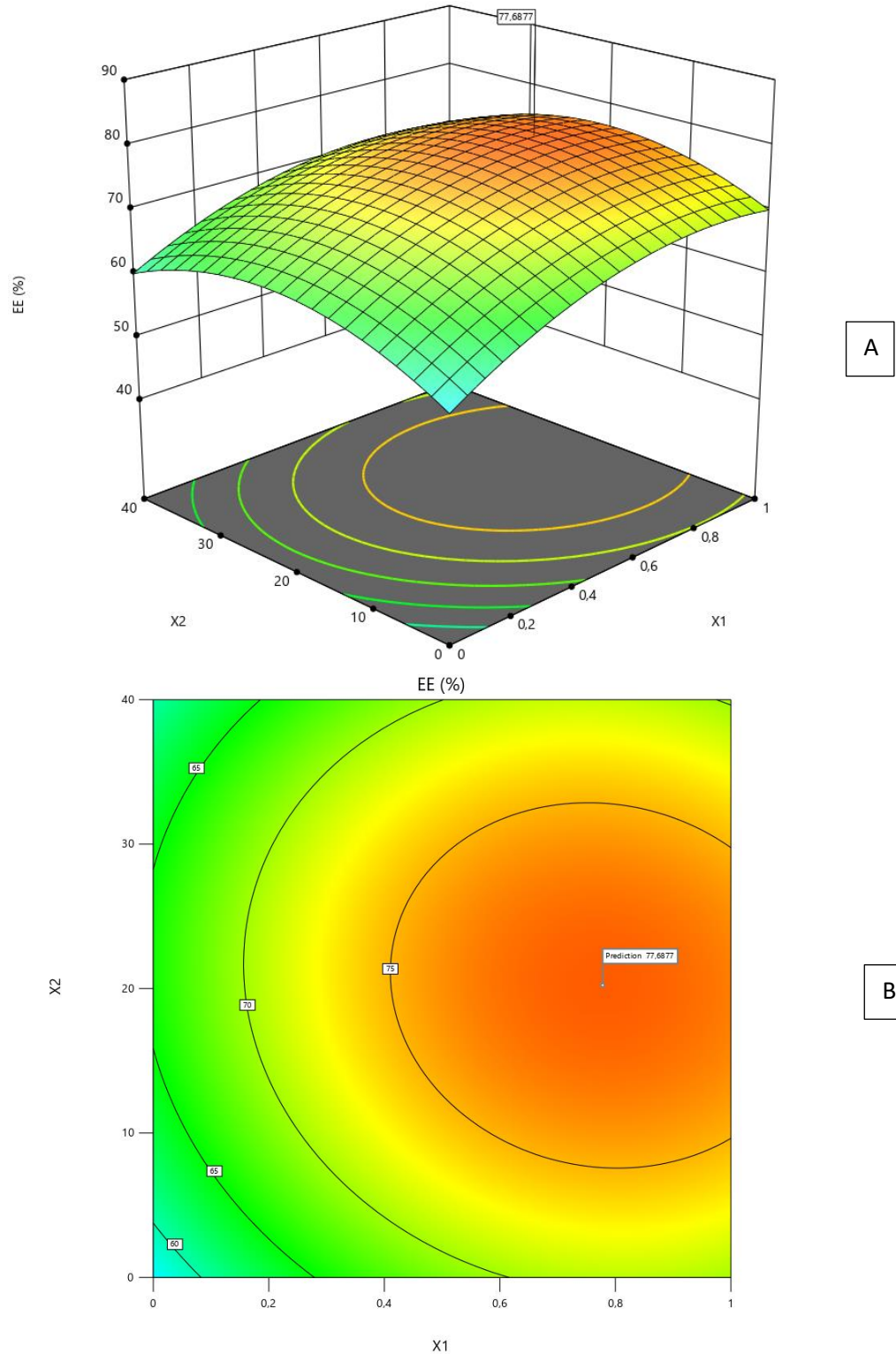
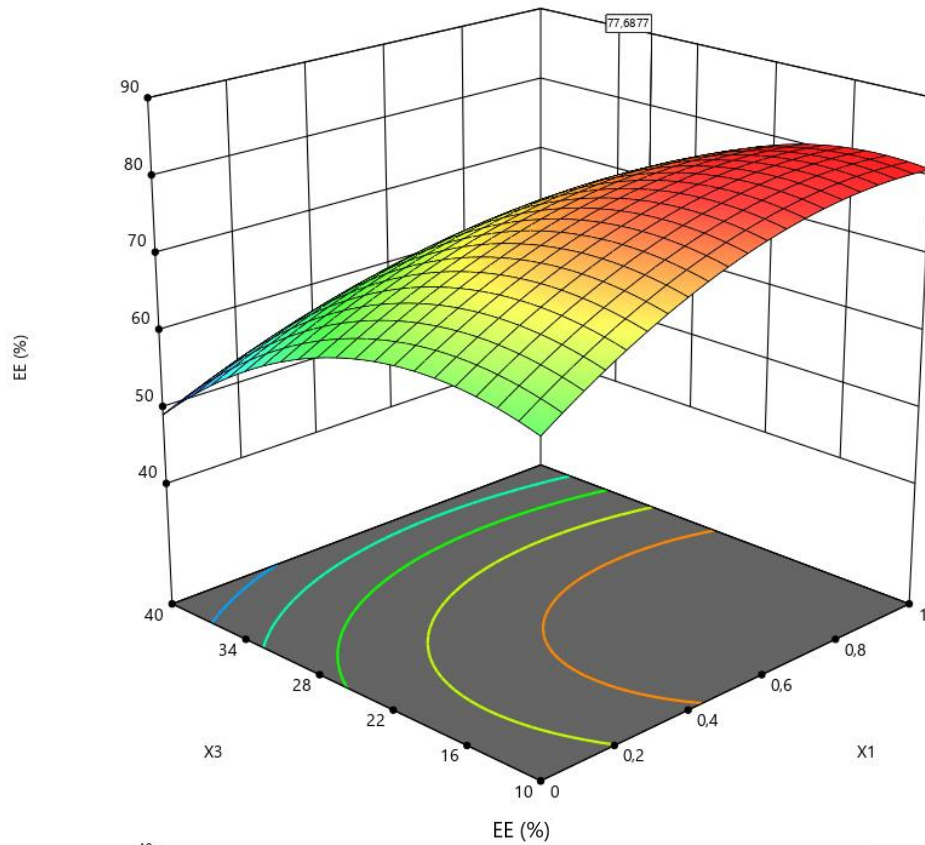
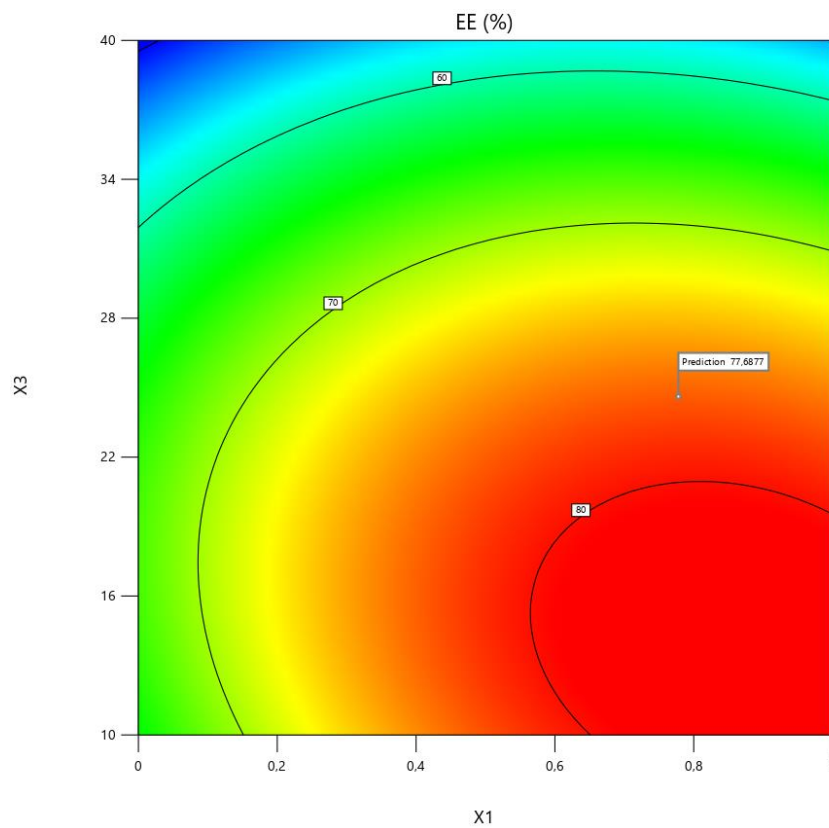


Figure 21. Surface plot (A) and contour plot (B) for EE response (X1; X2) (variables are the ratio between maltodextrin and Gum arabic MD/GA (X1) and the concentration of modified starch in wall material % (X2))

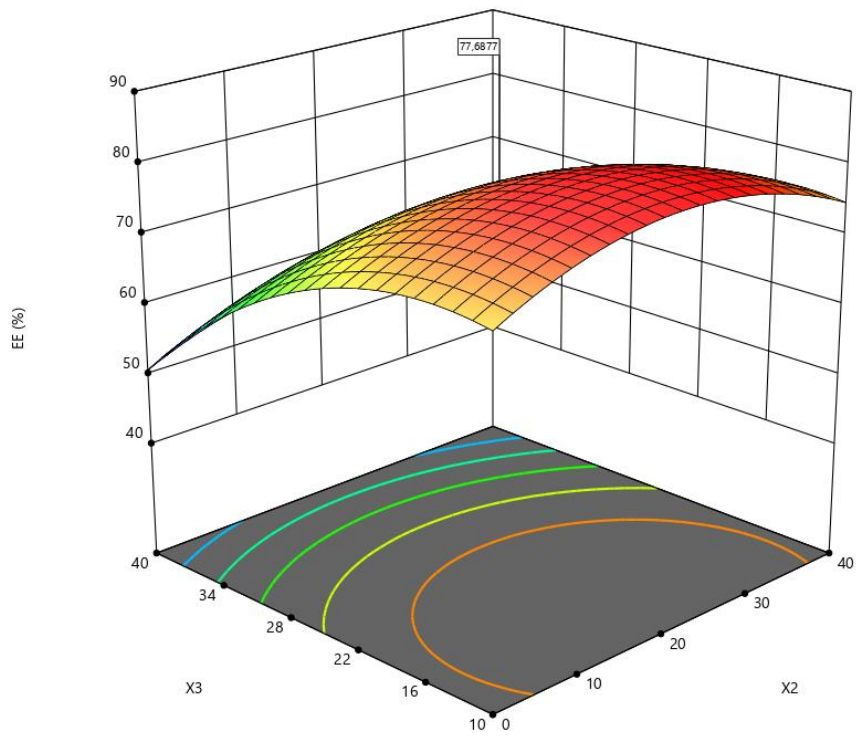


A

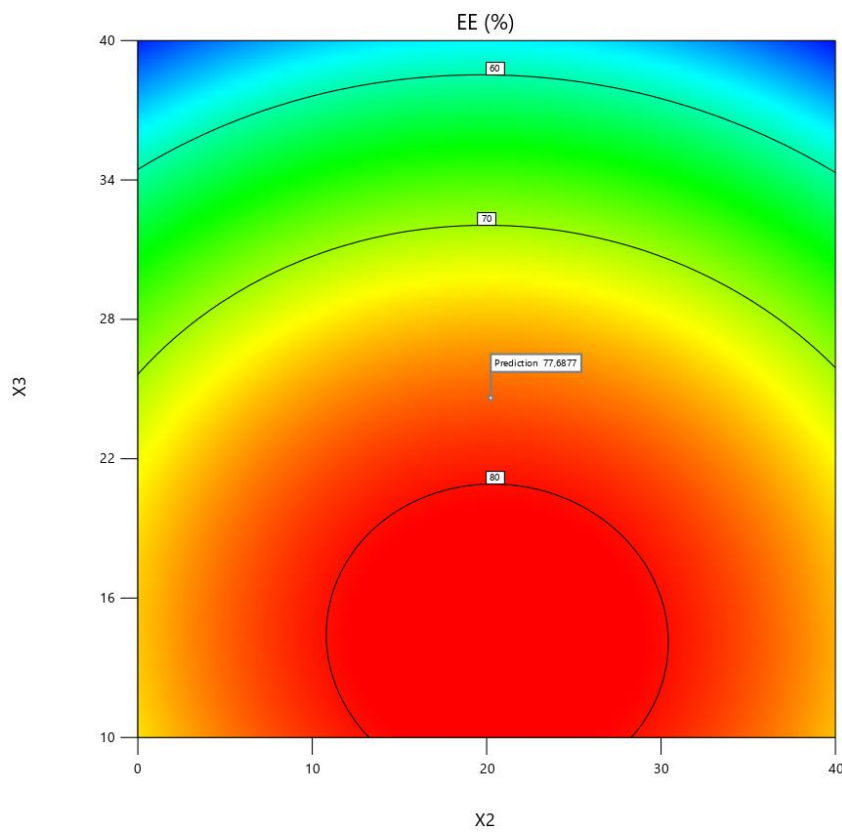


B

Figure 22. Surface plot (A) and contour plot (B) for EE response (X1; X3) (variables are the ratio between maltodextrin and Gum arabic MD/GA (X1), and flaxseed oil content % (X3))



A



B

Figure 23. Surface plot (A) and contour plot (B) for EE response (X2; X3) (variables are the concentration of modified starch in wall material % (X2), and flaxseed oil content % (X3))

Surface plots showed similar aptitude as the one obtained for EE using ME. EE% was in the same way affected by different oil content and wall material. This emphasizes the role drying technique has on the behaviors of capsules.

5.3.2.1. Optimization and verification formula of flaxseed oil microcapsules

The optimum formula with high-shear emulsification suggested by the software according to the constraints set in Table 17 is 0.79 MD/GA, 20.23% MS and 24.62% FO content giving an optimized EE of 77.68 % with 0.76 desirability.

Table 17: Constraints

Name	Goal	Lower Limit	Upper Limit	Lower Weight	Upper Weight	Importance
X1	is in range	0	1	1	1	2
X2	is in range	0	40	1	1	2
X3	maximize	10	40	1	1	2
EE%	maximize	49.87	80.43	1	1	5

The optimum formula obtained from RSM was further confirmed by experimenting with the optimum condition. The verified result of the optimum formula obtained EE values of 77.34. Compared with the predicted value, the verification result value is in the range of 95% PI low (76.49) and 95% PI high (78.94).

This result means that the chosen formula recommended by the Design Expert program is adequately good. Verification was then strengthened by the one sample t-test using SPSS. The results showed that the values were not significantly different (p value > 0.05). The experimental data is closer to the predicted value. It can be concluded that the RSM models could be used to study the quadratic effects of MD, GA, MS and oil on EE. Therefore, the application of the RSM with Box-Behnken was suitable for optimizing flaxseed particles with desirable EE%.

5.3.3. Encapsulation of flaxseed oil using combination of membrane emulsification and freeze drying

The experimental settings and responses of the optimization experimental design are mentioned in the Table 18.

Table 18: Experimental responses of the optimization experimental design

Run	X1	X2	X3	EE%
1	0	-1	1	50.1
2	-1	0	1	56.76
3	0	0	0	72.43
4	-1	0	-1	76.42
5	0	0	0	71.86
6	1	1	0	71.93
7	0	-1	-1	73.43
8	1	0	-1	76.19
9	-1	1	0	73.95
10	0	1	-1	76.26
11	-1	-1	0	72.47
12	1	-1	0	68.39
13	1	0	1	49.05
14	0	1	1	52.03
15	0	0	0	72.59

Run 4 had the best encapsulation efficiency (76.42%) out of all the runs performed, followed by run 10 and 8 with and EE% of 76.26% and 76.19% respectively. The formulation in Run 4 had a ratio MD/GA equal to 0 so no MD was used, 20% of MS with 10% of FO load. Run 1 in the other hand, had the lowest encapsulation efficiency (50.1%). Run 1 don't have MS in its formulation and had a ratio MD/GA of 0,5 with 40% of FO. These results although still accentuate the inversed proportionality between oil load and encapsulation efficiency, it rejects the importance of MD in microencapsulation through FD contrary to SD technique. The fact that the 76% EE could be exceeded with more formulations (4, 8, 10) allows more option for future applications e.g. when some of the wall material compounds cannot be used due to nutritional or financial purpose.

For the optimization of encapsulated FO sample, a quadratic polynomial model was suggested as a fit model with an adjusted R^2 of 0.9984 and a predicted R^2 of 0.9939 and a non-significant lack of fit (p value > 0.05) (Table 19)

Table 19: Fit summary

Source	Sequential p-value	Lack of Fit p-value	Adjusted R ²	Predicted R ²	
Quadratic	< 0.0001	0.4986	0.9984	0.9939	Suggested

For the effect of independent variables on response, ANOVA of all responses is shown in Table 20.

Table 20: Box-Behnken design and observed responses

Source	Sum of Squares	df	Mean Square	F-value	p-value	
Model	1419.84	9	157.76	988.08	< 0.0001	significant
X1	24.64	1	24.64	154.33	< 0.0001	
X2	11.96	1	11.96	74.88	0.0003	
X3	1112.98	1	1112.98	6970.77	< 0.0001	
X1X2	1.06	1	1.06	6.64	0.0496	
X1X3	13.99	1	13.99	87.61	0.0002	
X2X3	0.2025	1	0.2025	1.27	0.3112	
X1²	1.00	1	1.00	6.27	0.0542	
X2²	4.71	1	4.71	29.49	0.0029	
X3²	248.83	1	248.83	1558.44	< 0.0001	
Residual	0.7983	5	0.1597			
Lack of Fit	0.5038	3	0.1679	1.14	0.4986	not significant
Pure Error	0.2945	2	0.1472			
Cor Total	1420.64	14				
Std. Dev.	0.39		R ²	0.998		
Mean	67.59		Adjusted R ²	0.996		
C.V. %	0.59		Predicted R ²	0.982		
			Adeq Precision	62.76		

According to Table 20 showing the results of analysis of variance ANOVA it can be observed that the model F-value of 988.08 and the p-value which is less than 0.05 implies the model is significant. Same as for the encapsulation through SD with ME or with rotor stator homogenizer, the ratio between MD and GA, the concentration of MS in wall material and FO content in emulsion was proving to significantly affects microencapsulation efficiency

with a p-values <0.05 for the three independent variables. In this case the interaction between MS and oil had a non-significant effect with p values of 0.31>0.05.

The equation in terms of coded factors obtained from the model to describe the behavior of EE is the following:

$$EE\% = 72.29 - 1.76X_1 + 1.22X_2 - 11.80X_3 + 0.52X_1X_2 - 1.87 X_1X_3 - 1.13 X_2^2 - 8.21X_3^2 \quad (17)$$

The actual equation is as follow:

$$EE\% = 66.10 - 0.39 \frac{MD}{GA} + 0.17MS + 1.18FO + 0.05 \frac{MD}{GA} MS - 0.25 \frac{MD}{GA} FO - 0.01 MS^2 - 0.04FO^2 \quad (18)$$

Plot of residuals and of actual response in comparison with the predictive values of the model can be seen in Figure 24.

In plot (A) and (C) the data points are falling roughly close to the plot indicating a normal distribution and an adequate fit with the predicted data. Plot (B) shows that the residuals are randomly scattered around zero line and are situated within the limits ± 6.25 . This indicates that the model's has good accuracy.

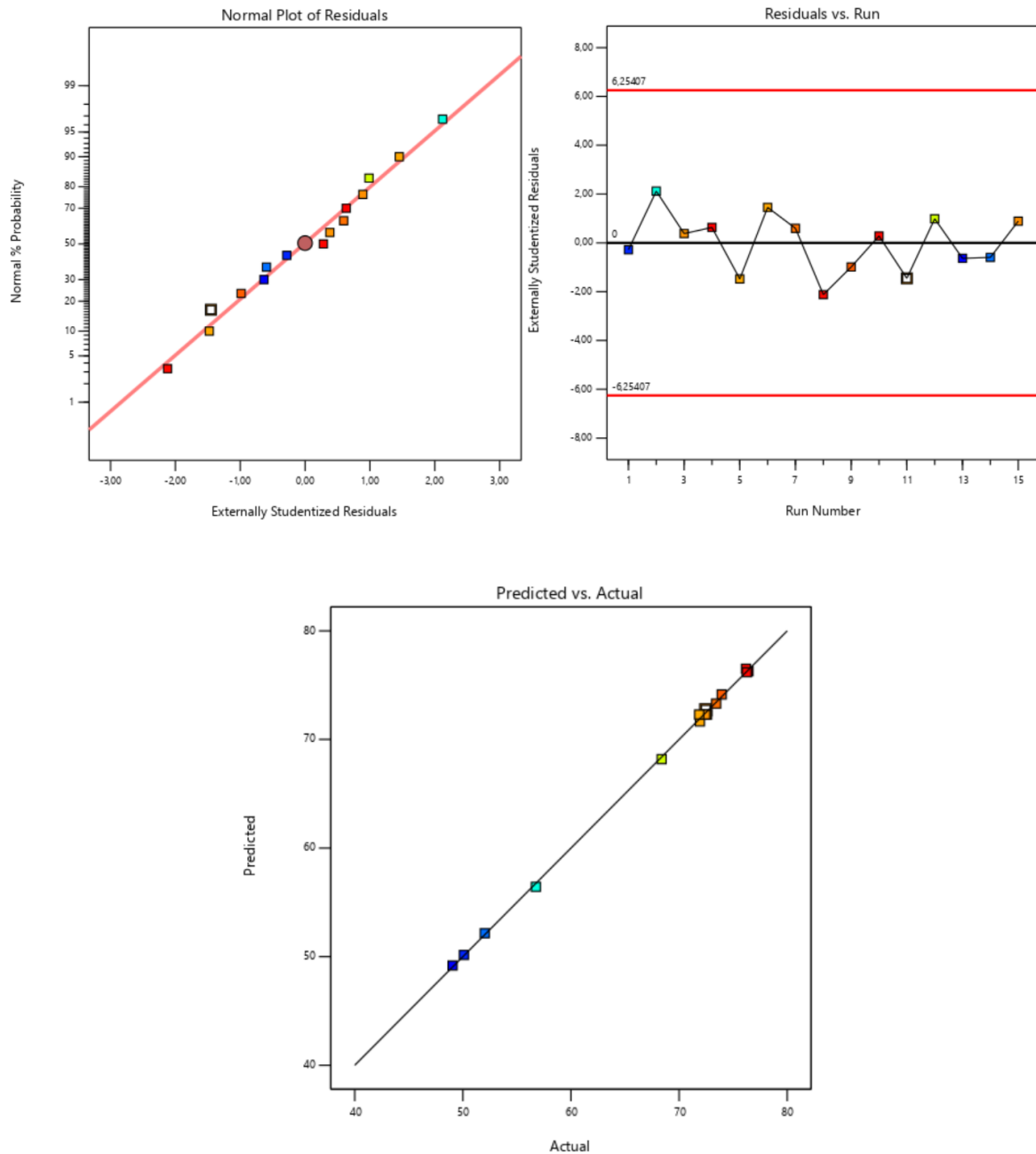


Figure 24. Plots of residuals for response and plot of actual response against predictive values, where (A) normal plot of residuals (B) externally studentized residuals vs run and (C) plot of predicted responses vs actual.

The results of the different response surfaces are shown in the following Figures 25, 26 and 27. These figures shows that the maximums are typically big plateaus in this case, the effect of X1 and X2 is more like linear, but X3 has a big quadratic effect on EE. Oil load is very determinative, with Figure 27 showing a negative correlation exhibit by X3 with EE% significantly increasing as X3 decreases.

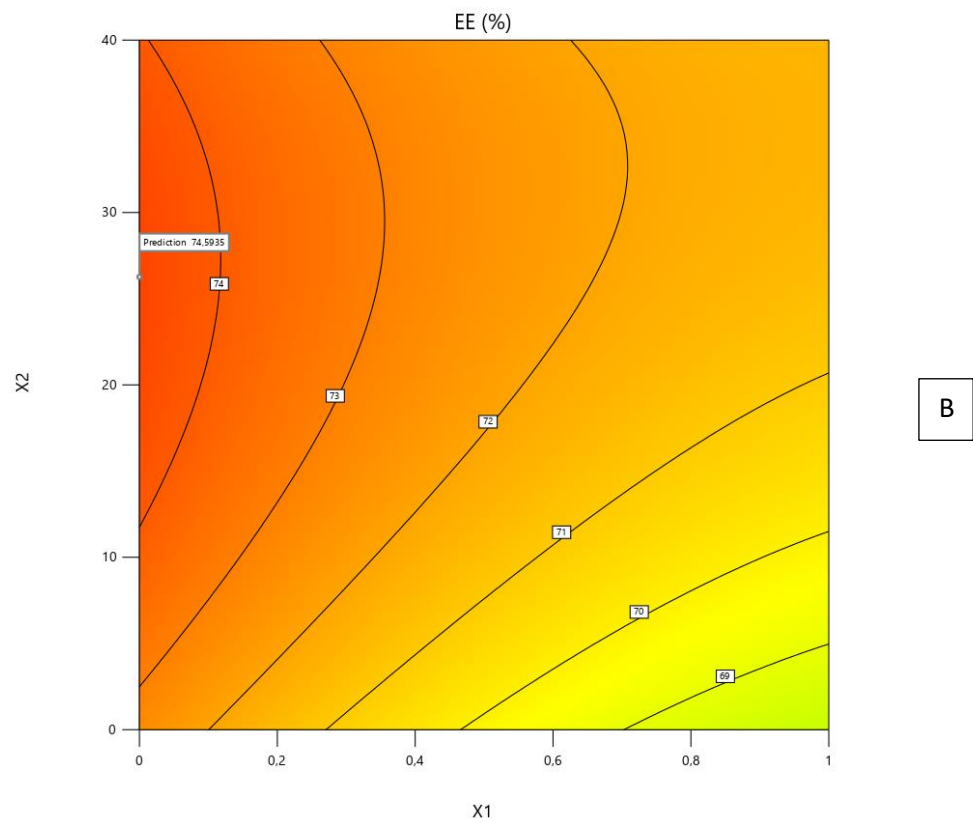
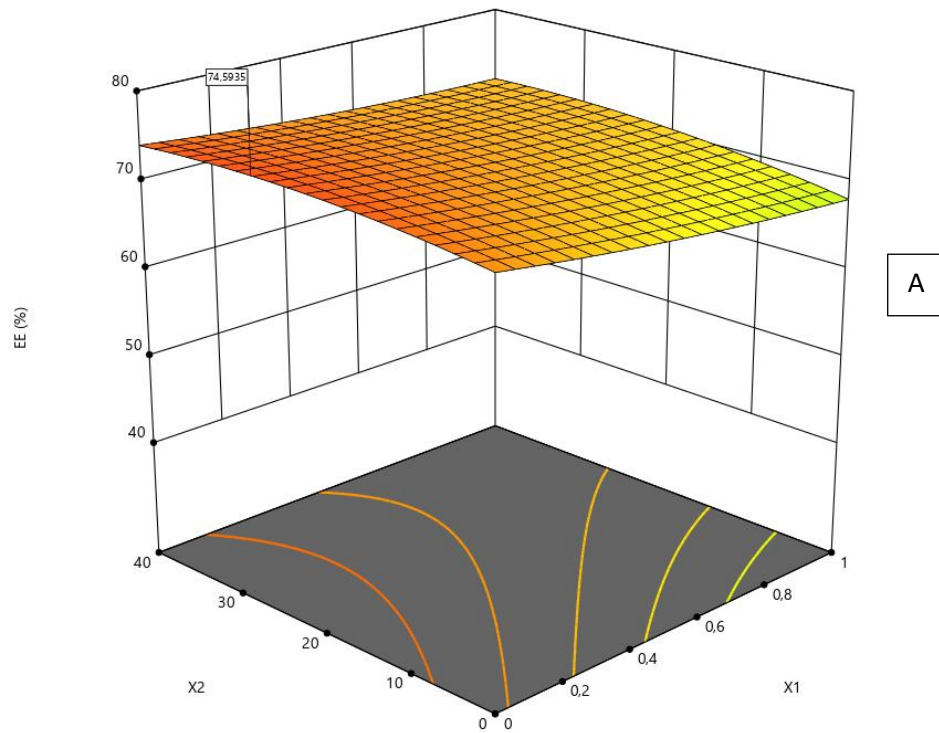


Figure 25. Surface plot (A) and contour plot (B) for EE response (X1;X2) (variables are the ratio between maltodextrin and Gum arabic MD/GA (X1) and the concentration of modified starch in wall material % (X2))

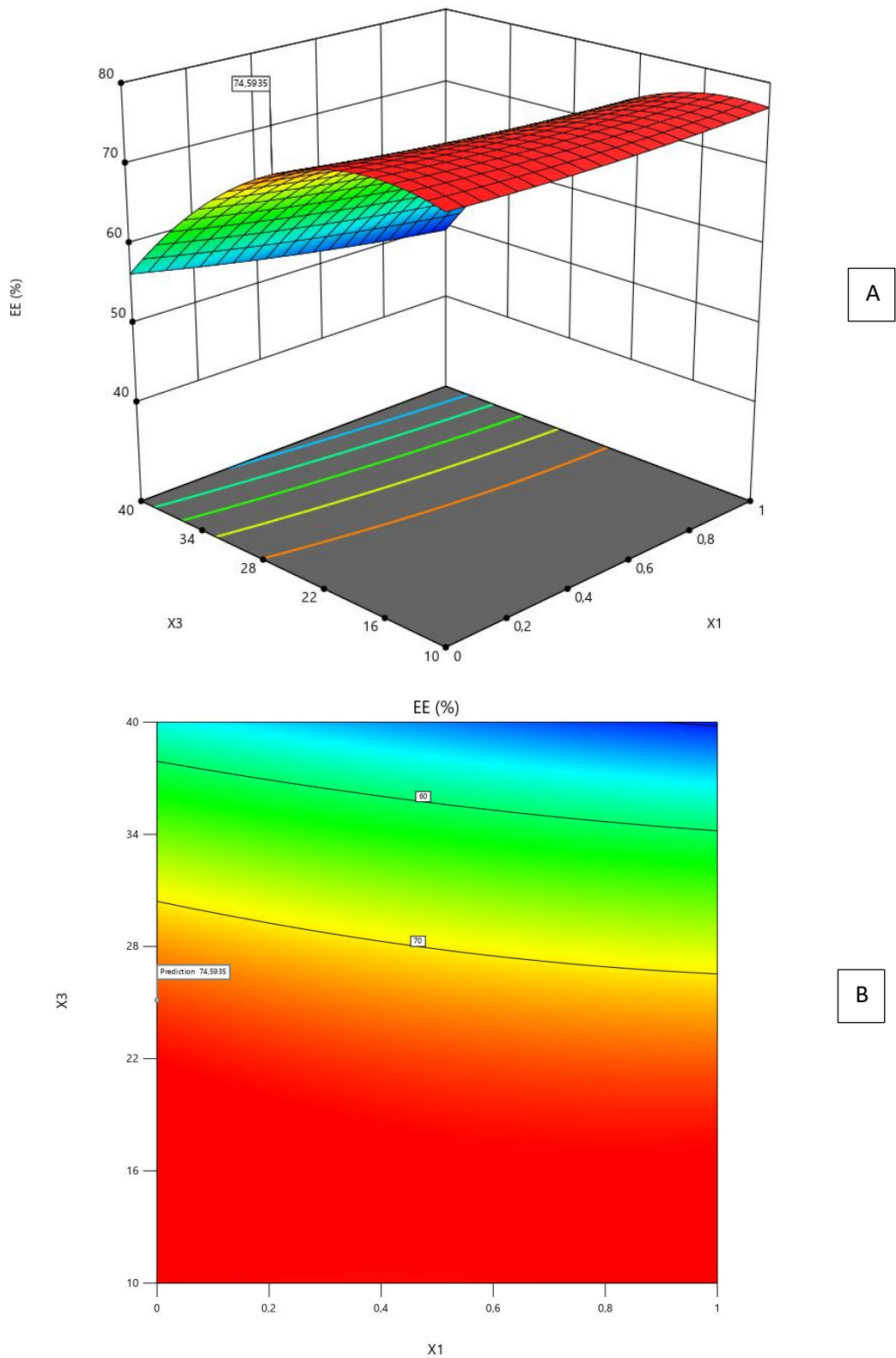


Figure 26. Surface plot (A) and contour plot (B) for EE response (X1;X3) (variables are the ratio between maltodextrin and Gum arabic MD/GA (X1), and flaxseed oil content % (X3))

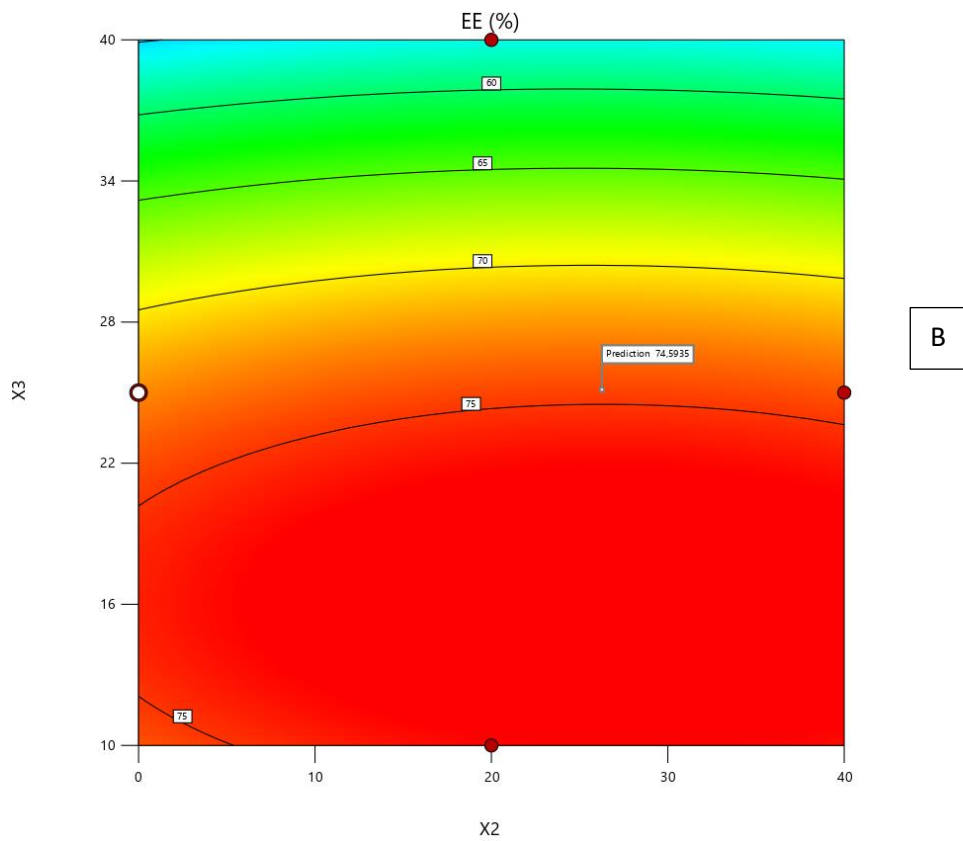
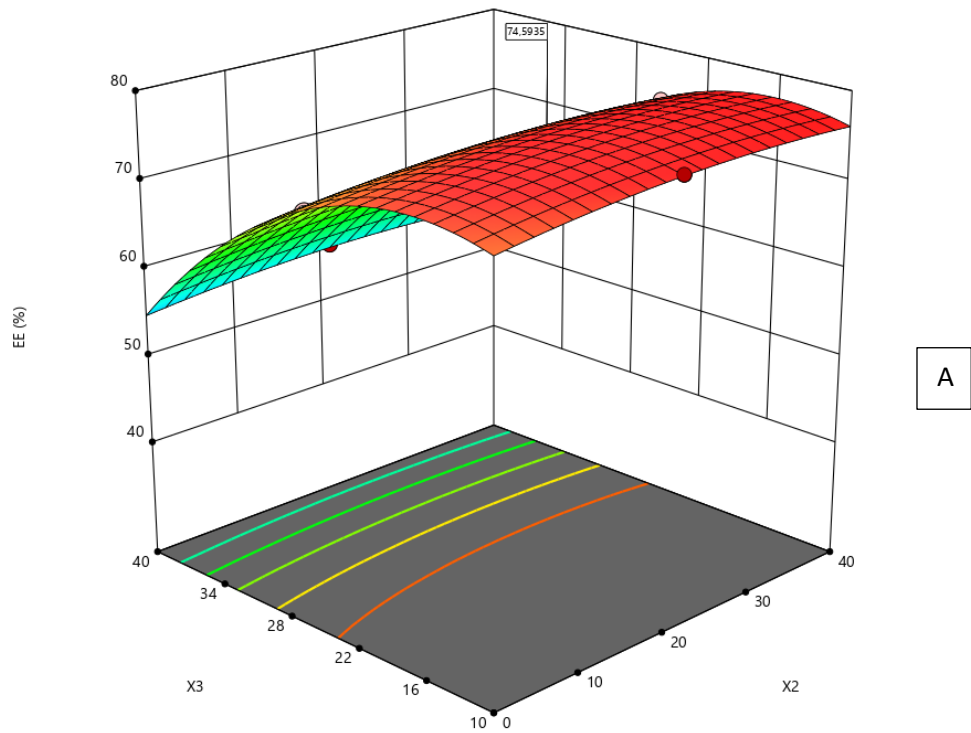


Figure 27. Surface plot (A) and contour plot (B) for EE response (X2;X3) (variables are the concentration of modified starch in wall material % (X2), and flaxseed oil content % (X3))

Surface plots show that the maximum encapsulation efficiency was achieved by minimizing the oil content. In the other hand, the optimum EE would be solely with GA and MS with no MD. This observation is matching with the findings of Chranioti and Tzia, (2013) where it was found, while studying the effect of different wall materials in fennel oleoresin encapsulation through FD, that the use of mixture of GA and MS provided a great encapsulating mixture in terms of microencapsulation efficiency and storage stability, and additionally lower EE were observed in mixtures containing MD.

5.3.3.1. Optimization and verification formula of flaxseed oil microcapsules

The optimum formula suggested by the software according to the constraints set in Table 21 is 0 MD/GA, 26.26% MS and 25.13% FO content giving an optimized EE of 74.59 % with 0.78 desirability.

Table 21: Constraints

Name	Goal	Lower Limit	Upper Limit	Lower Weight	Upper Weight	Importance
X1	is in range	0	1	1	1	2
X2	is in range	0	40	1	1	2
X3	maximize	10	40	1	1	2
EE	maximize	49.05	76.42	1	1	5

The optimum formula obtained from RSM was further confirmed by experimenting with the optimum condition. The verified result of the optimum formula obtained EE values of 74.33%. Compared with the predicted value, the verification result value is in the range of 95% PI low (73.71) and 95% PI high (75.47).

This result means that the chosen formula recommended by the Design Expert program is adequately good. Verification was then strengthened by the one sample t-test using SPSS. The results showed that the values were not significantly different (p value > 0.05). The experimental data is closer to the predicted value. It can be concluded that the RSM models could be used to study the quadratic effects of MD, GA, MS and oil on EE. Therefore, the application of the RSM with Box-Behnken was suitable for optimizing microencapsulated flaxseed oil particles with desirable EE.

5.4. Optimized emulsions and microcapsules characterization

Emulsions with the optimized formulations for each emulsification and drying technique were produced and were used to conduct the following analysis of both, emulsions, and microcapsules. Which means that in total we had three optimized formulations as follow: 1) from ME and SD technique the emulsion prepared had 0.69 MD/GA, 19.84% MS and 30.15 % FO; 2) from rotor stator homogenization and SD the emulsion prepared had 0.79 MD/GA, 20.23% MS and 24.62% FO; 3) and finally from ME and FD the emulsification prepared contained 0 MD/GA, 26.26% MS and 25.13% FO.

5.4.1. Emulsions stability

Zeta potential

Optimized sample prepared using ME for the aim of spray drying (ME-SD-E) has a ZP of $-37.8 \pm 1,1$ mV (Figure 28), which falls within the moderate stability range. This suggests that the oil droplets have a moderately negative charge, leading to some electrostatic repulsion between them. Optimized sample produced with rotor stator homogenization (RSH) for the aim of SD (RSH-SD-E) has the least negative ZP value of $-29.5 \pm 0,5$ mV (Figure 29) among the three samples meaning a weaker electrostatic repulsion force between the droplets which can consequently make the more susceptible to destabilization mechanisms during storage. The use of rotor-stator homogenization in RSH-SD-E might be a contributing factor, in fact RSH applies higher shear forces compared to ME which could disrupt the adsorption of charged groups from the wall material onto the oil droplets, leading to a less negative ZP. Optimized sample produced through ME for the aim of FD (ME-FD-E) in the other hand exhibits a slightly more negative ZP of $-41.3 \pm 1,5$ mV (Figure 30) compared to ME-SD-E indicating a slightly stronger electrostatic repulsion between the droplets and potentially a higher stability compared to both ME-SD-E and RSH-SD-E. This could be due to the lower content in MD, in fact having less MD with lower affinity for oil could lead to less competition between it and other wall materials for adsorption sites on the oil droplet surface.

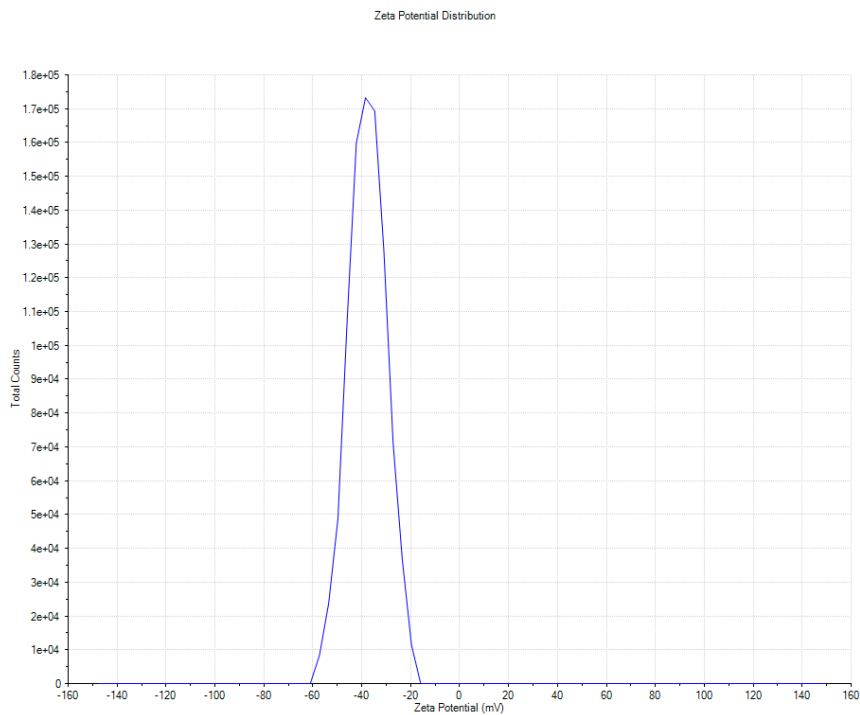


Figure 28. Zeta potential distribution of ME-SD-E

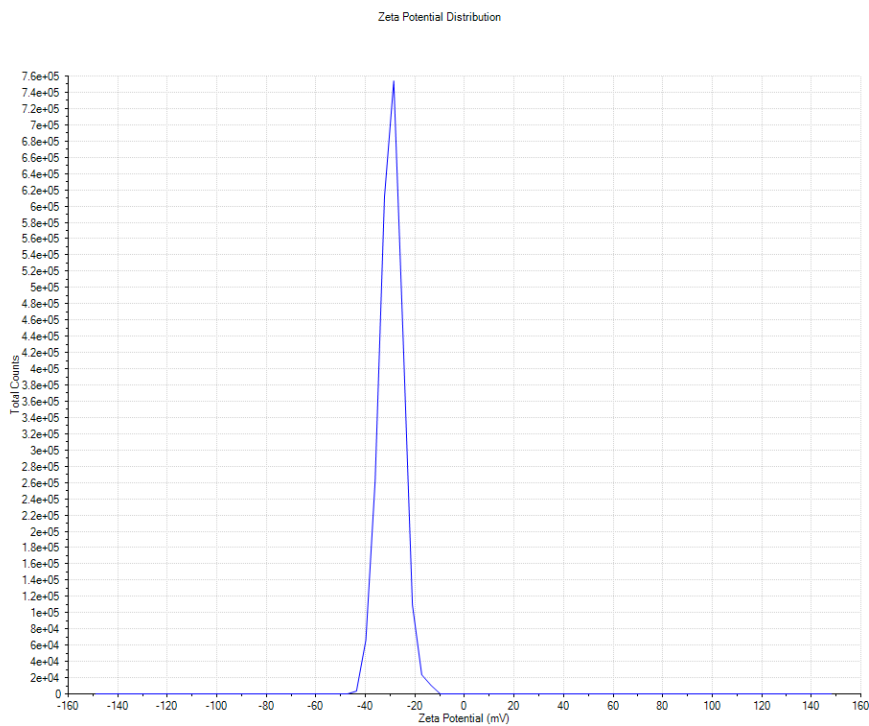


Figure 29. Zeta potential distribution of RSH-SD-E

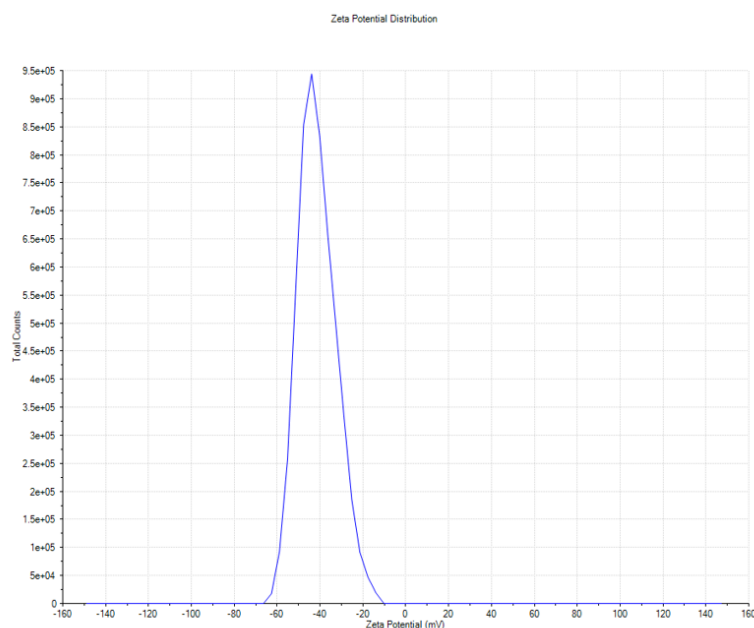


Figure 30. Zeta potential distribution of ME-FD-E

Another study of emulsion stability was conducted, in fact the zeta potential and separation percentages offer complementary insights into emulsion stability as a higher absolute value of ZP generally indicates stronger electrostatic repulsion between droplets leading to better stability with lower separation. This was evident in the result obtained in Table 22, where the lower separation% was observed in ME-FD-E and the highest was observed in sample RSH-SD-E:

Table 22: Evaluation of separation % of different optimized formulation

	ME-SD-E	RSH-SD-E	ME-FD-E
Separation %	10±0.5 ^b	17±0.25 ^c	7±0.5 ^a

Where: ME-SD-E is membrane emulsification emulsion prepared for spray drying;

RSH-SD-E is rotor stator homogenization emulsion and ME-FD-E is membrane emulsification emulsion prepared for freeze drying. Results are represented by mean value with standard deviation (\pm values). In superscript, significantly different groups are noted by different letters (a,b,c), interpretation is performed with one-way ANOVA, and evaluated by the Tukey’s HSD post hoc method.

5.4.2. Size and morphology study of emulsion

Analyzing the microscopic images in Figure 31, we can see that ME-SD-E, exhibits the largest average droplet size of approximately 16 μ m. ME-FD-E, also produced via ME,

exhibits a smaller average droplet size of 12 μm . Finally, RSH-SD-E produced through rotor-stator homogenization, has the smallest average droplet size of just 7 μm .

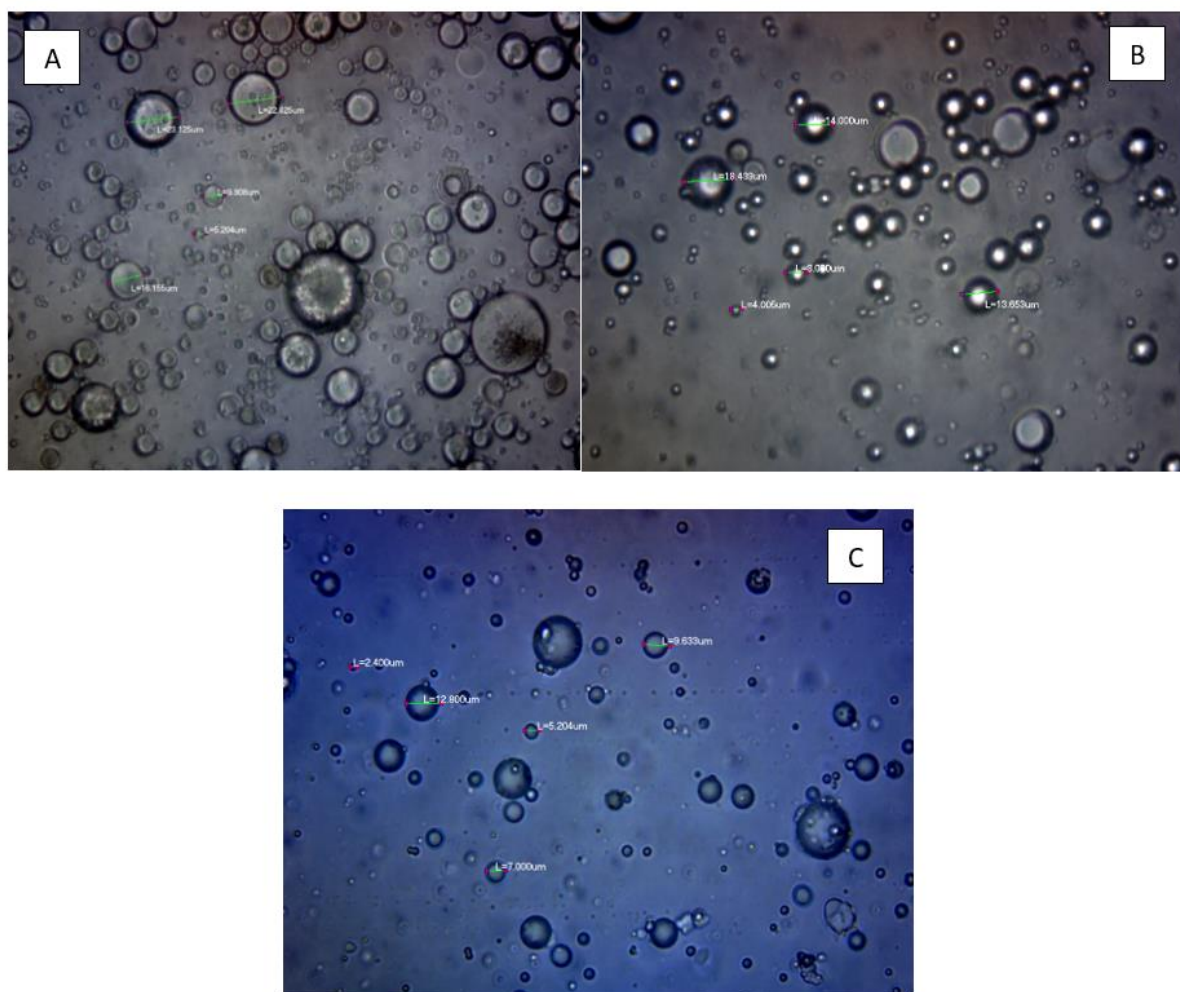


Figure 31. Microscopic images of ME-SD-E (A), ME-FD-E (B) and RSH-SD-E (C)

These results emphasize the fact that emulsification technique and wall material can influence the droplet size. In fact, for ME-SD-E and ME-FD-E ME's gentle pressure-driven process typically results in larger droplets compared to high shear methods. In our case the stability results mentioned earlier contradict the common notion that smaller droplets lead to better stability as from previous analysis ME-FD-E exhibits the highest stability. This can be attributed to the thicker steric barrier due to the larger surface area which allows more adsorbed wall material and reduced Brownian motion of the larger droplets which contributes to lower risks of collisions and aggregation. In the other hand ME-FD-E lower average droplet size compared to ME-SD-E despite using the same emulsification technique can be attributed to the lower content in MD and higher in GA and MS. In fact, generally,

MD is considered as a low viscosity emulsifier that do not create a very thick steric barrier while in the other hand GA is known for its good emulsifying properties due to its branched structure and ability to form a good interfacial film which can potentially lead to smaller droplets. RSH-SD-E average droplet size can be due to high shear forces applied by the Rotor-stator homogenization that break down the oil phase into significantly smaller droplets compared to ME. To have a more concrete idea about the droplet size and distribution, analyses were conducted according to description in paragraph 4.2.7.2. and results were recorded in Table 23.

Table 23: Evaluation of separation % of different optimized formulation

	ME-SD-E	RSH-SD-E	ME-FD-E
D_[3,2] (µm)	14.49 ±0.026 ^c	7.71 ±0.01 ^a	13.53±0.080 ^b
D_[4,3] (µm)	26.73 ±0.045 ^c	13.62 ±0.085 ^a	23.59±0.036 ^b
Span	0.53 ±0.07 ^a	1.3 ± 0.02 ^b	0.50±0.035 ^a

Where ME-SD-E is membrane emulsification emulsion prepared for spray drying; RSH-SD-E is rotor stator homogenization emulsion and ME-FD-E is membrane emulsification emulsion prepared for freeze drying. Results are represented by mean value with standard deviation (\pm values). In superscript, dissimilar alphabet represents the significant difference between different groups of wall materials composition within diameter ($D_{[4,3]}$ µm), ($D_{[3,2]}$ µm) and span, separately (horizontal way), interpretation is performed with MANOVA, with the output of Wilks' Lambda ($p < 0,001$) and evaluated by the Tukey's HSD post hoc method.

According to Post hoc Tuckey's test, there is no significant difference between the span of ME-SD-E and ME-FD-E. A lower span (closer to 1) indicates a more uniform distribution while a higher span signifies a wider range of particle sizes within the particles. These two values are significantly lower than the value obtained for RSH-SD-E emphasizing the effect ME has on homogenizing the size distribution of droplets in the emulsion which can offer a better stability and thus a better emulsification quality and protection for FO.

5.4.3. Flaxseed oil microcapsules size and morphology

Size distribution analysis provides valuable insights into the physical characteristics of powders and their potential implications for encapsulation efficiency and stability. Result obtained are mentioned in Table 24. Combining the fact that microcapsules obtained through ME and SD (ME-SD-C) has a median particle size (D_{50}) closer to the center of the overall

distribution compared to microcapsules obtained through rotor stator homogenization and SD (RSH-SD-C) and that span value for ME-SD-C is lower than RSH-SD-C, this suggests that ME might generate a more uniform range of particle sizes distribution.

Additionally, particles produced through ME and FD (ME-FD-C) had smaller particle size than those produced through SD, this could be due to the more abundant presence of MD in both ME-SD-C and RSH-SD-C that could have contributed to larger size.

Structural analysis of the freeze-dried powders was conducted by scanning electron microscope (SEM). A comparison of the images (Figure 32) showed a notable difference in terms of particle structure, shape, and size. ME-SD-C had the most homogeneous structure with clear spheric particles. RSH-SD-C image shows a probable agglomeration and hallow particle proving that some oil was released from the capsules. ME-FD-C images in the other hand presented the most irregular shape, which is logical knowing that, unlike SD that produce spheric powder, the freeze-dried samples were manually ground into a fine powder.

Table 24: Evaluation of particle size and distribution of different optimized formulation

	ME-SD-C	RSH-SD-C	ME-FD-C
$D_{[3,2]} \mu\text{m}$	17.72 ± 0.035^b	18.15 ± 0.075^c	12.50 ± 0.13^a
$D_{[4,3]} \mu\text{m}$	82.70 ± 0.3^b	120.0 ± 0.43^c	49.88 ± 0.34^a
$D_{10} \mu\text{m}$	9.73 ± 0.041^b	9.833 ± 0.068^b	6.462 ± 0.072^a
$D_{50} \mu\text{m}$	70.47 ± 0.24^b	91.05 ± 0.23^c	35.80 ± 0.48^a
$D_{90} \mu\text{m}$	171.3 ± 0.39^b	272.6 ± 0.68^c	112.1 ± 0.1^a
Span	2.29 ± 0.18^a	2.89 ± 0.95^b	2.95 ± 0.26^b

Where ME-SD-C is membrane emulsification and spray drying capsules; RSH-SD-C is rotor stator homogenization and spray drying capsules and ME-FD-C is membrane emulsification and freeze-drying capsules. Results are represented by mean value with standard deviation (\pm values). In superscript, dissimilar alphabet represents the significant difference between different groups of wall materials composition within ($D_{[3,2]} \mu\text{m}$), ($D_{[4,3]} \mu\text{m}$), ($D_{10} \mu\text{m}$), ($D_{50} \mu\text{m}$), and ($D_{90} \mu\text{m}$). According to Post hoc Tuckey's test, there is no significant difference between the span of RSH-SD-C and ME-FD-C. A span closer to 1 indicates a more uniform distribution while a higher span signifies a wider range of particle sizes within the particles.

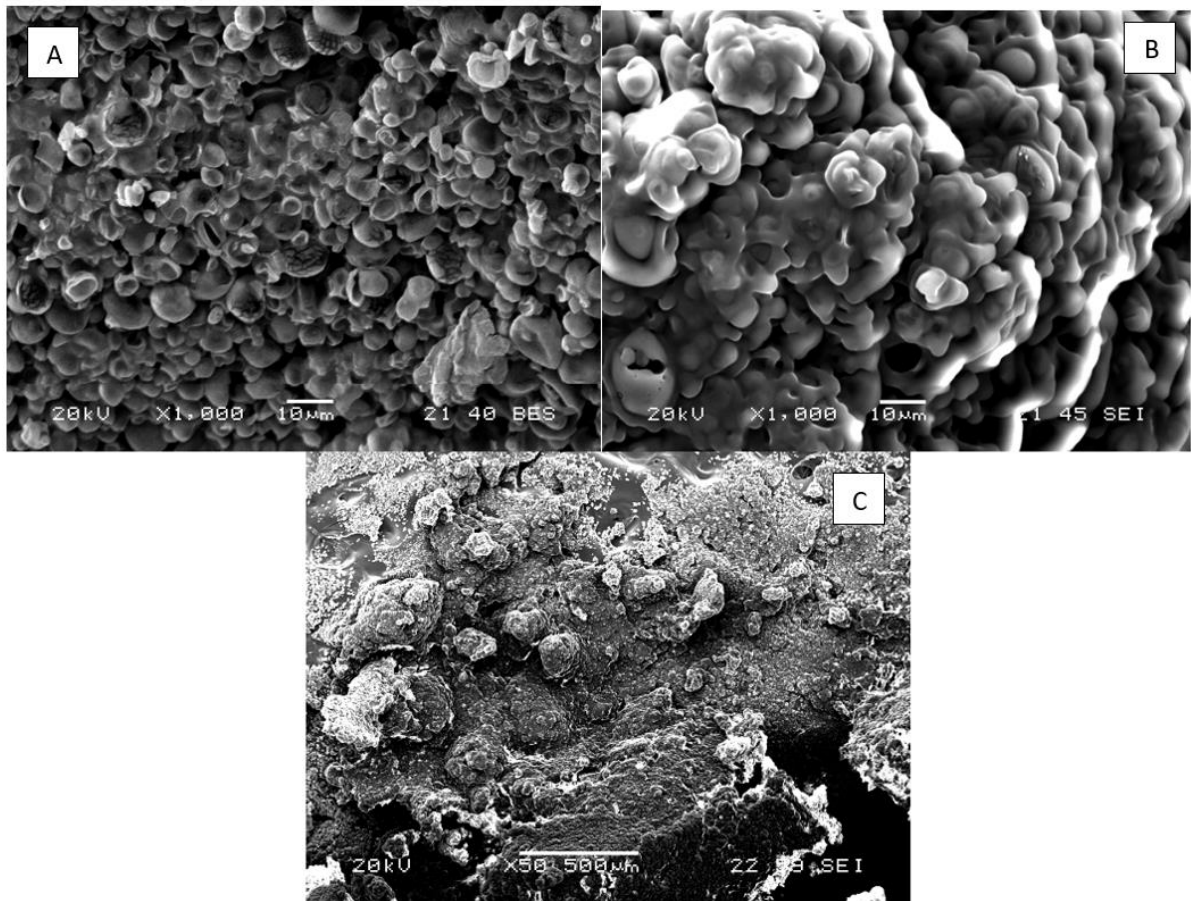


Figure 32. SEM images of ME-SD-C (A), RSH-SD-C (B) and ME-FD-C (C)

Where ME-SD-C is membrane emulsification and spray drying capsules; RSH-SD-C is rotor stator homogenization and spray drying capsules and ME-FD-C is membrane emulsification and freeze-drying capsules.

5.4.4. Oxidative stability of encapsulated flaxseed oil

The TBARS (Thiobarbituric Acid Reactive Substances) values presented in Figure 33 for the three samples after one month of storage provide insights about the oxidative stability of the oil.

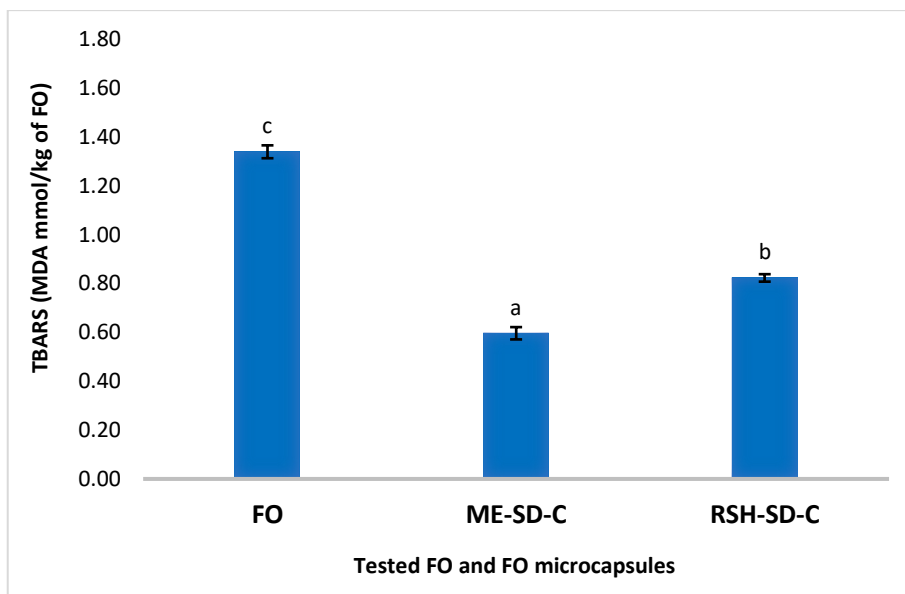


Figure 33. TBARS measurements in FO, ME-SD-C and RSH-SD-C after 30 days storage. Results are represented by mean value with standard deviation (\pm values). In superscript, dissimilar alphabet represents the significant difference between results, interpretation is performed with one-way ANOVA, and evaluated by the Tukey's HSD post hoc method.

Freeze dried capsules were not analyzed as the aim is to investigate the variation of emulsification technique in the oxidation stability of the microcapsules.

For the solely FO sample, the TBARS value of 1.34 mmol/kg indicates lipid oxidation likely due to the absence of any protection. In fact, FO is known for its high unsaturated fatty acid content, making it prone to oxidation when exposed to air, light, and heat. Therefore, the oil is vulnerable to oxidation, resulting in the observed high TBARS value.

In the other hand oil in ME-SD-C and RSH-SD-C had undergone protective techniques aiming to enhance the stability by providing a protective barrier against environmental factors which explains the lower TBARS values of 0.60 mmol/kg and 0.82 mmol/kg respectively. This suggest that both encapsulation processes were effective in reducing lipid oxidation during storage by creating a protective matrix around the oil droplets. It's also worth to mention that the difference in TBARS values between ME-SD-C and RSH-SD-C suggests that ME might have provided slightly better oxidative stability compared to rotor-stator homogenization. This can be explained by the higher stability of emulsion obtained through ME and the higher encapsulation efficiency. On the other hand, the droplet distribution can also have an effect as rotor-stator homogenization may not produce droplets as uniform as those obtained through ME so this slight difference in droplet size and distribution could influence the overall stability.

5.4.5. Powder characteristics

Moisture content, wettability, and solubility are crucial factors in optimized microcapsules. Lower moisture content generally indicating better stability. Wettability impacts the dispersion and absorption of the microcapsules, and solubility in the other hand is vital for ensuring effective delivery of the encapsulated compounds. In this regard, controlling these parameter helps with enhancing the functionality of microencapsulated FO. The results of these parameters are indicated in Table 25.

Table 25: Evaluation of moisture%, wettability and solubility% of optimized formulations

	Moisture%	Wettability (s)	Solubility%
ME-SD-C	1.21±0.9 ^a	166±5.5 ^a	71.20±0.75 ^b
RSH-SD-C	1.6±0.13 ^b	192±5.5 ^b	75.49±1.3 ^c
ME-FD-C	2.1±0.15 ^c	317±5.3 ^c	57.99±1.04 ^a

Where ME-SD-C is membrane emulsification and spray drying capsules; RSH-SD-C is rotor stator homogenization and spray drying capsules and ME-FD-C is membrane emulsification and freeze-drying capsules. Results are represented by mean value with standard deviation (\pm values). In superscript, dissimilar alphabet represents the significant difference between different groups of wall materials composition within Moisture% Wettability and, Solubility%, vertical way, interpretation is performed with MANOVA, with the output of Wilks' Lambda ($p < 0,001$) and evaluated by the Tukey's HSD post hoc method. According to Post hoc Tuckey's test, there is a significant difference between the moisture% wettability and, solubility% for ME-SD-C, RSH-SD-C and ME-FD-C.

Spray-dried samples (ME-SD-C and RSH-SD-C) showed lower moisture content of 1.21% and 1.6% compared to ME-FD-C 2.1%, which was expected as SD removes more moisture during heat processing. In the other hand ME-FD-C exhibited the highest wettability compared to RSH-SD-C and ME-SD-C, this could be explained by the higher presence of MD with its hydrophilic nature in the spray dried samples that might promote water absorption on the particle surface. Solubility result can also be explained by the abundant presence of MD in spray dried capsules and the higher microencapsulation efficiency these samples have compared to ME-FD-C. A more even distribution can also affect the solubility as it allows for easier access of water to some of the oil.

The wettability of a powder is considered the time needed for the particles to sink which is relate to the ability to rehydrate in water (Bae and Lee, 2008). Encapsulation efficiency could

have had an effect of the obtained results mentioned in Table 25 as wettability is significantly decreasing with the increase of EE% obtained for each optimized emulsion as due to the amount of non-encapsulated oil available on the surface the particles are more floating of the particles on the water. This was probably due to the high amount of not encapsulated oil available on the surface, which made the particles more susceptible to float on the water surface and not sink.

Table 26: Evaluation of bulk and tapped density for ME-SD-C and RSH-SD-C

	Bulk density (g/mL)	Tapped density (g/mL)	CI (%)	HR
ME-SD-C	0.39±0.020	0.43±0.01	9.30±0.02	1.10±0.01
RSH-SD-C	0.31±0.025	0.36±0.01	13.88±0.01	1.16±0.01

Where ME-SD-C is membrane emulsification and spray drying capsules; RSH-SD-C is rotor stator homogenization and spray drying capsules and ME-FD-C is membrane emulsification and freeze drying capsules. Results are represented by mean value with standard deviation (\pm values). In superscript, dissimilar alphabet represents the significant difference between different groups of wall materials composition within (Bulk density (g/mL)), (Tapped density (g/mL)), (CI (%)) and (HR). Interpretation is performed with MANOVA, with the output of Wilks' Lambda ($p < 0.001$) and evaluated by the Tukey's HSD post hoc method.

Bulk density and tapped density are critical factors for food industries as these characteristics can affect many stages of manufacturing, packaging, and handling in the food manufacturing process. Bulk density refers to the natural packing behaviour of food powder that indicates the volume occupied by a unit mass with minimal manipulation. On the other hand, tapped density, measures the packing efficiency achieved by a tapping technique which results in a more compact arrangement of particles. (Finney et al., 2002; Quispe-Condori et al., 2011). In our case in both bulk density and tapped density measurements the ME-SD-C had the highest values indicating that ME-SD-C can make better use of space and thus can be stored in a small container. The density values for ME-FD-C were not measured due the non-consistency of the results caused mainly by the method of obtaining the powder after FD as these were manually grounded. This result can be linked to the encapsulation efficiency results in which ME-SD-C had 86.05% and RSH-SD-C had 77.34 % which means ME-SD-C had more encapsulated oil load than RSH-SD-C leading to higher density. This can be

beneficial as it was investigated before that having high densities means that there is less free space between the particles which means lower risk of oxidation due to lower exposure to oxygen (Ndayishimiye, 2019).

Higher bulk density in Capsules ME-SD-C can also be related to the surface regularity of the microcapsules and the particle size homogeneity. In fact, the external morphology of the microcapsules especially if they are spherical shaped without much irregularity can be packed more closely and will result in a higher bulk density. Carr index (CI) and Hausner ratio (HR) are determined based on the Bulk Density and tapped density and they are important in analysing flowability and cohesiveness of the powders. ME-SD-C and RSH-SD-C had CI values of 9.30 and 13.88 and HR values of 1.10 and 1.16 respectively.

Values of Carr index lower than 15% and HR between 1 and 1.11 indicate excellent flow behaviour. HR between 1.12 and 1.18 indicates good flow behaviour, while values higher than 1.35 are associated to powders with poor flowability (Schlick-Hasper et al., 2022). Particles obtained through both emulsification processes have showed excellent to good flow properties with ME-SD-C being significantly better than RSH-SD-C.

6. SUMMARY

FO, a rich source of α -linolenic acid (ALA), exhibit many valuable health benefits. However, this very characteristic also bring some challenges as exposure to light, heat, and oxygen can degrade these delicate fatty acids, diminishing their nutritional value and introducing potentially harmful byproducts. This is where encapsulation technology steps in as a well-known process that can protects the oil that is prone to oxidation and improves its handling properties. This study investigates the use of response surface methodology (RSM) to optimize the encapsulation of FO using different combinations of wall materials and processing methods.

At the first stage, RSM, statistical technique was used with Box-Behnken design to optimize processes by evaluating the relationships between multiple independent variables and a desired response variable. In this study, the independent variables were Ratio of MD to GA; concentration of MS (wall material) and FO content. The response was expressed as encapsulation efficiency (EE). The encapsulation efficiency was measured for each experiment. The data was then analyzed using RSM software to develop a mathematical model that describes the relationship between the variables and the EE.

Results The RSM analysis showed that all three independent variables and their interactions significantly affected the encapsulation efficiency. The optimal conditions for maximizing EE through ME and SD were found to be: 0.689 MD/GA, 19.835% MS and 30.148% FO. Under these conditions, the predicted encapsulation efficiency was predicted at 85.93%. The optimal conditions for maximizing EE through Rotor stator homogenization and SD were found to be 0.79 MD/GA, 20.23% MS and 24.62% FO. Under these conditions, the predicted encapsulation efficiency was 77.68 %, and finally, the optimal conditions for maximizing EE through ME and FD were found to be: 0 MD/GA, 26.26% MS and 25.13% FO. Under these conditions, the predicted encapsulation efficiency was 74.59 %.

At a second stage the optimal composition from each encapsulation method was produced and analyzed through the study of the produced oil in water emulsion and the study of oil capsules after drying. The stability of the emulsions prepared using different encapsulation methods was assessed by measuring the zeta potential and separation percentage. Zeta potential is an indicator of the electrostatic repulsion between the oil droplets, which influences emulsion stability. The results showed that all emulsions had moderate stability, with zeta potential values between -29.5 mV and -41,3 mV. Emulsion droplet size was also analyzed giving the conclusion that ME samples resulted in larger droplets compared to the

rotor-stator homogenization one due to its gentler pressure-driven process. ME-FD-E, with no MD and more GA, had a smaller average droplet size compared to ME-SD-E despite using the same emulsification technique. This highlights the impact of wall material properties on droplet formation.

Powder characteristics was evaluated through the study of PSD and Oxidative Stability: ME-SD-C and ME-FD-C displayed a narrower distribution of particle sizes compared to RSH-SD-C. This suggests that ME might generate a more uniform distribution, potentially impacting encapsulation efficiency. Regarding oxidation all ME-SD-C and RSH-SD-C demonstrated significantly lower TBARS values compared to unencapsulated FO, indicating reduced lipid oxidation due to the protective barrier formed by the encapsulation materials. ME-SD-C exhibited a slightly lower TBARS value compared to RSH-SD-C, suggesting potentially better protection from ME. Additional observations were also done on encapsulated FO including moisture content, solubility, and bulk density.

As a conclusion, this study has made into light the effectiveness of encapsulation in protecting FO against environmental factors. ME appears to offer advantages in terms of emulsion stability, PSD which on its turn affect in a positive way the encapsulation efficiency and oxidative stability. It is worth to mention the importance of the choice of wall material composition as it plays a significant role in influencing these properties. Further research could explore the impact of these factors on other functionalities of the encapsulated oil.

7. NEW SCIENTIFIC RESULTS

[1] Statistical modeling of flaxseed oil encapsulation through membrane emulsification and spray drying technologies: By studying the impact of different formulations of carbohydrates namely Maltodextrin with 19 dextrose equivalent (MD), Gum arabic (GA), and High amylose maize modified starch (MS) in combination with varied amount of the different cold-pressed, filtered Flaxseed oil (FO) bioactive loads, on the Encapsulation efficiency (EE%) in case of a combined microcapsule production technology via membrane emulsification and spray drying, with the application of Response Surface Methodology RSM (Box-Behnken experimental design) as modeling tool, the encapsulation efficiency was determined with the following actual equation ($R^2=0.999$):

$$EE\% = 63.01 + 58.35 \frac{MD}{GA} + 0.76MS + 0.14FO - 0.16 \frac{MD}{GA} MS - 0.34 \frac{MD}{GA} FO - 32.60 \left(\frac{MD}{GA} \right)^2 - 0.02 MS^2 - 0.01FO^2$$

where MD/GA is the ratio between MD and GA ranging from 0 to 1, MS is the concentration of modified starch in wall material ranging from 0 to 40% (w/w), and FO is the Flaxseed load ranging from 10% to 40% (w/w).

[2] Statistical modeling of flaxseed oil encapsulation through rotor-stator homogenization and spray drying technologies: By studying the impact of different formulations of carbohydrates namely Maltodextrin with 19 dextrose equivalent (MD), Gum arabic (GA), and High amylose maize modified starch (MS) in combination with varied amount of the different cold-pressed, filtered Flaxseed oil (FO) bioactive loads, on the Encapsulation efficiency (EE%) in case of a combined microcapsule production technology via rotor stator homogenizer and spray drying, with the application of Response Surface Methodology RSM (Box-Behnken experimental design) as modeling tool, the encapsulation efficiency was determined with the following actual equation ($R^2=0.998$):

$$EE\% = 46.75 + 41.05 \frac{MD}{GA} + 0.78MS + 1.34FO - 0.08 \frac{MD}{GA} MS - 0.34 \frac{MD}{GA} FO - 19.98 \left(\frac{MD}{GA} \right)^2 - 0.02 MS^2 - 0.04FO^2$$

where MD/GA is the ratio between MD and GA ranging from 0 to 1, MS is the concentration of modified starch in wall material ranging from 0 to 40% (w/w), and FO is the flaxseed oil load ranging from 10% to 40% (w/w).

[3] Statistical modeling of flaxseed oil encapsulation through membrane emulsification and freeze drying technologies: By studying the impact of different formulations of carbohydrates namely Maltodextrin with 19 dextrose equivalent (MD), Gum arabic (GA), and High amylose maize modified starch (MS) in combination with varied amount of the different cold-pressed, filtered Flaxseed oil (FO) bioactive loads, on the Encapsulation efficiency (EE%) in case of a combined microcapsule production technology via membrane emulsification and freeze drying, with the application of Response Surface Methodology RSM (Box-Behnken experimental design) as modeling tool, the encapsulation efficiency was determined with the following actual equation ($R^2=0.998$):

$$EE\% = 66.10 - 0.39 \frac{MD}{GA} + 0.17MS + 1.18FO + 0.05 \frac{MD}{GA} MS - 0.25 \frac{MD}{GA} FO - 0.01 MS^2 - 0.04FO^2$$

where MD/GA is the ratio between MD and GA ranging from 0 to 1, MS is the concentration of modified starch in wall material ranging from 0 to 40% (w/w), and FO is the flaxseed load ranging from 10% to 40% (w/w).

[4] By setting the importance, the range, and the limit of our factors (maltodextrin (DE=19), Gum arabic, high amylose maize modified starch and cold-pressed, filtered flaxseed oil bioactive loads), I was able to determine an optimal combination to maximize the encapsulation efficiency while keeping a balanced oil load. The optimal wall material carbohydrate and oil combinations for the three investigated complex technology mentioned in the table below yielded good results in term of encapsulation efficiency.

Table 1: Composition of optimized formulation for flaxseed oil microencapsulation

	Optimized formulations of wall material and flaxseed oil		
	Membrane emulsification – Spray drying	Rotor stator homogenization – Spray drying	Membrane emulsification – Freeze drying
Ratio Maltodextrin/Gum arabic	0.69	0.79	0
Modified starch %	19.84	20.23	26.26
Flaxseed oil %	30.15	24.62	25.13
Encapsulation efficiency %	87.93	77.68	74.59

[5] Comparison between cross flow Membrane emulsification (ME) and Rotor stator homogenization (RSH) as emulsification techniques for producing flaxseed oil

microcapsules of optimized formulations: I found that the RSH (15000 rpm for 5min) produced smaller droplet sizes but exhibited less homogeneous distribution than membrane emulsification (1.4 um pore size, pressure 2 bar). Spray-dried microcapsules showed superior encapsulation efficiency for capsules achieved by cross flow ME and offered better oxidation protection than RSH for the resultant microcapsules. Results are mentioned in the table 2.

Table 2: Comparison between optimized flaxseed oil microcapsule obtained through membrane emulsification and rotor stator homogenization.

	ME	RSH
D _[4,3] Emulsion (µm)	26.73 ± 0.04	13.62 ± 0.08
Span (emulsion)	0.53 ± 0.07	1.3 ± 0.02
EE (%)	85.93	77.68
Oxidative stability (MDA mmol/kg of FO)	0.6 ± 0.03	0.82 ± 0.02

[6] Comparison between emulsions and microcapsules properties of optimized formulations produced through membrane emulsification (ME) intended for spray drying (SD) and freeze drying (FD): I found that, for emulsion intended for FD (Temperature -109°C, vacuum pressure 12Pa) excluding maltodextrin and using only Gum arabic alongside high amylose maize modified starch resulted in smaller droplet size and enhanced stability. Furthermore, SD (nozzle diameter 0.5mm, inlet temperature of 185 ± 5°C and outlet temperature of 105 ± 5°C) offered a more homogeneous distribution and lower moisture content compared to FD. Additionally, SD microcapsules exhibited increased solubility and higher encapsulation efficiency (EE%) compared to FD, thereby establishing ME and SD as the optimal combination for achieving high EE% with moderate flaxseed oil load. Results are mentioned in the table 3.

Table 3: Comparison between optimized flaxseed oil microcapsule obtained through membrane emulsification followed by spray drying and freeze drying

	Membrane emulsification – Spray drying	Membrane emulsification – Freeze drying
D _[4,3] (µm) (droplets)	26.73 ± 0.04	23.59 ± 0.04
Span (capsules)	2.29 ± 0.18	2.95 ± 0.26
Separation (%)	10 ± 0.5	7 ± 0.5
Moisture content (%)	1.21 ± 0.9	2.1 ± 0.15
Solubility (%)	71.20 ± 0.75	57.99 ± 1.04

8. Appendix

Appendix Table 1. Characteristics of matrix used for microencapsulation of flaxseed oil.

Matrix	Source	Characteristics	Advantages	Disadvantages	Reference
Gum arabic	Extracted from <i>Acacia senegal</i> (L.) or <i>Acacia seyal</i> (L.).	<ol style="list-style-type: none"> 1. It is a mixture of polysaccharides, oligosaccharides, and glycoproteins. 2. Hydrolysis of polysaccharides produce arabinose, galactose, rhamnose, and glucuronic acid. 3. It is soluble in water. 	<ol style="list-style-type: none"> 1. Well accepted film-forming ability. 2. It has emulsifying property due to presence of protein. 3. Low viscosity in aqueous solution. 4. Stable in aqueous emulsion. 5. High solubility in aqueous solution. 6. Good retention of flavor. 	<ol style="list-style-type: none"> 1. Expensive. 2. Variable availability and quality. 3. Limited potentiality to prevent oxidation of encapsulated item. 	(Anandharamakrishnan and Padma Ishwarya, 2015; Fang and Bhandari, 2012)
Maltodextrin	Enzymatically derived from corn (<i>Zea mays</i>), potato (<i>Solanum tuberosum</i> L.), rice (<i>Oryza sativa</i>) and wheat (<i>Triticum aestivum</i> L.) starches.	MD consists of D-glucose, linked with $\alpha(1\rightarrow4)$ glycosidic bond. MD can be of variable length according to degree of polymerization. Typically, it varies from 3 to 17 glucose units. MDs are classified according to dextrose equivalent. The higher value of dextrose equivalent signifies shorter glucose chain, higher solubility, higher sweetness, and lower heat resistance.	<ol style="list-style-type: none"> 1. Low cost. 2. High potentiality to prevent oxidation of encapsulated item. 3. Easily digestible in intestine. 4. Highly soluble in water. 5. Low viscosity with high solid content in emulsion. 6. Heat resistance. 	<ol style="list-style-type: none"> 1. Poor emulsifying property. 2. Poor flavor retention. 3. Sometimes offer allergenic activity. 	(Anandharamakrishnan and Padma Ishwarya, 2015)
Modified starch	Native starch is collected from corn (<i>Zea mays</i>), potato (<i>Solanum tuberosum</i> L.), rice (<i>Oryza sativa</i>)	It is prepared by physical, enzymatic, or chemical treatment of native starch, which changes according to the property of native starch.	<ol style="list-style-type: none"> 1. Well soluble in water. 2. Low viscosity. 3. Excellent volatile compound retention. 4. Excellent emulsifying property. 	Provide allergenicity to food due to presence of gluten.	(Anandharamakrishnan and Padma Ishwarya, 2015; Fang and

Matrix	Source	Characteristics	Advantages	Disadvantages	Reference
	and wheat (<i>Triticum aestivum</i> L.) starches.		5. Provide stability in emulsion. 6. Heat stable. 7. Odorless and tasteless. 8. Low cost.		Bhandari, 2012; Mishra, 2015)
Methyl cellulose	Methyl cellulose is not present in plant cell wall. After collection of natural cellulose from plant cell wall, it is produced by heat treatment of native cellulose with sodium hydroxide solution and treating with methyl chloride.	Different types of methyl cellulose are produced by substitution of different number of hydroxyl group. It has amphiphilic property.	1. Stable viscosity over a wide range of pH (pH 3-11). 2. Heat stable. 3. Odorless and tasteless. 4. High emulsifying property due to its amphiphilic structure. 5. Satisfactory film-forming ability.	Low solubility with higher degree of polymerization.	(Mishra, 2015; Shahidi and Han, 1993)
Whey protein	Dairy milk	Is a mixture of α -lactalbumin (molecular weight: 14.2 kDa, isoelectric point: 4.2), β -globulin (molecular weight: 18.3 kDa, isoelectric point: 5.2–5.4), serum albumin (molecular weight: 66 kDa, isoelectric point: 4.9–5.1), lactoperoxidase (molecular weight: 78 kDa, isoelectric point: 9.6), lactoferrin (molecular weight: 78 kDa, isoelectric point: 8), immunoglobulin G (molecular weight: 150 kDa, isoelectric point: 6.5–9.5), immunoglobulin A	1. High solubility in aqueous solution. 2. Satisfactory film-forming ability. 3. Efficient to protect from oxidation. 4. Good emulsifying property due to its amphiphilic structure.	1. Coagulate at lower pH of the emulsion. 2. Heat sensitive. 3. Provide allergenicity to food.	(Anandharamakrishnan and Padma Ishwarya, 2015)

Matrix	Source	Characteristics	Advantages	Disadvantages	Reference
		(molecular weight: 320 kDa, isoelectric point: 4.5–6.5) and immunoglobulin M (molecular weight: 900 kDa, isoelectric point: 4.5–6.5). 2. All whey proteins may denature with heat treatment ~70 °C for 20 min, but does not aggregate due to renneting or acidification of milk.			
Sodium caseinate	Dairy milk	Casein is a phospho protein. There are different types of casein proteins, such as α_{s1} -casein, α_{s2} -casein, β -casein and κ -casein are present in casein fraction of milk. It is produced by neutralisation of acid precipitated casein with sodium hydroxide.	<ol style="list-style-type: none"> 1. Highly soluble in aqueous solution. 2. Good film-forming ability. 3. High denaturation temperature. 4. Good emulsifying property due to presence of hydrophilic and hydrophobic amino acids in protein structure. 	<ol style="list-style-type: none"> 1. Coagulate at lower pH of the emulsion. 2. Provide allergenicity to food. 	(Anandharamakrishnan and Padma Ishwarya, 2015)
Vegetable proteins, such as Lentil, Chickpea, Flaxseed, Soya, Pea protein etc.	Proteins from lentil (<i>Lens culinaris</i>), chickpea (<i>Cicer arietinum</i>), flaxseed (<i>Linum usitatissimum</i>), soybean (<i>Glycine max</i>), pea (<i>Pisum sativum</i>)	Proteins from different plant sources have unique amino acid sequence. Because of it, they offer variety of biochemical activities.	<ol style="list-style-type: none"> 1. Inexpensive and available throughout the year. 2. Highly soluble in aqueous solution. 3. Good film-forming ability. 4. Efficient to protect from oxidation. 5. Good emulsifying property due to amphiphilic structure. 	<ol style="list-style-type: none"> 1. Coagulate at lower pH of the emulsion. 2. Heat sensitive. 3. Some of vegetable proteins, such as chickpea and soya-based proteins may provide allergenicity to food product. 	(Can Karaca et al., 2013; Fang and Bhandari, 2012; Mishra, 2015)

Appendix Table 2. Process conditions for producing encapsulated flaxseed oil and their biochemical characterization.

Process	Wall material (matrix)	Oil content	Emulsifier	Particle size	Encapsulation efficiency (%)	Moisture content %	Oxidative stability	References
Bench top spray dryer	Combinations of chickpea protein isolate and maltodextrin	10%	-	16.3-24.0 μm	88.72	3.66 - 4.07	Peroxide value 6.68 - 7.31 meq active O_2 / kg for chickpea protein isolate.	(Can Karaca et al., 2013)
		15%			86.69			
		20%			83.62			
	Combinations of lentil protein isolate and maltodextrin	10%		21.0 – 26.1 μm	90.42	3.65 - 4.12	Peroxide value 6.62- 6.86 meq active O_2 / kg for lentil protein isolate.	
		15%			87.89			
		20%			85.61			
Spray drying	Combinations of whey protein isolate, methyl cellulose, maltodextrin, Gum arabic and soya lecithin	>20%	Soya lecithin	10 - 50 μm	~ 90	1.8 - 3.1	Rancimat induction period after 10 months (h) for GA + soya lecithin: 5.9, GA + MD + soya lecithin: 2.8, GA + MD + whey protein isolate + soya lecithin: 6.8	(Gallardo et al., 2013)
Coacervation, Spray drying, Freeze drying	Flaxseed gum, Flaxseed protein isolate	Oil-to-wall ratios 1:2, 1:3 and 1:4	-	For liquid microcapsules 90 - 130 μm	Maximum value 87.60 by SD and 67.06 by FD	3.20 - 3.70 for spray drying and 4.18 - 4.47 for freeze drying	Peroxidase value (meq active O_2 /kg) after 30 days are 2.85-5.52 for SD and 3.25-8.72 for FD.	(Kaushik et al., 2016)
Spray drying	Combination of maltodextrin and Gum arabic	14% and 20%	-	17.6 - 23.1 μm	54.6 - 90.7. The highest encapsulation efficiency was achieved with 14% oil.	-	Induction time 2.83 ± 0.62 h, Oxidative stability index 3.78 h for 14% oil.	(Rubilar et al., 2012)

Process	Wall material (matrix)	Oil content	Emulsifier	Particle size	Encapsulation efficiency (%)	Moisture content %	Oxidative stability	References
Spray drying	Combination of maltodextrin, whey protein concentrate, Gum arabic, Modified starch 100 Hi-Cap	20%	-	Droplet diameter: 0.6 - 26 μm	62.3 - 95.7, The lowest value obtained for MD and whey protein concentrate	1% - 3%	Peroxidase value (meq peroxide/kg oil) after 4 weeks for GA + MD: 138, MS + MD 138, Hi-Cap + MD: 124, Whey protein concentrate + MD: 107	(Carneiro et al., 2013)
Spray drying, Freeze drying	Zein	-	-	-	For SD 93.26 ± 0.95 and for FD 59.63 ± 0.36	For SD 3.49 - 5.06 and FD 4.94 - 5.33	-	(Quispe-Condori et al., 2011)
Spray drying	Gum arabic Whey protein concentrate Modified starch Hi-Cap 100	10% 20% 30% 40%	-	0.24 - 180 μm	37 - 97. Emulsions prepared with MS had the highest encapsulation efficiency, whereas emulsion prepared with whey protein concentrate had lowest encapsulation efficiency.	0.36 - 0.78 for whey protein concentrate, 0.89- 1.74 for GA, 0.19 - 0.53 for MS Hi-Cap 100	Peroxidase value (meg peroxide/kg oil) for MS Hi-Cap 100 is 0.5 – 1.8, 3.1-4 for GA and 1,3-2 for whey protein concentrate.	(Tonon et al., 2012)
Freeze drying	Combination of lentil protein isolates and maltodextrin	10%, 20% 30%	-	4.2 - 6.7 μm	Highest encapsulation efficiency ~62.8	< 6.0%	Peroxide value on day 30 for 4.0% native lentil protein isolates + 36% MD + 10% oil 25.57 and 14.75 meq of active O_2 / kg for free oil and entrapped oils, respectively.	(Avramenko et al., 2016)

Process	Wall material (matrix)	Oil content	Emulsifier	Particle size	Encapsulation efficiency (%)	Moisture content %	Oxidative stability	References
Spray drying	Combination of whey proteins concentrate, sodium caseinate, lactose and ascorbyl palmitate	12.5%	-	0.54 - 70.6 μm	86.77% - 84.51%	3.88 - 3.98	Peroxide value after 6 months varied from 0.81 to 0.99 meq peroxides/ kg	(Goyal et al., 2015)
Spray drying	Modified starch	30%	-	0.5 - 100 μm	90.9%	3.5%	Induction period of the microcapsules exceeded 50 h for all times.	(Barroso et al., 2014)
Spray drying	Combination of Gum arabic, maltodextrin, skimmed milk powder and tween 80	8% - 22%	Tween 80	-	70% - 86%	3.2% - 4.8%	Peroxide value varied from 1 - 1.28 meq/ kg	(Thirundas et al., 2014)
Spray drying	Gum arabic	10% - 30%	-	0.1 - 477 μm	51% - 92%	-	Peroxide value 0.017 - 0.106 meq peroxide/ kg oil	(Tonon et al., 2011)
Spray drying	Combination of whey protein concentrate, sodium alginate and maltodextrin	4.5% - 5%	-	1 - 10 μm	30.69% - 84.39%	-	Peroxidase value (meq/ kg oil) 3.46 - 6.84	(Fioramonti et al., 2019)
Freeze drying	Combination of whey protein isolate, maltodextrin and, sodium alginate	10%	-	-	27.01% - 95.44%	-	Peroxide value for emulsion with 20.24 total solids content (g/100 g emulsion) was increased from 1.5 to 46.5 meq/kg oil after FD.	(Fioramonti et al., 2017)

Process	Wall material (matrix)	Oil content	Emulsifier	Particle size	Encapsulation efficiency (%)	Moisture content %	Oxidative stability	References
Freeze drying	Combination of tertiary conjugate of gelatin, flaxseed mucilage and oxidized tannic acid	15 %, 30% and 50%	-	-	>90%	-	Peroxide value increased from 3.0 - 5.3 meq O ₂ / kg	(Mohseni and Goli, 2019)
Spray drying	Combination of maltodextrin and pea protein Isolate	20% and 40%	-	Particle size distribution (PSD) ~ 24 µm	35.2% - 95.6% for 20% oil and 22.3% - 93.6% for 40% oil	-	-	(Bajaj et al., 2017)
Spray drying	Combination of maltodextrin and whey protein concentrate	20%	-	5.47 - 7.09 µm	ranged between 81.3% - 95.3%	3.16 - 4.91% (weight basis)	-	(Tontul and Topuz, 2014)
Spray drying	Different combinations of soya protein isolate, pea protein isolate, wheat dextrin soluble fiber and trehalose	35%	-	Mean diameter of particles 18 - 40 µm	Microcapsules with the protein-trehalose matrix 98% - 94%. Microcapsules with the protein-soluble fibre matrix 81% - 62%	1.5% - 2.3%	Peroxide value of microencapsulated oil before storage: 1.80 - 7.90 meqO ₂ / kg and after 12 weeks 4 - 27 meqO ₂ /kg.	(Domian et al., 2017)

Process	Wall material (matrix)	Oil content	Emulsifier	Particle size	Encapsulation efficiency (%)	Moisture content %	Oxidative stability	References
Spray drying	Gum arabic	10%		Droplets mean diameter 1.854 μm	~92 %	-	Peroxide value ~0.032 meq/kg oil	(Pedro et al., 2011)
		20%		Droplets mean diameter 2.191 μm	~75%		Peroxide value ~0.036 meq/kg oil	
		30%		Droplets mean diameter 2.479 μm	~52%		Peroxide value ~0.036 meq/kg oil	
		40%		Droplets mean diameter 3.464 μm	~40%		Peroxide value ~0.04 meq/kg oil	



Appendix - Figure 1: Spectrophotometer (U-2900 Hitachi Ltd., Japan)



Appendix - Figure 2: Membrane module



Appendix - Figure 3: Fritsch Analysette 22



Appendix - Figure 4: Laser Diffraction: Bettersize ST



Appendix - Figure 5: A Malvern Zetasizer



Appendix - Figure 6: Picture of a selection of dried microcapsule.

9. REFERENCES

Alam, M. N., Aqueous Dispersions of Curcumin: Preparation and Applications, INTECH Open Access (2015)

Anandharamakrishnan C.; Padma Ishwarya S. spray drying Techniques for Food Ingredient Encapsulation. spray drying Techniques for Food Ingredient Encapsulation. 2015. 1–296 p.

Aronson M.P. The Role of Free Surfactant in Destabilizing Oil-in-Water Emulsions. Langmuir. 1989.

Avramenko N.A.; Chang C.; Low N.H.; Nickerson M.T. Encapsulation of Flaxseed oil within native and modified lentil protein-based microcapsules. Food Res Int. 2016.

Bae, E. K., and Lee, S. J. (2008). Microencapsulation of avocado oil by spray drying using whey protein and MD. Journal of Microencapsulation, 25(8), 549–560

Bai L, Huan S, Rojas OJ, McClements DJ. Recent Innovations in Emulsion Science and Technology for Food Applications. J Agric Food Chem. 2021 Aug 18;69(32):8944-8963.

Bajaj P.R.; Bhunia K.; Kleiner L.; Joyner (Melito) H.S.; Smith D.; Ganjyal G.; et al. Improving functional properties of pea protein isolate for microencapsulation of Flaxseed oil. J Microencapsul. 2017.

Bakry A.M.; Abbas S.; Ali B.; Majeed H.; Abouelwafa M.Y.; Mousa A.; et al. Microencapsulation of Oils: A Comprehensive Review of Benefits, Techniques, and Applications. Compr Rev Food Sci Food Saf. 2016;15(1):143–82.

Bakry, A.M., Abbas, S., Ali, B., Majeed, H., Abouelwafa, M.Y., Mousa, A. and Liang, L. (2015): Microencapsulation of Oils: A Comprehensive Review of Benefits, Techniques, and Applications; Comprehensive Reviews in Food Science and Food Safety; 15(1); 143-182.

Balić A.; Vlašić D.; Žužul K.; Marinović B.; Mokos Z.B. Omega-3 versus Omega-6 polyunsaturated fatty acids in the prevention and treatment of inflammatory skin diseases. International Journal of Molecular Sciences. 2020.

Barroso A.K.M.; Pierucci A.P.T.R.; Freitas S.P.; Torres A.G.; Rocha-Leão M.H.M. Da. Oxidative stability and sensory evaluation of microencapsulated Flaxseed oil. *J Microencapsul.* 2014.

Bas, D., and Boyacı, I. H. (2007). Modelling and optimization II: Comparison of estimation capabilities of response surface methodology with artificial neural networks in a biochemical reaction. *Journal of Food Engineering*, 78, 846–854.

Beikzadeh, S., Shojaee-Aliabadi, S., Dadkhodazade, E., Sheidaei, Z., Abedi, A., Mirmoghtadaie, L., Hosseini, S.M. (2020). Comparison of Properties of Breads Enriched with Omega-3 Oil Encapsulated in β -Glucan and *Saccharomyces cerevisiae* Yeast Cells.

Bolger, Z., Brunton, N. P., & Monahan, F. J. (2018). Impact of inclusion of flaxseed oil (pre-emulsified or encapsulated) on the physical characteristics of chicken sausages. *Journal of Food Engineering*, 230(August), 39–48

Buffo, Roberto and Reineccius, G.A. (2000). Optimization of gum acacia/modified starch/maltodextrin blends for the spray drying of flavors. *Perfumer and Flavorist*. 25. 45-54.

Can Karaca A.; Low N.; Nickerson M. Encapsulation of Flaxseed oil using a benchtop spray dryer for legume protein-MD microcapsule preparation. *J Agric Food Chem.* 2013.

Carneiro H.C.F.; Tonon R. V.; Grosso C.R.F.; Hubinger M.D. Encapsulation efficiency and oxidative stability of Flaxseed oil microencapsulated by spray drying using different combinations of wall materials. *J Food Eng.* 2013.

Chao Wang, Guogang Xu, Xinyue Gu, Peng Zhao, Yuanhui Gao, Recycling of waste attapulgite to prepare ceramic membranes for efficient oil-in-water emulsion separation, *Journal of the European Ceramic Society*, Volume 42, Issue 5, 2022, Pages 2505-2515,

Charcosset C. Preparation of emulsions and particles by microencapsulation for the food processing industry. *J Food Eng.* 2009;92(3):241–9.

Charcosset C.; Limayem I.; Fessi H. (2004). The microencapsulation process - A review. *J Chem Technol Biotechnol.*79(3):209–18.

Charcosset, C. (2009). Preparation of emulsions and particles by microencapsulation for the food processing industry. *Journal of Food Engineering*.

Chranioti, C., and Tzia, C. (2013). Arabic Gum Mixtures as Encapsulating Agents of Freeze-Dried Fennel Oleoresin Products. *Food and Bioprocess Technology*

Comunian T.A.; Favaro-Trindade C.S. Microencapsulation using biopolymers as an alternative to produce food enhanced with phytosterols and omega-3 fatty acids: A review. *Food Hydrocolloids*. 2016.

Dell C.A.; Likhodii S.S.; Musa K.; Ryan M.A.; Burnham W.M.I.; Cunnane S.C. Lipid and fatty acid profiles in rats consuming different high-fat ketogenic diets. *Lipids*. 2001.

Desai K.G.H.; Park H.J. Recent developments in microencapsulation of food ingredients. *Drying Technology*. 2005.

Desobry S.A.; Netto F.M.; Labuza T.P. Desobry1997_J Food Sc_comparison of spray dryingDD freeze drying for beta carotene preservation. 1997;62(6):1158–62.

Domian E.; Brynda-Kopytowska A.; Marzec A. Functional Properties and Oxidative Stability of Flaxseed oil Microencapsulated by spray drying Using Legume Proteins in Combination with Soluble Fiber or Trehalose. *Food Bioprocess Technol*. 2017.

El-Beltagi, H. & Amin Mohamed, A., (2010). Variations in fatty acid composition, glucosinolate profile and some phytochemical contents in selected oil seed rape (*Brassica napus* L.) cultivars. *Grasas y Aceites*. 61. 143-150.

Elik, A., Koçak Yanık, D., and Göğüş, F. (2021). A comparative study of encapsulation of carotenoid enriched flaxseed oil and Flaxseed oil by spray freeze drying and spray drying techniques. *LWT*, 143, 111153.

Ezhilarasi, P. N., Indrani, D., Jena, B. S., and Anandharamakrishnan, C. (2013). freeze drying technique for microencapsulation of *Garcinia* fruit extract and its effect on bread quality. *Journal of Food Engineering*, 117, 513–520

Fang Z.; Bhandari B. Spray drying, freeze drying and related processes for food ingredient and nutraceutical encapsulation. In: Encapsulation Technologies and Delivery Systems for Food Ingredients and Nutraceuticals. 2012.

Finney, J., Buffo, R., and Reineccius, G. A. (2002). Effects of type of atomization and processing temperatures on the physical properties and stability of spray-dried flavors. *Journal of Food Science*, 67, 1108–1114.

Fioramonti S.A.; Rubiolo A.C.; Santiago L.G. Characterisation of freeze-dried Flaxseed oil microcapsules obtained by multilayer emulsions. *Powder Technol.* 2017.

Fioramonti S.A.; Stepanic E.M.; Tibaldo A.M.; Pavón Y.L.; Santiago L.G. Spray dried Flaxseed oil powdered microcapsules obtained using milk whey proteins-alginate double layer emulsions. *Food Res Int.* 2019.

Friberg S.E.; Corkery R.W.; Blute I.A. Phase inversion temperature (PIT) emulsification process. *J Chem Eng Data.* 2011.

Fuchs, M., et al. (2006). Encapsulation of oil in powder using spray drying and fluidised bed agglomeration. *Journal of Food Engineering*, 75(1), 27–35.

Gaikwad S.G.; Pandit A.B. Ultrasound emulsification: Effect of ultrasonic and physicochemical properties on dispersed phase volume and droplet size. *Ultrason Sonochem.* 2008.

Gallardo G.; Guida L.; Martinez V.; López M.C.; Bernhardt D.; Blasco R.; et al. Microencapsulation of linseed oil by spray drying for functional food application. *Food Res Int.* 2013.

Gharsallaoui A.; Roudaut G.; Chambin O.; Voilley A.; Saurel R. Applications of spray drying in microencapsulation of food ingredients: An overview. *Food Research International.* 2007.

Gibson R.A.; Muhlhausler B.; Makrides M. Conversion of linoleic acid and alpha-linolenic acid to long-chain polyunsaturated fatty acids (LCPUFAs), with a focus on pregnancy, lactation and the first 2 years of life. *Maternal and Child Nutrition.* 2011.

Gouin S. Microencapsulation: Industrial appraisal of existing technologies and trends. In: Trends in Food Science and Technology. 2004.

Goula, A. M. (2004). spray drying of Tomato Pulp: Effect of Feed Concentration. *Drying Technology*, 22(10), 2309–2330.

Gowda A.; Sharma V.; Goyal A.; Singh A.K.; Arora S. Process optimization and oxidative stability of omega-3 ice cream fortified with Flaxseed oil microcapsules. *J Food Sci Technol*. 2018.

Gowda, A., Sharma, V., Goyal, A., Singh, A. K., and Arora, S. (2018). Process optimization and oxidative stability of omega-3 ice cream fortified with Flaxseed oil microcapsules. *Journal of Food Science and Technology*, 55(5), 1705–1715.

Goyal A.; Sharma V.; Sihag M.K.; Singh A.K.; Arora S.; Sabikhi L. Fortification of dahi (Indian yoghurt) with omega-3 fatty acids using microencapsulated Flaxseed oil microcapsules. *J Food Sci Technol*. 2016.

Goyal A.; Sharma V.; Sihag M.K.; Singh A.K.; Arora S.; Sabikhi L. Oxidative stability of alpha-linolenic acid (ω -3) in Flaxseed oil microcapsules fortified market milk. *Int J Dairy Technol*. 2017.

Goyal A.; Sharma V.; Sihag M.K.; Tomar S.K.; Arora S.; Sabikhi L.; et al. Development and physico-chemical characterization of microencapsulated Flaxseed oil powder: A functional ingredient for omega-3 fortification. *Powder Technol*. 2015.

Goyal A.; Sharma V.; Upadhyay N.; Gill S.; Sihag M. Flax and FO: an ancient medicine and modern functional food. *Journal of Food Science and Technology*. 2014.

Goyal, A., Sharma, V., Sihag, M. K., Tomar, S. K., Arora, S., Sabikhi, L., and Singh, A. K. (2015). Development and physico-chemical characterization of microencapsulated Flaxseed oil powder: A functional ingredient for omega-3 fortification. *Powder Technology*, 286, 527–537

Guesmi, R.; Benbettaieb, N.; Ben Romdhane, M.R.; Barhoumi-Slimi, T.; Assifaoui, A. In Situ Polymerization of Linseed Oil-Based Composite Film: Enhancement of Mechanical

and Water Barrier Properties by the Incorporation of Cinnamaldehyde and Organoclay. *Molecules* 2022, 27, 8089.

Gunstone F.D. *Vegetable Oils in Food Technology: Composition, Properties and Uses*, Second Edition. 2011.

Hall C.; Tulbek M.C.; Xu Y. *Flaxseed. Advances in Food and Nutrition Research*. 2006.

Harvey K.L.; Holcomb L.E.; Kolwicz S.C. *Ketogenic Diets and Exercise Performance. Nutrients*. 2019.

Haseley P.; Oetjen G.-W. *Foundations and Process Engineering. In: freeze drying 3e*. 2017.

Holstun J.; Zetocha D. *An analysis of flaxseed utilization in the health food industry*. 1994;(January).

Kairam, N., Kandi, S., and Sharma, M. (2021). Development of functional bread with Flaxseed oil and garlic oil hybrid microcapsules. *LWT*, 136, 110300.

Kaur N.; Chugh V.; Gupta A.K. *Essential fatty acids as functional components of foods- a review. Journal of Food Science and Technology*. 2014.

Kaushik P.; Dowling K.; McKnight S.; Barrow C.J.; Adhikari B. *Microencapsulation of Flaxseed oil in flaxseed protein and flaxseed gum complex coacervates. Food Res Int*. 2016.

Keogh M. *Spray-Dried Microencapsulated Fat Powders*. In 2005.

Kinyanjui T.; Artz W.E.; Mahungu S. *EMULSIFIERS | Organic Emulsifiers*. In: *Encyclopedia of Food Sciences and Nutrition*. 2003.

Kouadio Jean Eric-Parfait Kouamé, Awa Fanny Massounga Bora, Xiaodong Li, Yue Sun, Lu Liu, *Novel trends and opportunities for microencapsulation of Flaxseed oil in foods: A review, Journal of Functional Foods, Volume 87, 2021, 104812, ISSN 1756-4646,*

Krishnan S, Bhosale R, Singhal RS. *Microencapsulation of cardamom oleoresin: Evaluation of blends of GA, maltodextrin and a modified starch as wall materials. Carbohydrate Polymers*. 2005 Jul;61(1):95-102.

Krishnan, S., Kshirsagar, A. C., and Singhal, R. S. (2005). The use of Gum arabic and modified starch in the microencapsulation of a food flavoring agent. *Carbohydrate Polymers*, 62, 309–315.

Lopez-Montilla J.C.; Herrera-Morales P.E.; Pandey S.; Shah D.O. Spontaneous emulsification: Mechanisms, physicochemical aspects, modeling, and applications. *J Dispers Sci Technol*. 2002.

Li, S. (2010). Influence of wall materials on the properties of emulsions prepared by ME. *Journal of Food Engineering*, 97(4).

Li, X., Zhao, S., Guo, J., Li, W., and Zhang, J. (2022). Novel Rotor-Stator Assembly Promotes the Emulsification Performance in an Inline High-Shear Mixer. *Industrial and Engineering Chemistry Research*, 61(13), 4722–4737.

Liu T.T.; Yang T.S. optimization of emulsification and microencapsulation of evening primrose oil and its oxidative stability during storage by response surface methodology. *J Food Qual*. 2011.

Ludwig D.S. The Ketogenic Diet: Evidence for Optimism but High-Quality Research Needed. *J Nutr*. 2020.

Maa, Y. F., & Hsu, C. (1996). Liquid-liquid emulsification by rotor/stator homogenization. *Journal of Controlled Release*, 38(2–3), 219–228.

Malik M.A.; Wani M.Y.; Hashim M.A. Microemulsion method: A novel route to synthesize organic and inorganic nanomaterials. 1st Nano Update. *Arabian Journal of Chemistry*. 2012.

Mao, L., Yang, J., Yuan, F., Gao, Y., Zhao, J., (2009). Effects of Small and Large Molecule Emulsifiers on the Characteristics of β -Carotene Nanoemulsions Prepared by High Pressure Homogenization. *Food Technology and Biotechnology*. 47.

Massounga Bora A.F.; Li X.; Zhu Y.; Du L. Improved Viability of Microencapsulated Probiotics in a Freeze-Dried Banana Powder During Storage and Under Simulated Gastrointestinal Tract. *Probiotics Antimicrob Proteins*. 2019.

Matusiak, Jakub and Grządka, Elżbieta. (2017). Stability of colloidal systems-a review of the stability measurements methods. *Annales - Universitatis Mariae Curie-Sklodowska, Sectio AA*. LXXII. 33-45. 10.17951/aa.2017.72.1.33

Mawilai P.; Chaloeichitratham N.; Pornchaloempong P. Processing feasibility and qualities of freeze-dried mango powder for SME scale. In: *IOP Conference Series: Earth and Environmental Science*. 2019.

McClements, D. J., and Jafari, S. M. (2018). Improving emulsion formation, stability and performance using mixed emulsifiers: A review. *Advances in Colloid and Interface Science*, 251, 55–79.

McClements, D. J., *Food Emulsions: Principles, Practices, and Applications (Second Edition)*, John Wiley and Sons (2017)

Mishra M. Overview of Encapsulation and Controlled Release. In: *Handbook of Encapsulation and Controlled Release*. 2015.

Mohseni F.; Goli S.A.H. Encapsulation of Flaxseed oil in the tertiary conjugate of oxidized tannic acid-gelatin and flaxseed (*Linum usitatissimum*) mucilage. *Int J Biol Macromol*. 2019.

Mori C.; Kadota K.; Tozuka Y.; Shimosaka A.; Yoshida M.; Shirakawa Y. Application of nozzleless electrostatic atomization to encapsulate soybean oil with solid substances. *J Food Eng*. 2019.

Mourtzinis I.; Biliaderis C.G. Principles and applications of encapsulation technologies to food materials. In: *Thermal and Nonthermal Encapsulation Methods*. 2017.

Nabilah A.; Handayani S.; Setiasih S.; Rahayu D.U.C.; Hudiyono S. Emulsifier and antimicrobial activity against *Propionibacterium acnes* and *Staphylococcus epidermidis* of oxidized fatty acid esters from hydrolyzed castor oil. In: *IOP Conference Series: Materials Science and Engineering*. 2020.

Nazari M.; Mehrnia M.A.; Jooyandeh H.; Barzegar H. Preparation and characterization of water in sesame oil microemulsion by spontaneous method. *J Food Process Eng*. 2019.

Ndayishimiye, Ferrentino, G., Nabil, H., and Scampicchio, M. (2019). Encapsulation of Oils Recovered from brewer's Spent Grain by Particles from Gas Saturated Solutions Technique. *Food and Bioprocess Technology*, 13(2), 256–264.

Onsaard E.; Onsaard W. Microencapsulated Vegetable Oil Powder. In: *Microencapsulation - Processes, Technologies and Industrial Applications*. 2019.

Parikh M.; Maddaford T.G.; Austria J.A.; Aliani M.; Netticadan T.; Pierce G.N. Dietary flaxseed as a strategy for improving human health. *Nutrients*. 2019.

Pedro R.B.; Tonon R. V; Hubinger M.D. Effect of Oil Concentration on the Microencapsulation of Flaxseed oil By Spray Drying. *III Jornadas Int sobre Av en la Tecnol Film y Cober Funcionales en Aliment*. 2011;(December 2014):5.

Premi, M., and Sharma, R. (2017). Microencapsulation of Green Cardamom (*Elettaria cardamomum* Maton) Volatile Oil by Spray drying: Effect of Process Variables and Wall Materials on Encapsulation Efficiency and Release Profile. *Materials*, 10(12), 1477.

Quispe-Condori S.; Saldaña M.D.A.; Temelli F. Microencapsulation of flax oil with zein using spray and freeze drying. *LWT - Food Sci Technol*. 2011.

Quispe-Condori, S., Saldana, M. D. A., and Temelli, F. (2011). Microencapsulation of flax oil with zein using spray and Freeze drying. *LWT – Food Science and Technology*, 44, 1880–1887

Rabail, R.; Shabbir, M.A.; Sahar, A.; Miecznikowski, A.; Kieliszek, M.; Aadil, R.M. An Intricate Review on Nutritional and Analytical Profiling of Coconut, Flaxseed, Olive, and Sunflower Oil Blends. *Molecules* 2021, 26, 7187.

Rezvankhah A.; Emam-Djomeh Z.; Askari G. Encapsulation and delivery of bioactive compounds using spray and freeze-drying techniques: A review. *Dry Technol*. 2020.

Rosen M.J.; Kunjappu J.T. *Surfactants and Interfacial Phenomena: Fourth Edition*. Surfactants and Interfacial Phenomena: Fourth Edition. 2012.

Roohinejad, S., Greiner, R., Oey, I., Wen, J. (2018). Emulsion-based systems for delivery of food active compounds: Formation, application, health, and safety. In *Emulsion-based*

Systems for Delivery of Food Active Compounds: Formation, Application, Health and Safety.

Rubilar M.; Morales E.; Contreras K.; Ceballos C.; Acevedo F.; Villarroel M.; et al. Development of a soup powder enriched with microencapsulated linseed oil as a source of omega-3 fatty acids. *Eur J Lipid Sci Technol*. 2012.

Santana, R. C., Perrechil, F. A., & Cunha, R. L. (2013). High- and Low-Energy Emulsifications for Food Applications: A Focus on Process Parameters. *Food Engineering Reviews*, 5(2), 107–122.

Sarabandi, K., Jafari, S. M., Mahoonak, A. S., and Mohammadi, A. (2019). Application of Gum arabic and maltodextrin for encapsulation of eggplant peel extract as a natural antioxidant and color source. *International Journal of Biological Macromolecules*, 140, 59–68.

Schlick-Hasper, E., Bethke, J., Vogler, N., and Goedecke, T. (2022). Flow properties of powdery or granular filling substances of dangerous goods packagings—Packaging Technology and Science. *Packaging Technology and Science*, 35(10), 765–782

Schröder, V., Behrend, O., and Schubert, H. (1998). Effect of dynamic interfacial tension on the emulsification process using microporous ceramic membranes. *Journal of Colloid and Interface Science*, 202, 334–340.

Shahidi F. *Bailey's Industrial Oil and Fat Products, Volumes 1-6 (6th Edition)*. Bailey's Industrial Oil and Fat Products. 2005.

Shahidi F.; Han X.Q. Encapsulation of Food Ingredients. *Crit Rev Food Sci Nutr*. 1993.

Shima M.; Kobayashi Y.; Fujii T.; Tanaka M.; Kimura Y.; Adachi S.; et al. Preparation of fine W/O/W emulsion through membrane filtration of coarse W/O/W emulsion and disappearance of the inclusion of outer phase solution. *Food Hydrocoll*. 2004.

Simopoulos A.P. The importance of the omega-6/omega-3 fatty acid ratio in cardiovascular disease and other chronic diseases. *Experimental Biology and Medicine*. 2008.

Singh K.K.; Mridula D.; Rehal J.; Barnwal P. Flaxseed: A potential source of food, feed and fiber. *Crit Rev Food Sci Nutr*. 2011.

Solans C.; Morales D.; Homs M. Spontaneous emulsification. *Current Opinion in Colloid and Interface Science*. 2016.

Stang M.; Schuchmann H.; Schubert H. Emulsification in High-Pressure Homogenizers. *Eng Life Sci*. 2001.

Tarladgis, B. G., Watts, B. M., Younathan, M. T., and Dugan, L. (1960). A distillation method for the quantitative determination of malonaldehyde in rancid foods. *Journal of the American Oil Chemists Society*, 37(1), 44–48

Thirundas R.; Gadhe K.S.; Syed I.H. Optimization of wall material concentration in preparation of Flaxseed oil powder using response surface methodology. *J Food Process Preserv*. 2014.

Tonon R. V.; Grosso C.R.F.; Hubinger M.D. Influence of emulsion composition and inlet air temperature on the microencapsulation of Flaxseed oil by SD. *Food Res Int*. 2011.

Tonon R. V.; Pedro R.B.; Grosso C.R.F.; Hubinger M.D. Microencapsulation of Flaxseed oil by spray drying: Effect of Oil Load and Type of Wall Material. *Dry Technol*. 2012.

Tontul I.; Topuz A. Influence of emulsion composition and ultrasonication time on Flaxseed oil powder properties. *Powder Technol*. 2014.

Touré A.; Xueming X. Flaxseed lignans: Source, biosynthesis, metabolism, antioxidant activity, Bio-active components, and health benefits. *Compr Rev Food Sci Food Saf*. 2010.

Turchiuli, C., Fuchs, M., Bohin, M., Cuvelier, M. E., et al. (2004). Oil encapsulation by spray drying and fluidised bed agglomeration. *Innovations in Food Science and Emerging Technology*, 6, 29–35.

Urban, K., Wagner, G., Schaffner, D., Röglin, D., & Ulrich, J. (2006). Rotor-Stator and Disc Systems for Emulsification Processes. *Chemical Engineering & Technology*, 29(1), 24–31.

Van Der Graaf, S., Schroën, C. G. P. H., & Boom, R. M. (2005). Preparation of double emulsions by membrane emulsification - A review. *Journal of Membrane Science*, 251(1–2), 7–15.

Van Der Graaf, S., Schroën, C. G. P. H., Van Der Sman, R. G. M., & Boom, R. M. (2004). Influence of dynamic interfacial tension on droplet formation during membrane emulsification. *Journal of Colloid and Interface Science*.

Vladislavljević, G. T. (2019). microencapsulation in Pharmaceutics and Biotechnology. *Current Trends and Future Developments on (Bio-) Membranes*, 167–222.

Wang, Jun-Wei and Abadikhah, Hamidreza and Yin, Liangjun and Jian, Xian and Xu, Xin. (2023). Multilevel hierarchical super-hydrophobic ceramic membrane for water-in-oil emulsion separation. *Process Safety and Environmental Protection*. 175.

Yang X.; Li S.; Yan J.; Xia J.; Huang L.; Li M.; et al. Effect of different combinations of emulsifier and wall materials on physical properties of spray-dried microencapsulated swida wilsoniana oil. *J Bioresour Bioprod*. 2020.

Yarlina, V. P., Diva, A., Zaida, Z., Andoyo, R., Djali, M., and Lani, M. N. (2023). Ratio Variation of maltodextrin and Gum arabic as Encapsulant on White Jack Bean Tempe Protein Concentrate. *Current Research in Nutrition and Food Science*, 11(3).

Zou X.G.; Chen X.L.; Hu J.N.; Wang Y.F.; Gong D.M.; Zhu X.M.; et al. Comparisons of proximate compositions, fatty acids profile and micronutrients between fibre and oil flaxseeds (*Linum usitatissimum* L.). *J Food Compos Anal*. 2017

10. LIST OF PUBLICATIONS AND CONFERENCES

Articles in journals with impact factor and scopus cited
Publication
Yakdhane, A. , Labidi, S., Chaabane, D., Tolnay, A., Nath, A., Koris, A., & Vatai, G. (2021). Microencapsulation of Flaxseed Oil—State of Art. Processes, 9(2), 295. Doi:10.3390/pr9020295, IP = 3.5, Scimago rank Q2
Yakdhane, A. , Chaabane, D., Yakdhane, E., Molnár, M.A., Nath, A., & Koris, A., (2024) Microencapsulation of Flaxseed oil Produced by Sequential Rotor stator homogenization and Spray drying: Optimization of Emulsion composition; Progress in Agricultural Engineering Sciences; Manuscript number: 122, Doi: 10.1556/446.2024.00122, Scimago rank Q2
Chaabane, D., Mirmazloum, I., Yakdhane, A. , Ayari, E., Albert, K., Vatai, G., Ladányi, M., Koris, A., & Nath, A. (2023). Microencapsulation of Olive Oil by Dehydration of Emulsion: Effects of the Emulsion Formulation and Dehydration Process. Bioengineering, 10(6), 657. Doi: 10.3390/BIOENGINEERING10060657, IP = 4.6, Scimago rank Q2
Chaabane, D., Yakdhane, A. , Vatai, G., Koris, A., & Nath, A. (2022), Microencapsulation of Olive Oil: A comprehensive review. Periodica Polytechnica Chememical Engineering, 66(3), 354–366, Doi: 10.3311/ppch.19587, IP = 1.4, Scimago rank Q3
Proceeding at international conference
Yakdhane, A. , Nath, A., Koris, A., (2020), Preparation of food-grade oil-in-water emulsions using membrane emulsification technology - a review the 44th conference for students of agriculture and veterinary medicine, ISBN 978-86-7520-519-7, P216-221.
Nath, A., Yakdhane, A. , Eren, B.A., Csighy, A., Bánvölgyi, S., Páztorné Huszár, K., Szerdahelyi, E., Takács, K., Koris, A., (2020), Biological activities of Peptides derived from Milk proteins through Membrane and Enzymatic routes. Ifjú Tehetségek Találkozója SZIENTific Meeting of Young Researches, ISBN: 978-963-269-937-0, P278-283
Chaabane, D., Yakdhane, A. , Koris, A., (2019): Present status of membrane emulsification and encapsulation by spray drying of vegetable oils with increased active ingredient content – A review; BiosysFoodEng 2019 - Proceedings: 3rd International Conference on Biosystems and Food Engineering; Budapest, Hungary: Szent István University, (2019), ISBN 978-963-269-878-6, E332

Nath, A., **Yakdhane, A.**, Bánvölgyi, S., Koris, A., (2020), Encapsulation of probiotics and their release in food matrix; Ifjú Tehetségek Találkozója SZIEntific Meeting of Young Researches; ISBN: 978-963-269-937-0, P284-287.

Abstract at international conference

Yakdhane, A., Koris, A., Labidi S., Nath, A., (2019): Microencapsulation of flaxseed oil – A review. BiosysFoodEng 2019 - Proceedings: 3rd International Conference on Biosystems and Food Engineering, ISBN 978-963-269-878-6, E326.

Yakdhane, A., Vatai, G., Márki, E., Koris, A., Nath, A., (2019): Encapsulation of prebiotics and probiotics for food fortification – A review. BiosysFoodEng 2019 - Proceedings: 3rd International Conference on Biosystems and Food Engineering, ISBN 978-963-269-878-6, E327.

Koris, A., Tolnay, A., Kárpáti, P., **Yakdhane, A.**, Pozsgai, E., Gerencsér-Berta, R., Galambos, I., Márki, E., Nath, A., (2019): Bioadsorbent for removal of organic micropollutant: charecterization of bioadsorbent, adsorption isotherm and sustainability of bioadsorbtion process. VI. Soós Ernő Nemzetközi Tudományos Konferencia: Víz- és szennyvízkezelés az iparban 2019.Nagykanizsa, Hungary: Pannon Egyetem. ISBN 978-615-81384-0-6

Chaabane, D., **Yakdhane, A.**, Tolnay, A., Nath, A., Koris, A., (2020) Membrane emulsification and encapsulation by spray drying of olive oil: selection of the wall material. 12th international congress on membranes and membrane processes. ICOM2020.

Nath, A., **Yakdhane, A.**, Mérő, K., Albert, K., Tolnay, A., Feczko, T., Trif, L., Koris, A., Vatai, G., (2019): Microencapsulation of vegetable oil through the combination of membrane emulsification and spray drying technologies-bioprocess engineering study, comprehensive product characterization and sustainability study. PERMEA 2019 - Membrane Conference of Visegrád Countries, ISBN 978-963-9970-97-7, P33

ACKNOWLEDGEMENT

I would like to express my sincere gratitude:

Firstly, to my supervisor, **Prof. András Koris** for accepting me as a PhD student at the Hungarian University of Agriculture and Life Sciences (MATE) and for his continuous support and believing in me which have been instrumental in motivating me to pursue this research. I am truly grateful for his encouragement.

Secondly, to my co-supervisor, **Dr. Habil Arijit Nath** for his unwavering support and guidance. His expertise and encouragement were instrumental in helping me navigate the challenges and achieve success. I am incredibly grateful for the opportunity to have learned from him.

Third, to **Tempus Public Foundation** (Stipendium Hungaricum Scholarship) for granting me a scholarship allowing me to study in the beautiful city of Budapest. I cannot thank them enough for their amazing support to that has played a vital role in making student life possible, and I deeply appreciate their commitment to alleviating the burdens of students.

I would like to address with great respect and gratitude to all those who helped me to accomplish this work in the best conditions, through their kindness and directives.

And finally, to my dearest Family, words cannot express how grateful I am for your support throughout my entire journey. Your constant love, caring, encouragement, and belief in me have been the fuel that kept me going through the challenges.